Solar Orbiter Environmental Specification

prepared by   J. Sørensen
Space Environment and Effects Analysis Section
ESA/ESTEC/TEC-EES

CHANGE LOG

date	issue	revision	pages	Reason for change
24/6-03	1.0	0	All	First issue Complete except for table 1 on page 35 (meteoroid fluences)
10/9-03	1.1	0	33-37	Meteoroid flux data added
23/3-05	1.2	0	3+18+21+25-26 30+33+48-97	LET and energy spectra for individual ions added NIEL data included
22/11-05		1	13, 18, 26, 48, 54-89	Wrong labeling corrected
12/12-05	1.3	0	3, 5-9. 12-13, 17-19, 21, 23-24, 27-33, 34, 37, 48-54, 56-59, 64-75, 81-95	New trajectory with launch in 2015 Separate data for nominal science phase Number of SPEs versus fluence threshold Data for specific SPEs
5/1-06		1	48-50	Correction and update of Appendix A
14/11-08	2.0	0	5-10, 13, 18-19, 25, 28-34, 38, 57-98	New trajectory with launch in 2017 or 2018 Change of solar proton model from JPL to ESP
9/6-10	3.0	0	5-15, 16-17, 27-29, 32-38, 42, 61, 63-102	New trajectory and launch options

Table of Content

Chapter

Appendix

1

Introduction

The Space Environment can cause severe problems for any space system including the Solar Orbiter on its mission to the innermost regions of the solar system. Proper assessment of the potential effects is an essential part of the engineering process leading to the construction of any element of the spacecraft. It is important that this is taken into account from the earliest phases of a project when consideration is given to mass budget, protection, component selection policy, etc. As the design of an element is developed, further engineering iteration is normally necessary with more detailed analysis.

This document is intended to assist the developers of instruments for the Solar Orbiter in assessing the effects of the space environment on their systems. The document is based on the ECSS-E-ST-10-04C Space Environment Standard [1], from which most of the background information has been taken (ECSS is a cooperative effort of the European Space Agency, National Space Agencies and European industry associations for the purpose of developing and maintaining common standards).

The Mission

The baseline is to launch Solar Orbiter between December 2016 and March 2017, with a backup possibility to launch in September 2018. The launch will be with a direct escape injection, after which the spacecraft will start its journey to the innermost regions of the solar system. Using successive Venus gravity assist manoeuvres an orbit with a perihelion down to 0.28AU (about 60 solar radii) and a period of about 150 days is obtained. The total duration of the mission is 9 to 10 years. The nominal science phase starts 3 to 4 years into the mission, and it has a duration of at least 3.2 years. For the baseline launch several launch windows are possible each with slightly different trajectories.

The different launch options are described in [2], and the trajectory for each option was received from ESOC [3]. Table 1 lists the various options, and Figure 1 to 5 gives an impression of the trajectory in terms of the distance to the sun as a function of time for each. The 2017 Case2 Late is regarded as the reference case.

Table 1: Launch options

	Case	Launch date*)
Baseline launch in 2017	Case 2 Early	15/12-2016
	Case 2 Late	23/1-2017
	Case 3	11/3-2017
	Case 4	28/12-2016
Backup launch in 2018	Case 1	6/9-2018

*) from the trajectory file – the actual launch window is described in [2]

The Space Environment

In general, when assessing the effects of the space environment on an instrument, the following environments should be included:

- Solar and Planetary Electromagnetic Radiation
- Neutral Atmosphere [1)]
- Plasmas
- Energetic Particle Radiation
- Particulates
- Contamination
- Thermal [2)]

For the environment in the innermost regions of the solar system only very little is known about many of these components. Indeed part of the purpose of the mission is to investigate the nature of several of these environments.

Because there is a direct escape injection of only short duration the earth orbit will not be discussed here except a short description of the radiation belts.

Each component of the space environment is treated separately, although synergies and cross-linking of models are specified. The natural environment is described together with the general models in use and principles for determining the local induced environment. Many of the models mentioned are also installed in the Space Environment Information System (Spenvis), which can be accessed via the WWW site http://www.spenvis.oma.be/spenvis/.

Many of the environments are strongly dependent on the heliospheric distance. Specifically several aspects are inverse proportional to the square of the distance to the Sun. Often models are not available for the range of heliospheric distances of Solar Orbiter. In these cases an appropriate scaling is applied to a model valid for 1AU. Figure 6 shows the heliospheric distance distribution of the Solar Orbiter trajectory in the different cases.

The trajectories for the various cases are very similar for what concerns the environment. The "2017 Case 2 Late" and the "2018 Case1" are identical (it is the same trajectory just shifted about 1.5 years and since a worst case w.r.t. the solar cycle is assumed, the results are practically identical. Similarly the difference between the "2017 Case 2 Late" and "2017 Case 2 Early" is extremely small (the first few months of the trajectory differ slightly, but is identical thereafter). The last 2 cases the "2017 Case 3" and the "2017 Case 4" are a bit different, but not spectacularly so. This document describe all the 5 cases, but combining the 3: Case 2 Early, Case 2 Late and 2018 Case1, as implied by the above. Table 2 shows the applied mission scaling factors for the various options given the trajectory of Solar Orbiter.

For many of the associated analyses it is necessary to take the geometry of the spacecraft into account, but such geometrical analyses are out of the scope of this document.

---

1) Not relevant for an interplanetary mission like the Solar Orbiter.

2) Although, also very important, the thermal environment is not treated in this document (except for the external heat sources).

Table 2: Mission scaling factors

		Duration [years]		Radius [AU]	r^{-2} scaling factor
Baseline launch in 2017 Case 2 Early Case 2 Late Backup launch in 2018	**Total Mission**	9.4-9.6	Max (min perihelion)	0.28	12.7
			Min (max aphelion)	1.37	0.53
			Mission average *)	0.60	**2.74**
	Nominal Science Phase	3.2	Max (min perihelion)	0.28	12.7
			Min (max aphelion)	0.91	1.20
			Mission average *)	0.56	**3.24**
Baseline launch in 2017 Case 3	**Total Mission**	9.4	Max (min perihelion)	0.28	12.7
			Min (max aphelion)	1.47	0.46
			Mission average *)	0.62	**2.61**
	Nominal Science Phase	3.5	Max (min perihelion)	0.28	12.7
			Min (max aphelion)	1.11	0.81
			Mission average *)	0.60	**2.74**
Baseline launch in 2017 Case 4	**Total Mission**	10.2	Max (min perihelion)	0.28	12.7
			Min (max aphelion)	1.32	0.58
			Mission average *)	0.59	**2.90**
	Nominal Science Phase	3.6	Max (min perihelion)	0.28	12.7
			Min (max aphelion)	0.91	1.20
			Mission average *)	0.56	**3.20**

*) calculated as $1/\sqrt{(\text{Average}(r^{-2}))}$

1.1 Figures
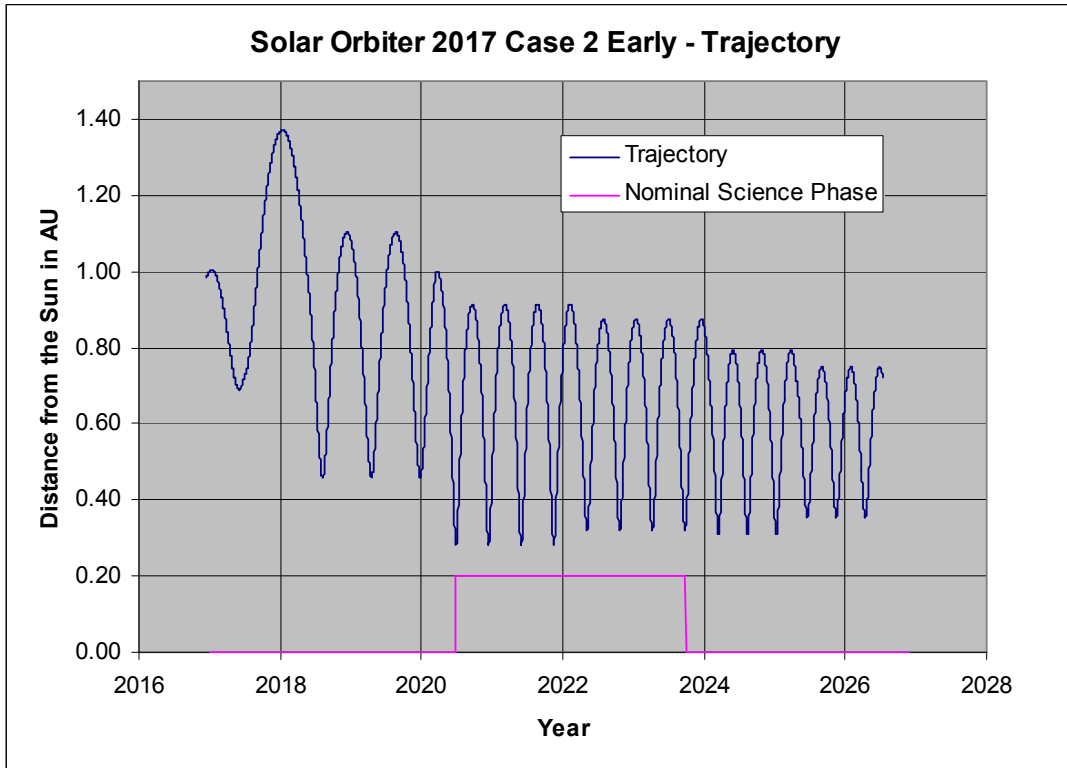
Figure 1: Solar Orbiter trajectory for launch in 2017 Case 2 Early
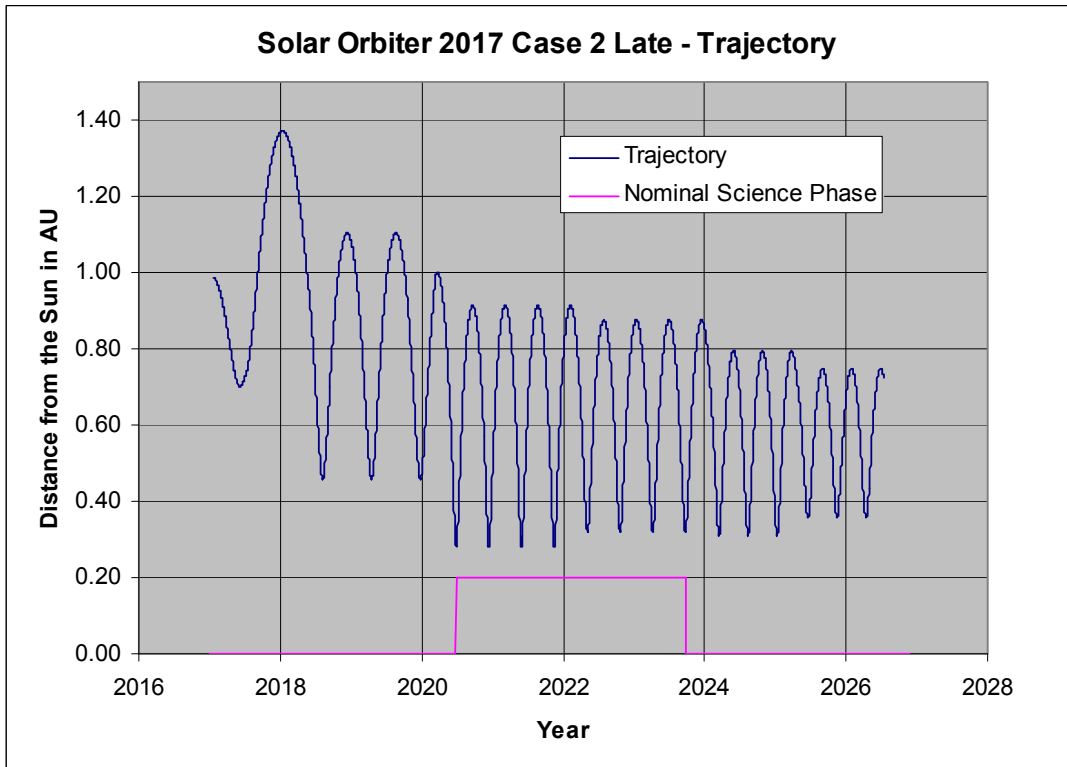
Figure 2: Solar Orbiter trajectory for launch in 2017 Case 2 Late
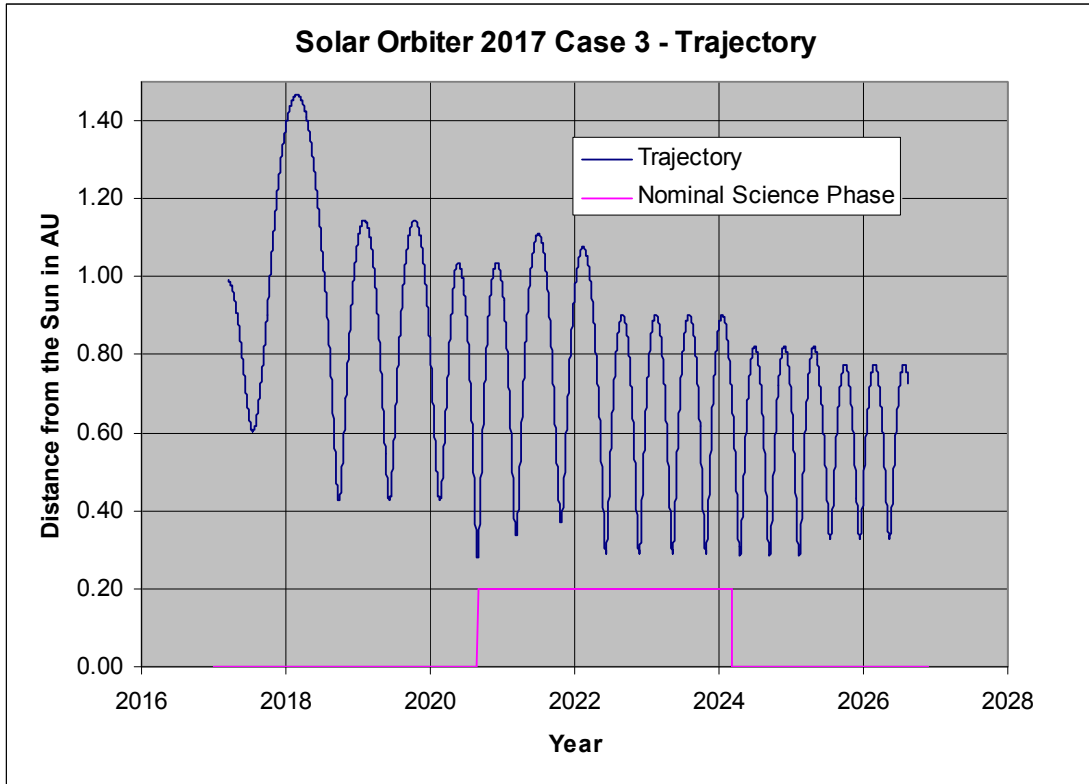
Figure 3: Solar Orbiter trajectory for launch in 2017 Case 3
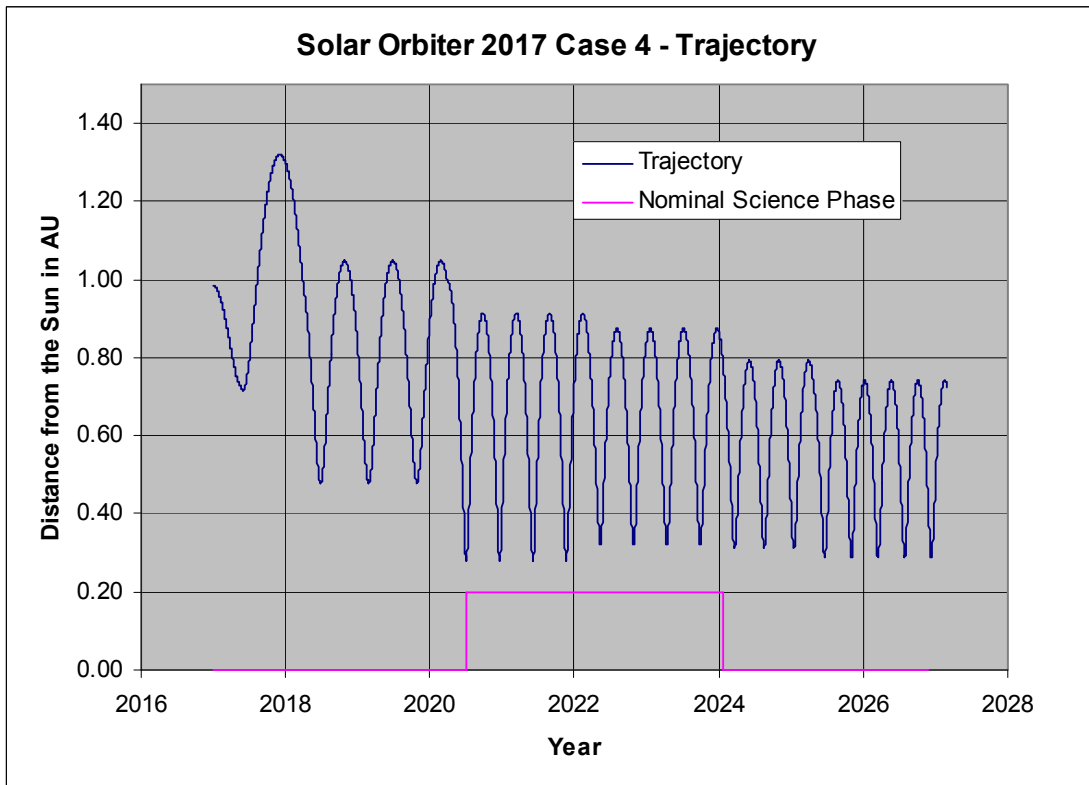
Figure 4: Solar Orbiter trajectory for launch in 2017 Case 4
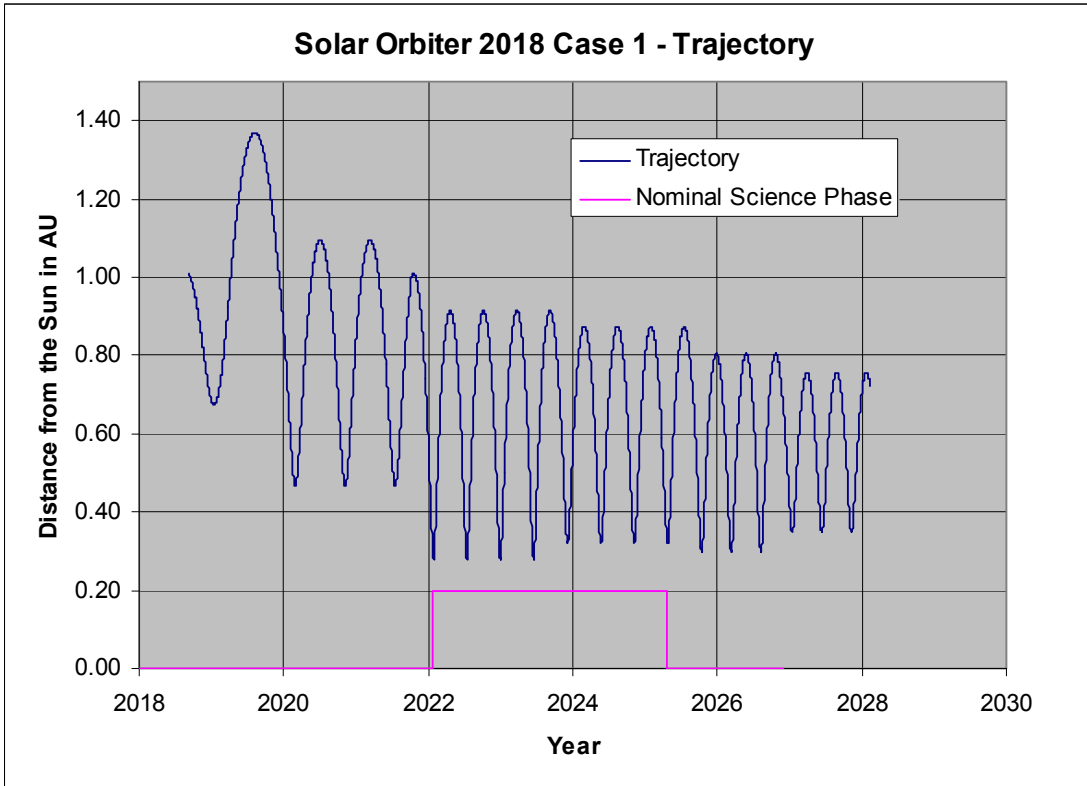
Figure 5: Solar Orbiter trajectory for launch in 2018 Case 1
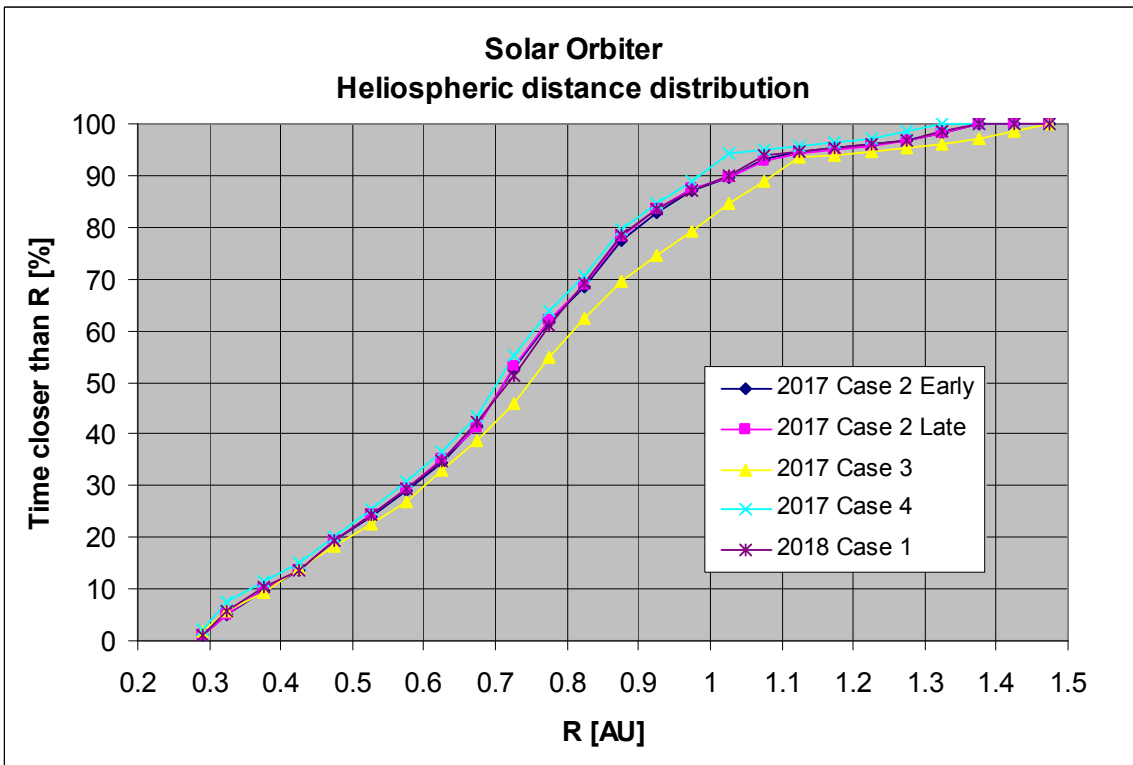
Figure 6: Solar Orbiter Heliosperic distance distribution

1.2 References

[1]   ECSS-E-ST-10-04C, System Engineering, Space Environment Standard
         WWW site: http://www.ecss.nl

[2]   Solar Orbiter: Consolidated Report on Mission Analysis, SOL-ESC-RP-05500,
         Issue 1, 12/5-2010, J.M. Sanchez Perez, ESA-ESOC/OPS-GFA

[3]   Orbit files received from ESOC 14/4-2010: SolO_Orbit_Files_14_04_201.zip

2

Solar and Planetary electromagnetic radiation environment

2.1 Introduction

In general spacecraft receive electromagnetic radiation from several external sources. The largest source is generally the direct solar flux. The fraction of incident sunlight that is reflected off a planet is termed albedo. When in orbit around a planet this will also contribute to the flux received by the spacecraft (depending on the sunlit part of the planet, which the spacecraft can see). A third source is the planet-emitted infrared radiation.

For the Solar Orbiter, in its interplanetary orbit, the albedo and the planet infrared radiation can be ignored, and only the direct solar flux needs to be taken into account.

The electromagnetic radiation varies with solar activities, which is highly variable over a solar cycle. The given data are mainly average values. For thermal analyses or certain special applications more detailed treatment is required, which is outside the scope of this document.

2.2 Solar electromagnetic radiation

Direct solar flux

The direct solar flux is inverse proportional to the square of the distance to the Sun. At the Earth's distance the value is fairly constant, but the Solar Orbiter in its very elliptical orbit will encounter extreme variations in the solar flux. The following values for the electromagnetic radiation shall be used for the Solar Orbiter (solar energy that falls on a unit area of surface normal to the line from the Sun, per unit time):

Table 1: Solar irradiance

	Solar flux $[W/m^2]$		
	Baseline (case2) and Backup	**Baseline (case3)**	**Baseline (case4)**
Average over the mission	3743	3565	3961
Maximum (at minimum perihelion)	17348 (at 0.28AU)		
Minimum (at maximum aphelion)	724 (at 1.37AU)	628 (at 1.47AU)	792 (at 1.32AU)
Average at the Earth (the solar constant)	1366		

(the average solar irradiance at the Earth has an uncertainty of about $\pm3W/m^2$)

The scaling factors applied in the calculation are shown in table 1 of Chapter 1.

Solar spectrum

The solar spectrum shall be approximated by a black body curve with a characteristic temperature of 5780K (this is the temperature that at 1AU gives the value of the solar constant reported above). A space sink temperature of 3 K shall be assumed.

The UV portion (wavelength, λ,< 300 nm) of the electromagnetic spectrum is of particular importance in determining effects of solar radiation on material properties. The integrated irradiance of the near UV electromagnetic radiation flux (180 nm < λ < 400 nm) is approximately (Baseline case 2 and Backup):

Mission average near UV	323 W/m^2
Maximum near UV (at minimum perihelion)	2499 W/m^2
Minimum near UV (at maximum aphelion)	63 W/m^2
Average near UV at the Earth	118 W/m^2

The far UV portion (λ < 180 nm) contributes about 0.023 W/m^2 at the Earth's distance (0.29 W/ m^2 at the minimum distance of the Solar Orbiter to the sun).

Certain parts of the spectrum are varying very much, both, over the 27-day solar rotation period and over the 11-year solar cycle. This variation ranges from about 50 % for the near UV part to a factor 2 for the UV and far UV portions and can reach orders of magnitude for flare X-rays.

Average and worst case irradiance levels for the high-energy spectrum are summarized in Table 2. The average values for the Earth's distance were taken from [1]. The Solar Orbiter values are for the Baseline Case2 and Backup options.

Table 2: High-energy solar electromagnetic flux

Type	Wavelength (nm)	At the Earth's distance		Solar Orbiter Mission	
		Average Flux (W/m^2)	Worst-Case Flux (W/m^2)	Average Flux (W/m^2)	Worst-Case Flux (W/m^2)
Near UV	180-400	118	177	323	2250
UV	< 180	2.3×10^{-2}	4.6×10^{-2}	6.3×10^{-2}	0.6
UV	100-150	7.5×10^{-3}	1.5×10^{-2}	2.1×10^{-2}	0.2
EUV	10-100	2×10^{-3}	4×10^{-3}	5×10^{-3}	5×10^{-2}
X-Rays	1-10	5×10^{-5}	1×10^{-4}	1.4×10^{-4}	1×10^{-3}
Flare X-Rays	0.1-1	1×10^{-4}	1×10^{-3}	3×10^{-4}	1×10^{-2}

For design purposes the worst-case values of Table 1 shall be used. The fluxes given for flare X-rays are peak values of large flares. For design, one such X-ray flare per week, lasting one hour, shall be assumed. More details on the solar spectrum can be found in [2] and on the X-ray part of the spectrum in particular in [3].

2.4 Directional and temporal variation

Apart from the global long term variation, the solar irradiation seen by a spacecraft element also varies through the orbit and from orbit to orbit, and with the direction in which the element is pointing.

To get the actual incident irradiation seen by an experiment, the shading by other elements of the spacecraft itself also has to be taken into account. For this a geometrical model is needed, which can simulate the pointing in the orbit and the kinematics of the spacecraft.

2.5 References

[1]   "Natural Orbital Environment Guidelines for Use in Aerospace Vehicle Development", B.J.Anderson, editor and R.E. Smith, compiler; NASA TM 4527, chapters 6 and 9, June 1994

[2]   ECSS-E-ST-10-04C, System Engineering, Space Environment Standard

          WWW site: http://www.ecss.nl

 [3]   Nieminen P., "Spectral Input Code for Induced X-Ray Emission Calculations from Solar System Bodies", ESA Working Paper 2009, February 1999

3

Plasmas

3.1 Introduction

A plasma is a partly or wholly ionised gas whose particles exhibit collective response to magnetic and electric fields. The collective motion is brought about by the electrostatic Coulomb force between charged particles. This causes the particles to rearrange themselves to counteract electric fields within a distance of the order of λ, the Debye length.

$$\lambda = \left(\frac{\varepsilon_0 k T_e}{ne^2} \right)^{1/2}$$

where:

> λ is in metres
> T_e is electron temperature in K
> e is electron charge in C
> n is density in m^{-3}
> k is the Boltzmann constant
> ε_0 is the permittivity of vacuum

On spatial scales larger than λ plasmas are electrically neutral.

The plasma regime experienced by the Solar Orbiter spacecraft is the **solar wind**, and varies through the mission as it travels from 1AU (Earth's heliocentric distance) to its closest distance to the sun (0.28AU at minimum perihelion).

The principal spacecraft engineering concerns for the Solar Orbiter spacecraft caused by space plasmas are outlined in Table 1.

Table 1: Main engineering concerns for Solar Orbiter due to space plasmas

System	Problem
Scientific experiments	Low level positive or negative charging and photoelectrons which interfere with plasma measurements Plasma entry and potential changes in sensitive detectors
Electric Propulsion	Interaction between generated plasma, ambient plasma, and the spacecraft

Remark that general surface charging with following possibly harmful electrostatic discharges is only a problem in earth orbit at high altitude or polar latitude.

3.2   The Solar Wind

Description

The solar wind is part of the Corona, the Sun's outer atmosphere. The high temperature of the plasma near the sun causes it to expand outwards against gravity, carrying the solar magnetic field along with it. The solar wind starts at the Sun as a hot dense, slowly moving plasma but accelerates outwards to become cool, rare and supersonic at the Solar Orbiter perihelion and beyond. Most of the solar wind's acceleration takes place near the sun and so the Solar Orbiter will not observe significant difference in velocity as its distance from the Sun varies.

The solar wind velocity typically lies in the range 300-1200km/s. It is most commonly around 400km/s but there are frequent high-speed streams with velocities around 700km/s. These streams are more commonly observed around solar minimum and recur generally with a 27-day period. The strong variability of the solar wind is the driving force, putting energy into the magnetosphere and ultimately causing surface charging and radiation effects. More severe but less frequent disturbances in the solar wind can be caused by coronal mass ejections.

Although solar wind plasma is cold, the ions carry considerable kinetic energy, typically ~1keV for protons and ~4keV for He^{++}. This can result in sputtering from surface materials. In the magnetosheath kinetic energy is lower, but sputtering still occurs.

Typical Parameters

Because the solar wind flows past the planets with negligible modification, unless it encounters the bow shock, it can be considered spatially uniform. Characteristic mean values for the solar wind environment are given in Table 2 (the values for the Baseline Case 2 and Backup options and the different distances from the sun are derived from the values at 1AU via simple scaling laws).

Table 2: Solar Wind parameters.

Parameter (average values)	1AU (Earth)	Mission average	0.28AU (minimum perihelion)
Density (cm^{-3})	8.7	24	110
Speed (km s^{-1})	468	468	468
T_p (K)	1.2×10^5	1.2×10^5	1.2×10^5
T_e (K)	1.0×10^5	1.0×10^5	1.0×10^5
λ (m)	7.3	4.1	2.0
N_{alpha}/N_{proton}	0.047	0.047	0.047

3.3   Induced Environments

The natural plasma environment can be augmented by a number of sources inside or on the satellite surface.

High-energy electron and ion populations can be generated by active experiments, i.e. electron and ion guns. These can be used to control surface charging or as a probe of the magnetic field. An ion thruster is a particularly high-flux ion gun.

Low-energy ion populations can be generated by ionisation (including charge exchange) of contaminant gasses i.e. those released from the spacecraft by "outgassing", emitted by thrusters, including ion thrusters and sputtered off the surface due to ion impacts. These contamination processes are described in a separate chapter.

Effects

Once outside the spacecraft, neutral atoms produced by outgassing and sputtering can be ionised by sunlight or charge-exchange with other ions, to create a low-energy (<10eV) ion population. These ions can be drawn to negatively charged surfaces and can adhere. This coating may alter optical properties e.g. of mirrors or solar panel covers, or change the secondary and photoemission yields and the susceptibility to surface charging. Within the spacecraft, e.g. in electronics boxes, residual gasses can facilitate electrostatic discharges from high voltage components.

Photo- and secondary electrons

The electron density at the spacecraft surface shall be determined from the incident UV and primary electron fluxes, multiplied by the yield for the surface in question. Away from the emitting surface the density shall be calculated from the following formula for a planar surface [2]:

$$\frac{N}{N_0} = (1 + \frac{z}{\sqrt{2}\lambda_0})^{-2}$$

where:

N is density (cm^{-3})

N_0 is density at emitter (cm^{-3})

z is distance from surface

λ_0 is shielding distance, calculated as the Debye length due to the emitted electrons

Once neutral gas is released into space by whatever mechanism, it becomes subject to photoionisation and dissociation by solar UV and ionisation by charge exchange with solar wind ions. Production of new ions can be calculated from the appropriate photoionisation rates and charge exchange cross-sections.

$$Q = N_i (\nu + \sigma n_{sw} v_{sw})$$

from [3] where:

Q is production rate, ions s^{-1}

N_I is ion density

ν is photoionisation rate coefficient

n_{sw} and v_{sw} are solar wind density and velocity

σ is charge exchange coefficient.

Photoionisation rates depends on the atom or molecule concerned, and UV intensity and spectrum. Huebner and Giguere [4] have tabulated a number of rate coefficients for different species, for sunlight at 1AU.

Table 3 gives typical photoelectron sheath parameters [5] (the values for the Solar Orbiter distance have been obtained assuming them inverse proportional to the square of the distance to the Sun).

Table 3: Photoelectron Sheath parameters

Parameter	1AU (Earth)	Mission average	0.28AU (minimum perihelion)
Temperature (eV)	3	3	3
Photoelectron current (Amps m^{-2})	1×10^{-5}	3×10^{-5}	1×10^{-4}
Surface electron density (m^{-3})	1×10^{8}	3×10^{8}	1×10^{9}

3.4 References

[1]   Feynman J, "Solar Wind", Chapter 3 of "Handbook of Geophysics and the Space Environment", Ed. A. Juram, USAF, 1985

[2]   Grard R.J.L. and J.K.E.Tunaley, "Photo Electron Sheath Near a planar Probe in Interplanetary Space", J. Geophys.Res, 76, p.2498, 1971

[3]   Huddleston D.E., A.D.Johnstone and A.J.Coates, "Determination of Comet Halley Gas Emission Characteristics from Mass Loading of the Solar Wind", J.Geophys.Res, 95, p.21, 1990

[4]   Huebner W.F. and P.T.Giguere "A Model of Comet Comae II. Effects of Solar Photodissociative Ionization", Astrophys.J, 238, p.753, 1980

[5]   Scialdone J.J. "An Estimate of the Outgassing of Space Payloads and Its Gaseous Influence on the Environment", J. Spacecraft and Rockets, 23, p.373, 1986

[6]   Hanson W.B., S.Santoni and J.H.Hoffman `Ion Sputtering from Satellite Surfaces', J.Geophys.Res, 86, p.11350, 1981

[7]   Olsen R.C. and C.W.Norwood, `Spacecraft-Generated Ions', J.Geophys.Res., 96, 15951-15962, 1991

4

Energetic particle radiation

4.1 Introduction: Overview of energetic particle radiation environment and effects

Radiation environments and effects always have to be considered early in the design cycle. Energetic charged particles, which can penetrate outer surfaces of spacecraft (for electrons, this is typically above 100keV, while for protons and other ions this is above 1MeV), are encountered throughout the Solar Orbiter mission, and the effects on the different components have to be considered. Neutrons, gamma-rays and X-rays are also considered energetic particles in this context.

Environments

Radiation belts

Energetic electrons and ions are magnetically trapped around the earth forming the radiation belts, also known as the Van Allen belts. The radiation belts are crossed by low altitude orbits as well as high altitude orbits (geostationary and beyond). The radiation belts consist principally of electrons of up to a few MeV energy and protons of up to several hundred MeV energy. The so-called south Atlantic anomaly is the inner edge of the inner radiation belt encountered in low altitude orbits. The offset, tilted geomagnetic field brings the inner belt to its lowest altitudes in the south Atlantic region. More information can be found in references [1] and [2].

Apart from during the direct escape injection, such radiation belts will not be encountered by the Solar Orbiter during its mission. However the duration is so short that the effect can be ignored.

Solar energetic particles

Energetic solar eruptions (*solar particle events - SPEs*) produce large fluxes of solar energetic particles (SEPs) which are encountered in interplanetary space as well as close to the planets. The Earth's magnetic field provides a varying degree of geomagnetic shielding in low Earth orbit.

Galactic cosmic-rays

There is a continuous flux of galactic cosmic-ray (GCR) ions. Although the flux is low (a few particles /cm²/sec), GCRs include energetic heavy ions which can deposit significant amounts of energy in sensitive volumes and so cause problems.

Secondary radiation

Secondary radiation is generated by the interaction of the above environmental components with materials of the spacecraft. A wide variety of secondary radiations are possible, of varying importance.

Effects survey

The above radiation environments represent important hazards to space missions. Energetic particles, particularly from the radiation belts in Earth's orbits and from solar particle events cause

radiation damage to electronic components, solar cells and materials. They can easily penetrate typical spacecraft walls and deposit considerable doses during a mission.

Energetic ions, primarily from cosmic rays and solar particle events, lose energy rapidly in materials, mainly through ionization. This energy transfer can disrupt or damage targets such as a memory element, leading to single-event upset (SEU) of a component, or an element of a detector (radiation background).

Energetic particles also interfere with payloads, most notably with detectors on astronomy and observation missions where they produce a `background' signal, which may not be distinguishable from the photon signal being counted, or which can overload the detector system.

Energetic electrons can penetrate thin shields and build up static charge in internal dielectric materials such as cable and other insulation, circuit boards, and on ungrounded metallic parts. These can subsequently discharge, generating electromagnetic interference.

Apart from ionizing dose, particles can lose energy through non-ionizing interactions with materials, particularly through "displacement damage", or "bulk damage", where atoms are displaced from their original sites. This can alter the electrical, mechanical or optical properties of materials and is an important damage mechanism for electro-optical components (solar cells, opto-couplers, etc.) and for detectors, such as CCDs.

4.2 Quantification of effects and related environments

Models of the radiation environment are needed to assist in orbit selection, component selection and shielding optimization. In engineering a space system to operate in the space environment, it is necessary to relate the environment to system degradation quantitatively. This also involves questions of testing systems and their components for verification that they meet the performance requirements in the presence of the space environment.

For example, testing with calibrated radioactive sources can establish the threshold for functional failure or degradation of an electronic component in terms of *total absorbed dose*. Radiation environment models, used together with mission orbital specifications can predict the dose and enable correct performance to be verified.

The table below gives the parameters which shall be used for quantification of the various radiation effects.

Table1: Parameters for quantification of radiation effects

Radiation effect	Parameter
Electronic component degradation	Total ionizing dose.
Material degradation	"
Material degradation (bulk damage)	Non-ionizing dose (NIEL).
CCD, sensor and opto-electronic component degradation	NIEL
Solar cell degradation	NIEL & *equivalent fluence.*
Single-event upset, latch-up, etc.	LET spectra (ions); proton energy spectra; explicit SEU/SEL rate of devices.
Sensor interference (background signals)	Flux above above energy threshold and/or flux threshold; explicit background rate.
Internal electrostatic charging	Electron flux and fluence; dielectric E-field.

Although some of these parameters are readily derivable from a specification of the environment, others either need explicit consideration of test data (for example single-event upset calculation) or the detailed consideration of interaction geometry and mechanisms (e.g. radiation background estimation).

In the following sections, the basic data on the environment are presented, along with models to be employed for deriving data beyond those presented. Effects and the specific methods for derivation of

engineering quantities will then be presented. Figure 1 shows the ranges of electrons and protons in aluminium.

4.3 Energetic particle radiation environment reference data, models and analysis methods

Standard Earth trapped radiation belts models

These are not applicable for the interplanetary orbit of the Solar Orbiter spacecraft, but are only mentioned here for completeness.

For trapped radiation, the standard models of radiation belt energetic particle shall be the AE-8 and AP-8 models for electrons [3] and protons [4] respectively. They were developed at the NSSDC at NASA/GSFC based on data from satellites flown in the '60s and early '70s. The models give omni-directional fluxes as functions of idealized geomagnetic dipole co-ordinates B/B_0 and L . This means that they must be used together with an orbit generator and geomagnetic field computation to give instantaneous or orbit-averaged fluxes. The user must define an orbit, generate a trajectory, transform it to geomagnetic co-ordinates and access the radiation belt models to compute flux spectra. Apart from separate versions for solar maximum and solar minimum, there is no description of the temporal behaviour of fluxes and no explicit flux directionality. For more information including information about which field model to use see [5].

Standard Solar particle event model

During energetic events on the sun, large fluxes of energetic protons are produced which can reach the Earth. Solar particle events, because of their unpredictability and large variability in magnitude, duration and spectral characteristics, have to be treated statistically. However, large events are confined to a 7-year period defined as solar maximum. Although large events are absent during the remaining 4 solar minimum years of the 11-year solar cycle the occasional small event can still occur. The reference model that shall be used for engineering consideration of time-integrated effects is the ESP model [6]. This statistical model is based on data from 3 solar cycles and gives the proton fluences at 1AU. The fluence from an event is dependent on the distance from the sun. To predict the fluences seen by the Solar Orbiter an inverse square law shall be applied for scaling of the 1 AU fluences given by the ESP model. As the orbit is at a variable distance, and the ESP model provides a long-term fluence, the average of the inverse square of the distance is used to scale the low energy fluences, see Chapter 2 Table 1. The confidence level applied when running the ESP model is 90% (appropriate for the total mission duration). For the science phase part of the mission the application of a higher confidence level would be justified, but for comparison reasons 90 % is also applied. The ESP model has superseded the JPL-91 model [7], which was a standard for many years, but was shown to underestimate the fluences.

The inverse square law provides for the "worst case" assumption of the proton event propagation and attenuation through the interplanetary medium. Research since the adoption of the inverse square law shows that a proton acceleration mechanism is also present during the propagation, which could result in a much smaller radial dependence than predicted by the inverse square law. However, the available data, which might support such research, is currently insufficient to confirm the pessimism of the inverse square law and so this worst case assumption has been applied to the analysis.

Figure 2 and 3 shows the predicted spectrum for the Solar Orbiter mission of solar protons based on this model both as plot and in tabular form.

The individual flare spectra are very variable, and what constitutes a worst-case event for a given energy is not necessarily worst-case at another. For the higher energies, which are the most important for nuclear interactions giving rise to certain types of background and single-event upsets, the October 1989 event is normally seen as a worst-case. This event produced a fluence of about 2.2 10^{10} protons.cm^{-2} with energies above 10 MeV (with a peak flux of 10^5 protons.cm^{-2}.s^{-1} with energies above 10 MeV).

More information of the expected number of solar proton events above a given > 10 MeV fluence threshold can be found in appendix A (both according to the JPL-1991 and a more recent model).

Concerning the directionality of the event flux, there is a streaming taking place, but it is usually of short duration (short compared with the duration of the individual event), with field disturbances quickly changing it into near isotropic distribution. Also it seems less pronounced in larger events. Therefore for the design the flux can be assumed to be isotropic. More information can be found in [26].

Individual Solar particle events

While the standard model provides data only for integrated effects analysis (dose, long-term degradation, total upset count, etc.), it is often necessary to consider individual events. Burrell, as reported in [10], developed a modified Poisson statistic to describe the probability p of a number of events n occurring during a time t, based on a previously observed frequency of N during time T:

$$p(n,t; N,T) = \{(n+N)! \, (t/T)^n\} / \{n!N! \, (1+t/T)^{N+n+1}\}$$

In this equation, $N=1$ and $T=7$ for the anomalous class of flare, while for ordinary flares, $N=24$ and $T=7$. This is sometimes useful in considering numbers of events in contrast to the total fluence.

Often it is necessary to consider instantaneous fluxes. For radiation background estimation for example, the fluxes are required above an energy threshold determined by sensor shielding and sensor sensitivity, and above a flux threshold determined by sensor signal-to-noise characteristics. Two reference environment data resources are available: NASA OMNIWEB database [11], and the NOAA GOES [12] database. With these databases, the durations and magnitudes of events above energy and flux thresholds can be analysed. Both databases are available on the WWW and provide a comprehensive long-term database of measurements of the interplanetary environment. OMNIWEB contains a complete database of energetic proton data from the IMP series of spacecraft. The NOAA GOES satellites have returned energetic proton and electron data from geostationary orbit since January 1986.

Data for some specific severe events can be found in appendix B.

Solar particle event ions

For analysing single event upset rates during solar particle events (SPE's), the CREME96 model shall be used. It can also be used for other applications where data on severe SPE conditions are needed, such as background estimation. CREME96 is described further in [13]. While the older CREME model contained models for the peak flux for various types of events, CREME96 contains models based on the October 1989 event. It provides models of energy spectrum, composition and LET spectrum for the worst week, worst day and peak 5 minutes. The older CREME model provided more choice of peak environments. However, some of the more severe options were unrealistic. More detailed information on the contribution of the different ions can be found in appendix C.

Cosmic ray environment and effects models

The Cosmic-Ray environment and effects models (CREME) were originally created by Adams and co-workers at the U.S. Naval Research Laboratory [14]. They provided a comprehensive set of cosmic ray and flare ion LET and energy spectra, including treatment of geomagnetic shielding and material shielding. CREME also included upset rate computation based on the path-length distribution in a sensitive volume and also treated in a simple manner trapped proton-induced SEUs. CREME has been superseded by CREME96 [14]. The major differences are in the inclusion of a model of the cosmic ray environment and its solar-cycle modulation due to Nymmik et al. [15], improved geomagnetic shielding calculation, improved material shielding calculation and more realistic solar energetic particle event (SEPE) ion environments. Cosmic ray fluxes are anti-correlated with solar activity so the highest cosmic ray fluxes occur at solar minimum. CREME96 shall be the standard model for cosmic ray environment assessment. It shall also be the standard for evaluation of single event effects from cosmic rays, from solar energetic particles and from energetic protons. In principle CREME96 gives predictions for 1AU, but these give a good upper limit (the actual cosmic ray fluxes can be expected to be slightly lower, due to the attenuation by the solar wind). In the evaluation ions from $Z=1$ to 92 shall be included and, in the absence of a reason to use another value, shielding of $1g/cm^2$ aluminium shall be assumed.

Figure 4 shows the predicted composite LET spectra for the Solar Orbiter mission for three CREME96 environments (predictions for 1AU): the nominal solar minimum cosmic ray flux; the average flux for a "worst week" of a large SEPE; and the peak flux from a large SEPE. More detailed information on the contribution of the different ions can be found in appendix C.

Electrons

The energetic electron environment encountered by the Solar Orbiter is dominated by two sources [23]. During solar quiet periods, the majority of high-energy (>100keV) are of Jovian origin, while at solar active periods, it is the solar electrons that are by far the dominating source. Figure 5 gives an impression of the predicted electron flux for the mission (from [23] assuming the flux being inverse proportional to the square of the distance to the Sun – the plot shows the predicted values for Mercury's distance from the sun, but given the uncertainty this gives a reasonable indication also for Solar Orbiter).

Spacecraft secondary radiation

For engineering purposes it is often only electron-induced Bremsstrahlung radiation that is considered as a significant secondary source. Bremsstrahlung is high-energy electromagnetic radiation in the X-γ energy range emitted by charged particles slowing down by scattering off atomic nuclei. The primary particle might ultimately be absorbed while the Bremsstrahlung can be highly penetrating. In space, the most common source of Bremsstrahlung is electron scattering. In special cases other secondaries need to be considered.

In evaluating the radiation background effects in detector systems, it is often secondary radiation that is important. This might be because of heavy shielding removing primaries, veto systems which actively protect against counting primary-induced signals, or secondary radiation generated within the sensing band of an instrument. Most secondary radiation is emitted at the instant of interaction ("prompt") while some is emitted some time after a nucleus has been excited by an incoming particle (induced radioactivity).

By its nature, secondary radiation has to be analysed on a case-by-case basis, possibly through Monte-Carlo simulation. For engineering estimates of Bremsstrahlung, the SHIELDOSE model [16] shall be used.

Neutrons

Neutrons are generated by energetic particles undergoing nuclear interactions with the material of spacecraft. These neutrons play a role in generating background in sensitive detector systems. A low-level flux of neutrons of between 0.5 cm^{-2}.s^{-1} and 4 cm^{-2}.s^{-1} is also present at low altitudes around the Earth due to cosmic ray interactions with the atmosphere.

4.4 Analysis methods for derived quantities

The following analysis methods shall be used.

The environment models specified in 4.3 shall be used to generate the primary data described in Section 4.2. The secondary data shall be derived as follows:

Ionizing dose:

The ionizing dose environment is represented by the dose-depth curve. This may provide dose as a function of shield thickness in planar geometry or as a function of spherical shielding about a point. The planar model is appropriate for surface materials or for locations near to a planar surface. In general, electronic components are not in such locations and a spherical model is recommended for general specification.

The SHIELDOSE model shall be used [16] for ionizing dose. This method uses a pre-computed data set of doses from electrons, electron-induced Bremsstrahlung and protons, as derived from Monte-Carlo analysis. The doses are provided as functions of material shielding thickness. The reference geometrical configuration for this dose-depth curve shall be a solid aluminium sphere. Figure 6 and 7 shows the expected doses for the Solar Orbiter mission as functions of the radius of the aluminium shielding. The accumulated dose of solar energetic protons are shown in the figures with a confidence level of 90% that higher dose will not be seen.

In cases where more careful analysis of the shielding of a component or of other sensitive locations is necessary, a sectoring calculation is performed on the geometry of the system. This might be necessary if the doses computed from simple spherical shielding are incompatible with the specification of the allowable radiation dose. The sectoring method traces rays from the point of interest through the shielding in a large number of directions. Along each direction the derived shielding, together with the data on dose as a function of shielding depth, d, is used to find the omni directional 4π dose contribution from each direction. The contributions, weighted by the solid angle increment around the rays, are then summed to give the total dose.

In some cases, it is efficient to derive a shielding distribution. This is the result of the ray tracing described above and provides the distribution of encountered shielding. To this distribution the shielding of the unit under investigation itself must be added and it can then be folded with the dose depth curve to derive the total dose.

It is important to recognise that a shielding analysis in the presence of significant anisotropies in the environment can result in serious error if the environment is assumed to be isotropic. This assumption is implicit in the sectoring method defined above since all directional contributions are derived from a common "omni directional" dose-depth curve.

Because of the very harsh environment seen by the Solar Orbiter spacecraft, not just the ionising radiation, but combined with the thermal and UV environment etc., directly exposed coatings and thin sheets in the micron range needs special attention. These cannot directly be analysed with the SHIELDOSE model. To assess the radiation dose in thin sheets due to protons the SRIM code can be used (Stopping and Range of Ions in Matter – SRIM-2000 [25]).

Figure 9 shows the predicted radiation dose per year as a function of depth in a thin sheet for some selected materials as calculated with SRIM and using the spectrum shown in figure 8. This spectrum is based on the average flux spectrum seen by the ACE satellite (located at about 1AU) scaled assuming the flux being inverse proportional to the square of the distance to the sun (a reasonable worst case assumption for this low energy end of the spectrum). It is seen that the materials Kapton, Mylar and Delrin give almost identical results. These 3 materials have quite different composition, but almost identical density (from 1.40 to 1.43g/cm^3), which seem to indicate that the density of the material mainly determines the deposited dose. The results for the 4th material Teflon (density 2.20g/cm^3) seem to support this – the difference being equal to the density ratio. Although also present, heavier ions like He are not expected to contribute significantly to the dose.

Single-event upset rate

The CREME/CREME96 method shall be used [13], [14]. It is possible to make upset rate predictions only when details of the device under consideration are known, particularly the critical charge and the sensitive volume dimensions. If a device is uncharacterised, tests shall be performed.

The test data shall show the normalised upset rate as a function of ion LET in the range 1 to 100 MeV.cm^2/mg and as a function of proton energy in the range 20-100MeV. These data shall be used to make an estimate of the upset rate from trapped protons and solar protons using the two-parameter Bendel method [17], and of upsets due to galactic and solar ions using the method of CREME/CREME96. This latter shall be modified to account for the non-ideal upset rate as a function of ion LET derived from component test data [18] (the so-called "IRPP" method) as described below. This method has been implemented in CREME96. CREME96 also includes the two-parameter Bendel method.

To compute an upset rate for an electronic device or a detector from the predicted fluxes, device characteristics must be specified, particularly the size of the sensitive volume and the *critical charge*, or equivalently, critical energy E_c, in the volume which results in upset or registers as a "count". For SEUs resulting from direct ionisation the rate is found by integrating over the composite differential

ion LET spectrum and the distribution of path-lengths for the sensitive volume [15], [18]. An estimate of the upset rate from nuclear interactions of energetic protons can be obtained by integration of the product of the measured proton-induced upset cross section $\sigma(E)$ and the differential proton flux $f(E)$ over all energies. $\sigma(E)$ can be derived directly from the test data, or the 2-parameter Bendel fit can be used.

Solar cell degradation

The EQFRUX-Si or EQFRUX-Ga models shall be used for silicon and gallium arsenide solar cell degradation calculations respectively [19]. In the absence of other test data, it shall be assumed that 10MeV protons cause equivalent damage to 3000 1 MeV electrons in silicon cells. Similarly it shall be assumed for gallium arsenide cells that the damage equivalence of a 10MeV proton is 400, 1000 and 1400 1 MeV electrons for short-circuit current, maximum power and open-circuit voltage degradation respectively. Since the default in these models is the assumption of infinite rear-side shielding of cells, this shall be the standard way of reporting results. However, account shall then be explicitly taken of radiation penetration though the rear-side of solar arrays. Figures 10 and 11 shows the predicted equivalent 1MeV electron fluence for the Solar Orbiter mission for Si and GaAs solar cells respectively.

Internal electrostatic charging

Internal electrostatic charging (or deep-dielectric charging) results from the build-up over a longer period of electrostatic charge. The charge build-up depends on the severity of the environment and the dielectric resistivity of the susceptible part (or lack of grounding of floating metalisation). The actual discharge may also depend on properties such as geometry and material condition. Charge build-up can therefore be mitigated by choice of material and grounding, but also by employing shielding to reduce the severity of the environment.

Tools are available to address these issues, such as DICTAT, which has been incorporated in the Space Environment Information System http://www.spenvis.oma.be/. More complex tools are also available like ESADDC [20], which employs a Monte-Carlo radiation transport method to compute the charge build-up in a dielectric material in a certain environment.

Non-ionizing dose

Damage to CCDs and other electro-optical components susceptible to displacement damage shall employ the NIEL function (non-ionising energy loss), N(E) [21], to derive a 10MeV equivalent proton damage fluence F_D:

$$F_D = \sum_E f(E). N_{10}(E) . \Delta E$$

or a non-ionizing dose, D_N:

$$D_N = \sum_E f(E). N(E) . \Delta E$$

where: $f(E)$ is the differential fluence spectrum

$N(E)$ is the NIEL function

$N_{10}(E)$ is the NIEL function normalised to 10MeV

ΔE is the energy step of the sum.

Figure 12 shows the NIEL function for protons and Silicon as target material.

Figure 13 and 14 show the equivalent 10MeV proton fluence for the Solar Orbiter mission. To turn this into a relative degradation (e.g. Charge Transfer Efficiency loss in a CCD) it is necessary to test the specific detector in question to find its response to such an environment.

The NIEL is strongly dependent on the particle type and to a lesser extent on the target material. Heavier ions causes far more damage per nucleon for the same particle energy than lighter ones. More detailed information on the contribution of the different ions can be found in appendix C.

4.5 Links with radiation testing

The table below recalls the parameter used for quantification of various radiation effects, and for illustration purposes, lists the types of testing which must be done to verify compatibility with the effects. See ECSS-E-20 for further details.

Table 3: Links with radiation testing

Radiation effect	Parameter	Test means
Electronic component degradation	Total ionising dose	Radioactive sources (e.g ^{60}Co), particle beams (e$^-$,p$^+$)
Material degradation	Total ionising dose	Radioactive sources (e.g ^{60}Co), particle beams (e$^-$,p$^+$)
Material degradation (bulk damage)	Non-ionising dose (NIEL)	Proton beams
CCD and sensor degradation	Non-ionising dose (NIEL)	Proton beams
Solar cell degradation	Non-ionising dose (NIEL) & *equivalent fluence.*	Proton beams (~ low energy)
Single-event upset, Latch-up,etc.	LET spectra (ions), proton energy spectra, explicit SEU/L rate.	Heavy ion particle beams Proton particle beams ⇦
Sensor interference (background signals)	Flux above energy threshold, flux threshold, explicit background rate.	Radioactive sources, particle beams ⇦
Internal electrostatic Charging	Electron flux and fluence dielectric E-field.	Electron beams ⇦ Discharge characterisation

⇦ = test data feed back to calculation

e, p = electron, protons

4.6 Sources of models

Most models mentioned are also installed in the Space Environment Information System (Spenvis). Further information on Spenvis and analysis of space radiation environments and effects can be found on various WWW sites:

ESTEC Space Systems Environment Analysis Site	http://www.esa.int/TEC/Space_Environment/index.html
ESA/BIRA Space Environment Information System	http://www.spenvis.oma.be/spenvis/
NASA Space Environment and Effects Site	http://see.msfc.nasa.gov/

4.7 Figures
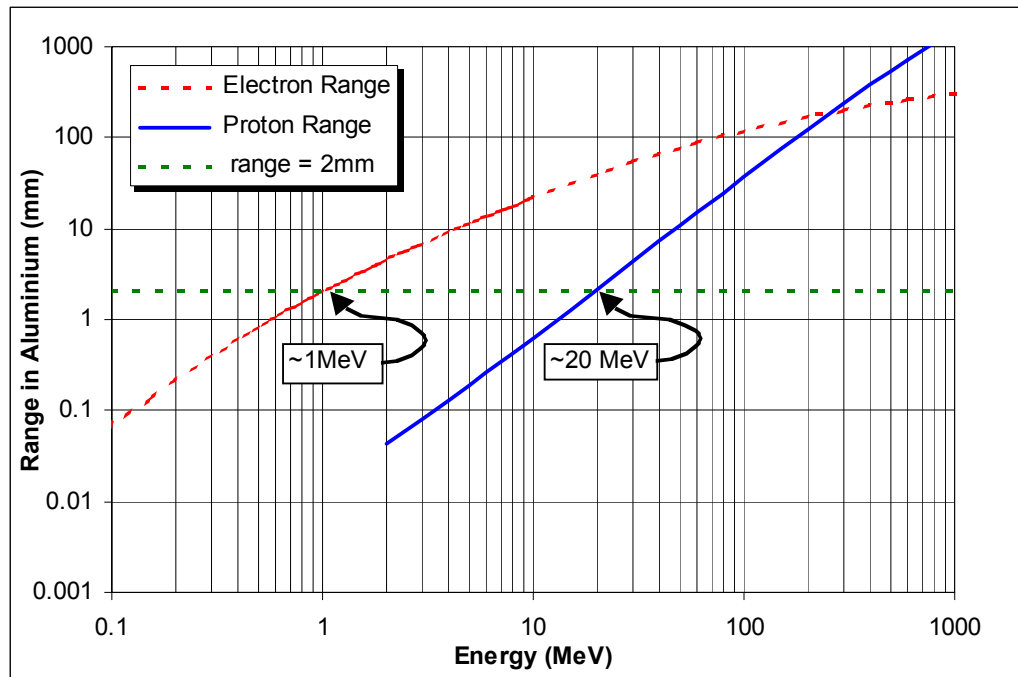
Figure 1: Mean ranges of protons and electrons in aluminium.
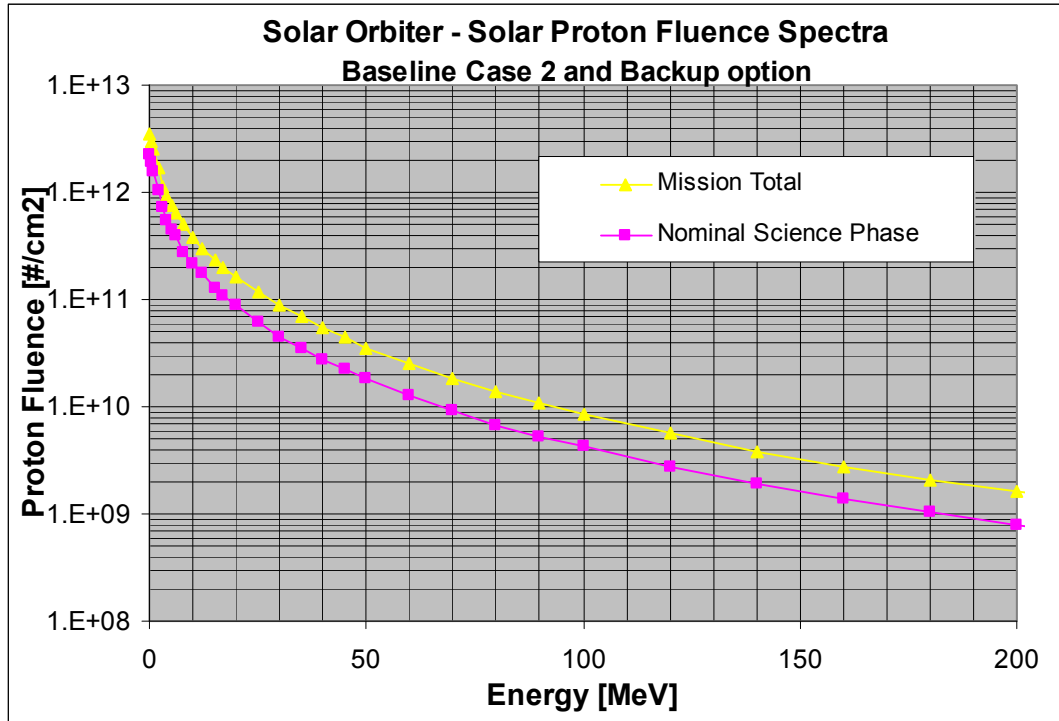
Figure 2. Solar Proton Spectrum for the mission.

Proton Energy [MeV]	Solar Orbiter - Integrated Solar Proton Fluence [#/cm2]					
	Baseline Case2 and Backup		Baseline Case 3		Baseline Case 4	
	Mission Total	Nominal Science Phase	Mission Total	Nominal Science Phase	Mission Total	Nominal Science Phase
1.00E-01	3.56E+12	2.24E+12	3.39E+12	2.03E+12	3.77E+12	2.40E+12
5.00E-01	3.01E+12	1.88E+12	2.87E+12	1.73E+12	3.19E+12	2.05E+12
1.00E+00	2.52E+12	1.56E+12	2.40E+12	1.42E+12	2.67E+12	1.70E+12
2.00E+00	1.70E+12	1.04E+12	1.62E+12	9.59E+11	1.80E+12	1.12E+12
3.00E+00	1.15E+12	7.13E+11	1.10E+12	6.30E+11	1.22E+12	7.68E+11
4.00E+00	9.32E+11	5.51E+11	8.87E+11	5.21E+11	9.86E+11	6.08E+11
5.00E+00	7.40E+11	4.54E+11	7.05E+11	4.11E+11	7.83E+11	4.80E+11
6.00E+00	6.30E+11	3.89E+11	6.00E+11	3.56E+11	6.67E+11	4.16E+11
8.00E+00	4.93E+11	2.79E+11	4.70E+11	2.58E+11	5.22E+11	3.07E+11
1.00E+01	3.84E+11	2.14E+11	3.65E+11	1.97E+11	4.06E+11	2.37E+11
1.20E+01	3.01E+11	1.75E+11	2.87E+11	1.62E+11	3.19E+11	1.95E+11
1.50E+01	2.36E+11	1.30E+11	2.24E+11	1.18E+11	2.49E+11	1.44E+11
1.70E+01	2.03E+11	1.10E+11	1.93E+11	1.01E+11	2.15E+11	1.22E+11
2.00E+01	1.62E+11	8.75E+10	1.54E+11	7.95E+10	1.71E+11	9.60E+10
2.50E+01	1.18E+11	6.16E+10	1.12E+11	5.75E+10	1.25E+11	6.72E+10
3.00E+01	8.77E+10	4.54E+10	8.35E+10	4.38E+10	9.28E+10	5.12E+10
3.50E+01	6.85E+10	3.56E+10	6.53E+10	3.29E+10	7.25E+10	3.84E+10
4.00E+01	5.48E+10	2.75E+10	5.22E+10	2.58E+10	5.80E+10	3.10E+10
4.50E+01	4.38E+10	2.24E+10	4.18E+10	2.08E+10	4.64E+10	2.50E+10
5.00E+01	3.56E+10	1.81E+10	3.39E+10	1.70E+10	3.77E+10	2.05E+10
6.00E+01	2.55E+10	1.26E+10	2.43E+10	1.18E+10	2.70E+10	1.44E+10
7.00E+01	1.86E+10	9.07E+09	1.77E+10	8.49E+09	1.97E+10	1.02E+10
8.00E+01	1.40E+10	6.80E+09	1.33E+10	6.30E+09	1.48E+10	7.68E+09
9.00E+01	1.07E+10	5.18E+09	1.02E+10	4.93E+09	1.13E+10	6.08E+09
1.00E+02	8.49E+09	4.21E+09	8.09E+09	3.84E+09	8.99E+09	4.80E+09
1.20E+02	5.75E+09	2.75E+09	5.48E+09	2.58E+09	6.09E+09	3.10E+09
1.40E+02	3.84E+09	1.91E+09	3.65E+09	1.78E+09	4.06E+09	2.18E+09
1.60E+02	2.74E+09	1.39E+09	2.61E+09	1.29E+09	2.90E+09	1.57E+09
1.80E+02	2.11E+09	1.04E+09	2.01E+09	9.59E+08	2.23E+09	1.15E+09
2.00E+02	1.62E+09	7.78E+08	1.54E+09	7.40E+08	1.71E+09	8.96E+08
2.20E+02	1.26E+09	6.16E+08	1.20E+09	5.75E+08	1.33E+09	7.04E+08
2.40E+02	1.01E+09	4.86E+08	9.66E+08	4.66E+08	1.07E+09	5.44E+08
2.60E+02	8.22E+08	3.89E+08	7.83E+08	3.84E+08	8.70E+08	4.48E+08
2.80E+02	6.58E+08	3.24E+08	6.26E+08	3.01E+08	6.96E+08	3.52E+08
3.00E+02	5.48E+08	2.66E+08	5.22E+08	2.49E+08	5.80E+08	3.01E+08
3.20E+02	4.66E+08	2.20E+08	4.44E+08	2.06E+08	4.93E+08	2.50E+08
3.40E+02	3.84E+08	1.81E+08	3.65E+08	1.70E+08	4.06E+08	2.05E+08
3.60E+02	3.01E+08	1.49E+08	2.87E+08	1.40E+08	3.19E+08	1.70E+08
3.80E+02	2.55E+08	1.23E+08	2.43E+08	1.15E+08	2.70E+08	1.41E+08
4.00E+02	2.08E+08	1.00E+08	1.98E+08	9.59E+07	2.20E+08	1.15E+08
4.20E+02	1.73E+08	8.42E+07	1.64E+08	7.95E+07	1.83E+08	9.60E+07
4.40E+02	1.42E+08	6.80E+07	1.36E+08	6.58E+07	1.51E+08	8.00E+07
4.60E+02	1.18E+08	5.83E+07	1.12E+08	5.48E+07	1.25E+08	6.40E+07
4.80E+02	9.59E+07	4.86E+07	9.14E+07	4.38E+07	1.02E+08	5.44E+07
5.00E+02	7.95E+07	3.89E+07	7.57E+07	3.56E+07	8.41E+07	4.48E+07

Figure 3. Solar Proton Spectrum for the mission.
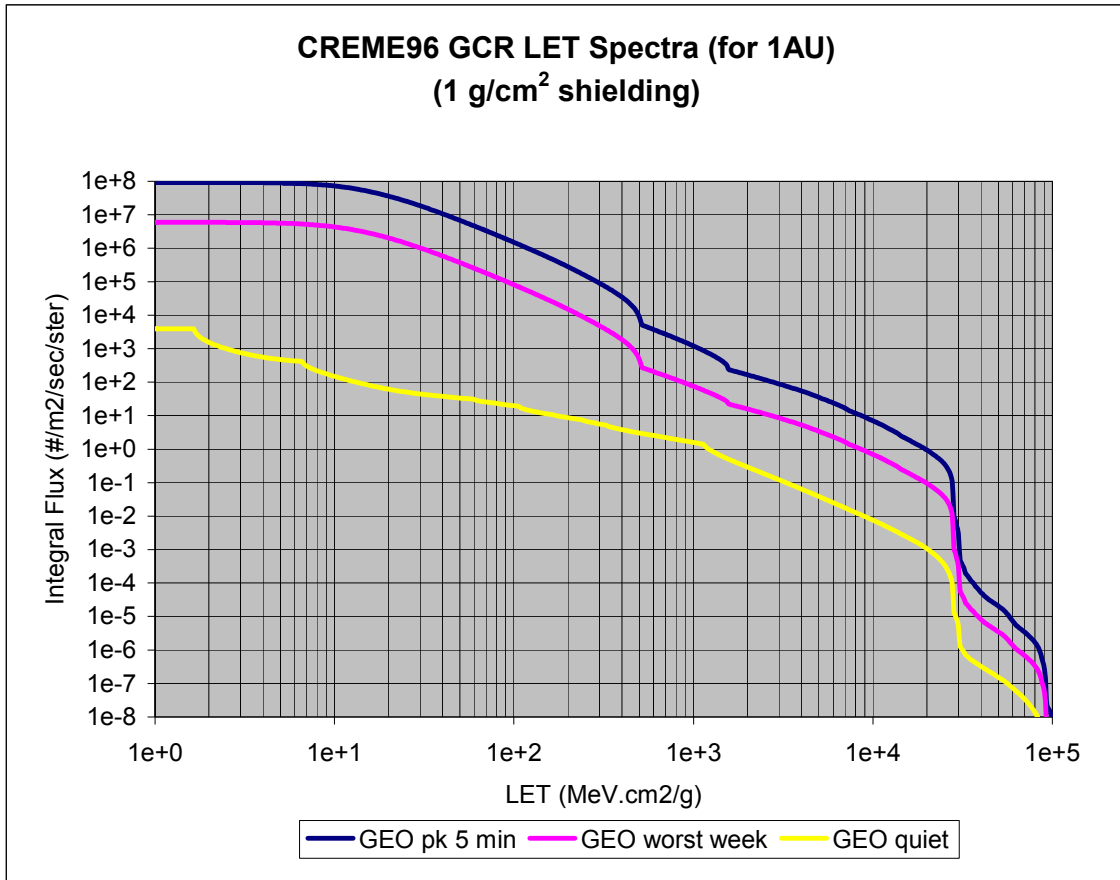
Figure 4. CREME96 Galactic Cosmic Ray LET Spectra for the three levels of activity, nominal (GEO quiet), worst week/worst case, and peak 5 minute for a component shielded by 1 g/cm². The predictions are for 1AU.

LET [MeV cm2/g]	Integral GCR Flux [#/m2/sec/sr]		
	Quiet	Worst Week	Peak 5 Min
1.00E+00	3.90E+03	5.94E+06	9.24E+07
1.52E+00	3.90E+03	5.94E+06	9.24E+07
2.31E+00	1.14E+03	5.93E+06	9.23E+07
3.52E+00	6.35E+02	5.85E+06	9.17E+07
5.36E+00	4.58E+02	5.58E+06	8.89E+07
8.15E+00	2.16E+02	4.89E+06	8.04E+07
1.24E+01	1.10E+02	3.68E+06	6.29E+07
1.89E+01	6.62E+01	2.26E+06	3.99E+07
2.87E+01	4.61E+01	1.15E+06	2.07E+07
4.36E+01	3.62E+01	5.12E+05	9.34E+06
6.64E+01	2.70E+01	2.12E+05	3.90E+06
1.01E+02	2.00E+01	8.37E+04	1.55E+06
1.54E+02	1.15E+01	3.14E+04	5.83E+05
2.34E+02	7.84E+00	1.07E+04	1.99E+05
3.56E+02	4.60E+00	3.14E+03	5.83E+04
5.41E+02	2.89E+00	2.68E+02	4.96E+03
8.23E+02	1.96E+00	1.20E+02	2.04E+03
1.25E+03	1.01E+00	5.01E+01	7.44E+02
1.91E+03	3.52E-01	1.79E+01	1.89E+02
2.90E+03	1.42E-01	9.62E+00	9.95E+01
4.41E+03	5.66E-02	4.74E+00	4.93E+01
6.71E+03	2.15E-02	2.00E+00	2.07E+01
1.02E+04	8.07E-03	7.40E-01	7.47E+00
1.55E+04	2.68E-03	2.31E-01	2.28E+00
2.36E+04	6.59E-04	6.21E-02	6.11E-01
3.59E+04	6.03E-07	2.05E-05	1.53E-04
5.47E+04	1.36E-07	3.09E-06	1.79E-05
8.32E+04	1.57E-08	3.74E-07	1.87E-06
1.03E+05	2.18E-10	2.95E-09	1.44E-08

Figure 4 (continued). CREME96 Galactic Cosmic Ray LET Spectra for the three levels of activity, nominal (quiet), worst week, and peak 5 minute (worst case) for a component shielded by 1 g/cm². The predictions are for 1AU.
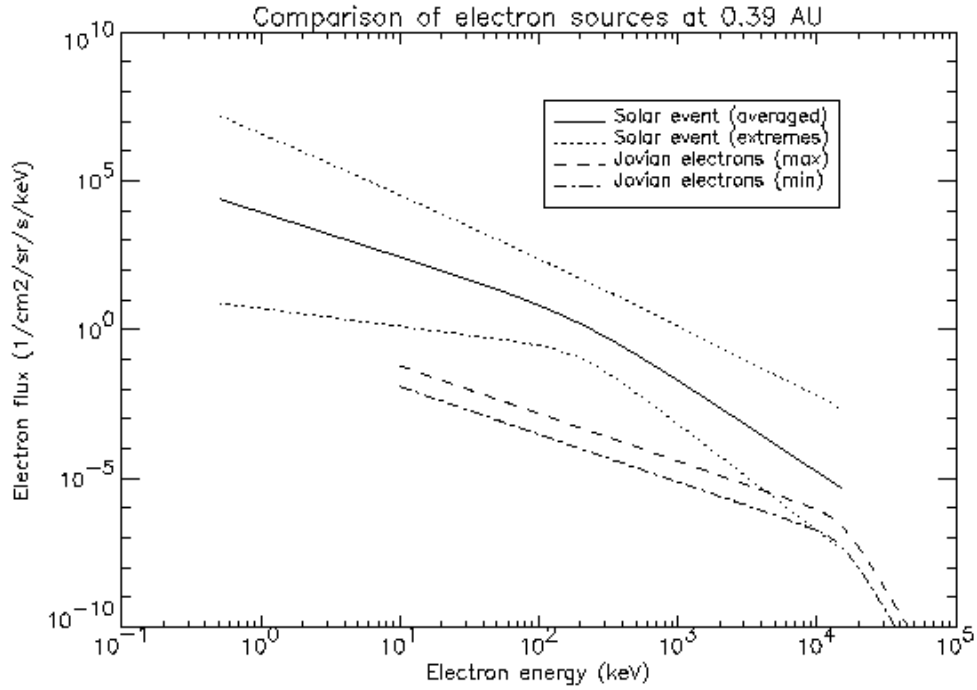
Figure 5: Predicted electron flux at 0.39AU (Mercury's distance from the sun) - given the uncertainty this gives an indication of the levels also for Solar Orbiter
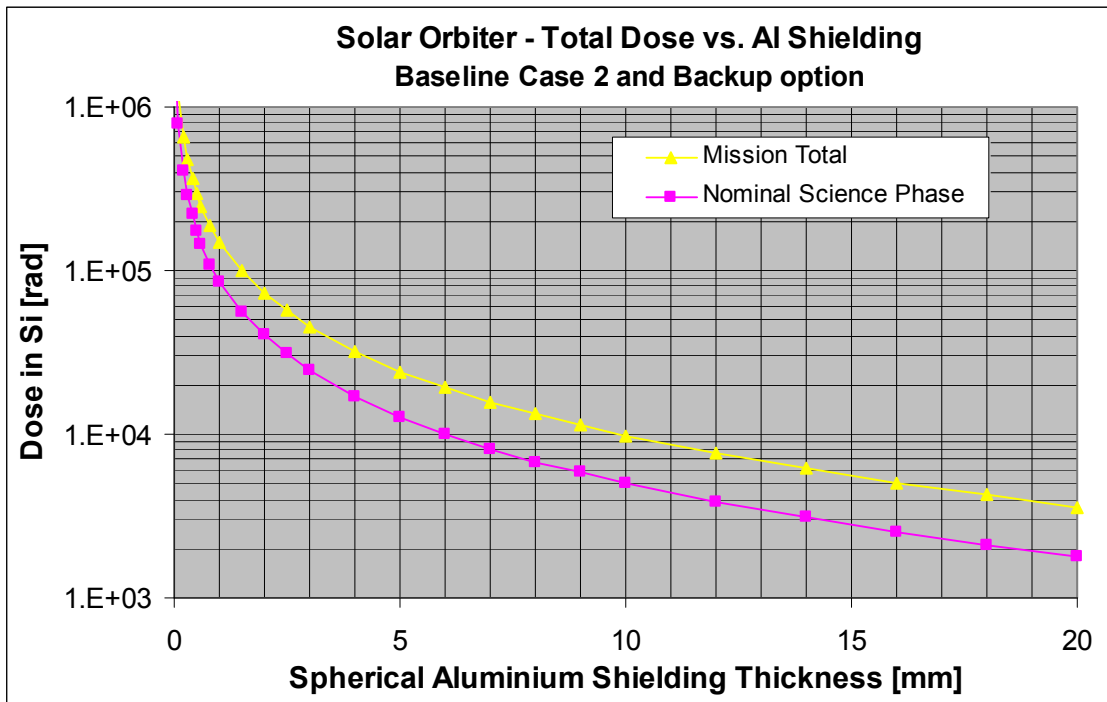
Figure 6. Mission dose in Silicon for spherical aluminium shielding.

Aluminium shielding thickness [mm]	Total ionising radiation dose in Si [rad]					
	Baseline Case2 and Backup		Baseline Case 3		Baseline Case 4	
	Mission Total	Nominal Science Phase	Mission Total	Nominal Science Phase	Mission Total	Nominal Science Phase
5.00E-02	2.48E+06	1.55E+06	2.36E+06	1.41E+06	2.62E+06	1.68E+06
1.00E-01	1.25E+06	7.84E+05	1.19E+06	7.15E+05	1.32E+06	8.54E+05
2.00E-01	6.60E+05	4.11E+05	6.29E+05	3.75E+05	6.99E+05	4.48E+05
3.00E-01	4.71E+05	2.89E+05	4.49E+05	2.64E+05	4.99E+05	3.16E+05
4.00E-01	3.67E+05	2.21E+05	3.50E+05	2.02E+05	3.89E+05	2.42E+05
5.00E-01	2.96E+05	1.77E+05	2.82E+05	1.62E+05	3.13E+05	1.94E+05
6.00E-01	2.47E+05	1.46E+05	2.35E+05	1.34E+05	2.61E+05	1.61E+05
8.00E-01	1.86E+05	1.08E+05	1.77E+05	9.97E+04	1.97E+05	1.19E+05
1.00E+00	1.50E+05	8.62E+04	1.43E+05	7.95E+04	1.59E+05	9.50E+04
1.50E+00	1.00E+05	5.61E+04	9.53E+04	5.18E+04	1.06E+05	6.21E+04
2.00E+00	7.34E+04	4.05E+04	6.99E+04	3.75E+04	7.77E+04	4.51E+04
2.50E+00	5.73E+04	3.11E+04	5.45E+04	2.88E+04	6.06E+04	3.46E+04
3.00E+00	4.58E+04	2.47E+04	4.36E+04	2.29E+04	4.84E+04	2.76E+04
4.00E+00	3.23E+04	1.71E+04	3.08E+04	1.59E+04	3.42E+04	1.91E+04
5.00E+00	2.42E+04	1.27E+04	2.31E+04	1.18E+04	2.57E+04	1.42E+04
6.00E+00	1.94E+04	1.01E+04	1.85E+04	9.40E+03	2.06E+04	1.13E+04
7.00E+00	1.58E+04	8.16E+03	1.51E+04	7.62E+03	1.68E+04	9.18E+03
8.00E+00	1.33E+04	6.80E+03	1.26E+04	6.36E+03	1.40E+04	7.65E+03
9.00E+00	1.14E+04	5.83E+03	1.09E+04	5.45E+03	1.21E+04	6.56E+03
1.00E+01	9.86E+03	5.02E+03	9.40E+03	4.69E+03	1.04E+04	5.63E+03
1.20E+01	7.73E+03	3.89E+03	7.36E+03	3.64E+03	8.18E+03	4.38E+03
1.40E+01	6.14E+03	3.09E+03	5.85E+03	2.88E+03	6.50E+03	3.49E+03
1.60E+01	5.04E+03	2.53E+03	4.80E+03	2.36E+03	5.34E+03	2.85E+03
1.80E+01	4.27E+03	2.13E+03	4.07E+03	1.99E+03	4.52E+03	2.40E+03
2.00E+01	3.59E+03	1.79E+03	3.42E+03	1.67E+03	3.80E+03	2.02E+03

Figure 7. Mission dose in Silicon for spherical aluminium shielding.
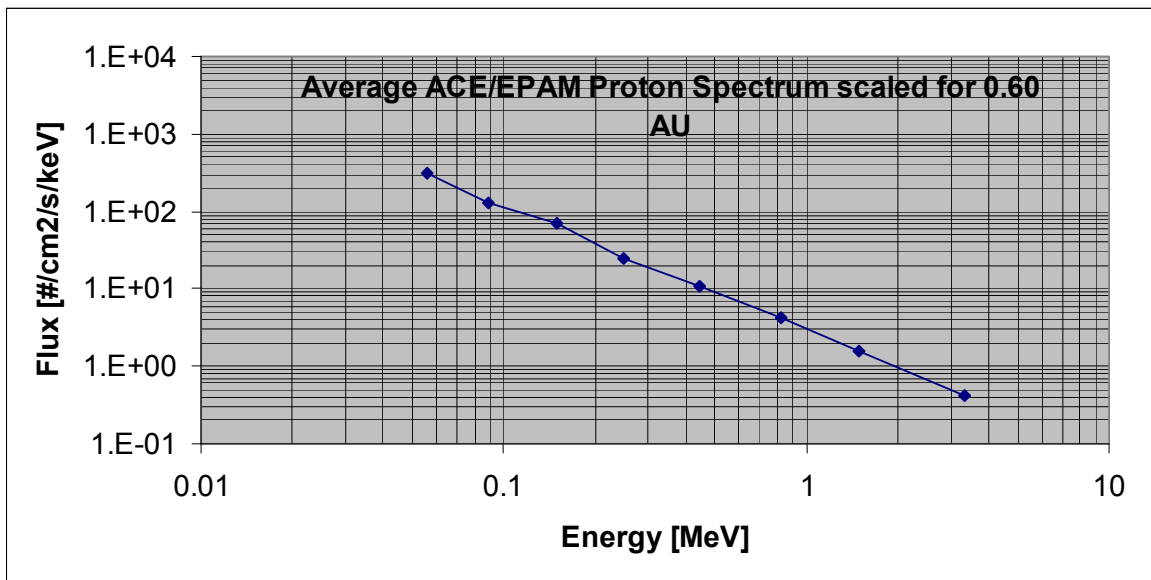
Figure 8: Average ACE/EPAM Proton Spectrum scaled for the Solar Orbiters average distance (0.60AU calculated as $1/\sqrt{(\text{Average}(r^{-2}))}$)
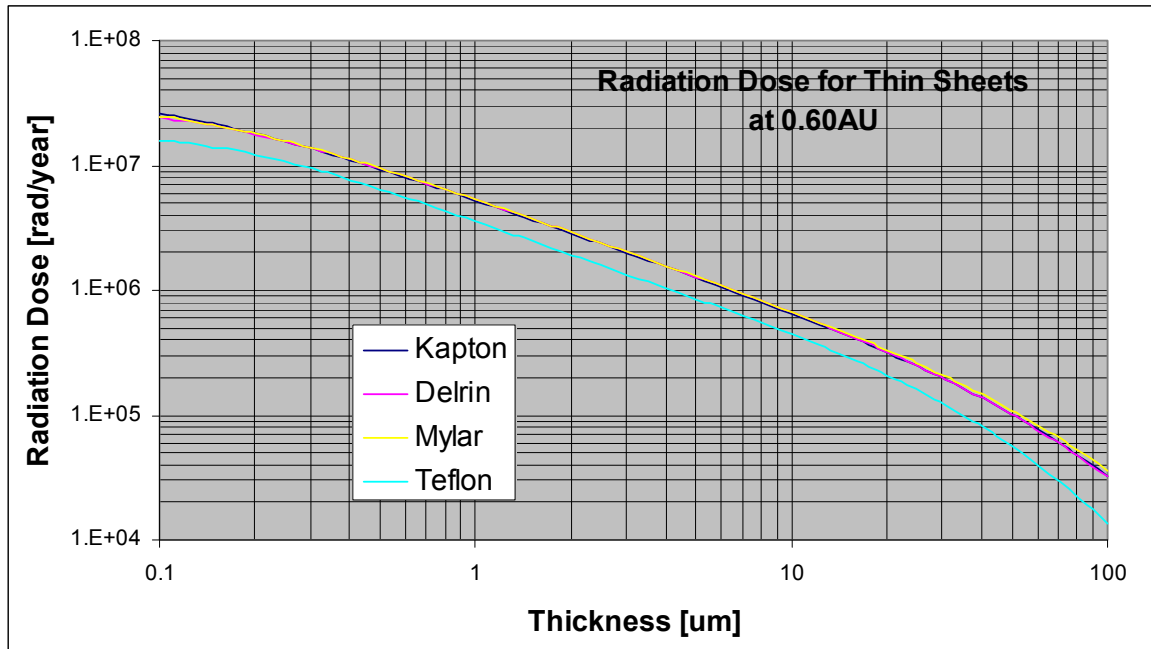
Figure 9: Radiation Dose for thin Sheets of certain Materials at the Solar Orbiters average distance (0.60AU calculated as $1/\sqrt{(Average(r^{-2}))}$)
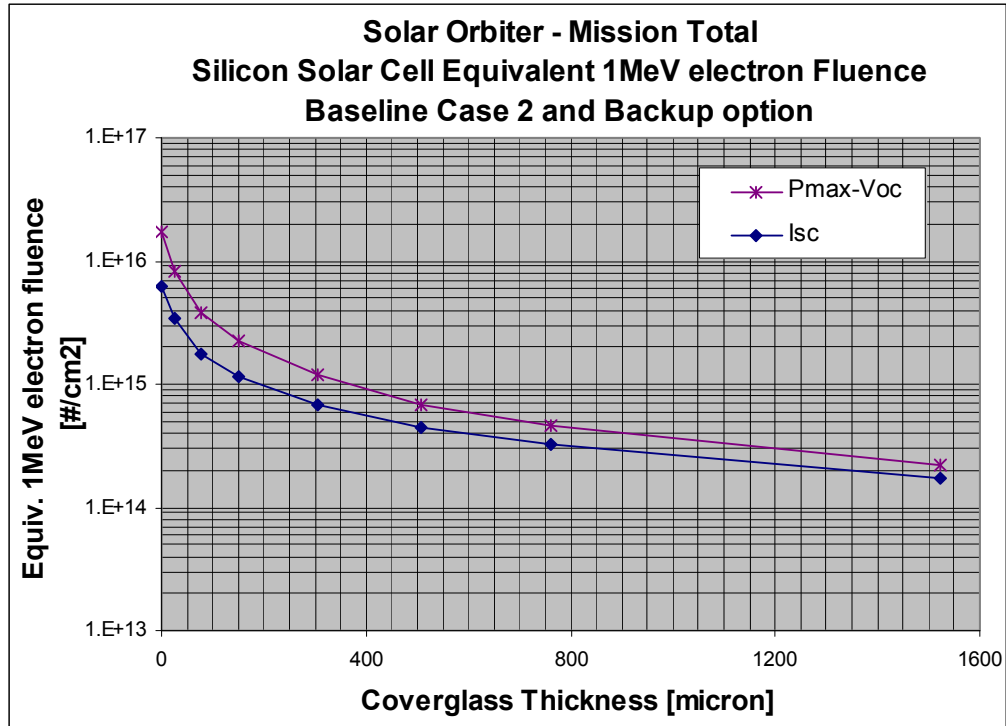
Silicon solar cells equivalent 1MeV electron fluence Mission total – Baseline case 2 and Backup		
Cover Glass Thick (Microns)	PMAX-VOC	ISC
0	1.73E+16	6.17E+15
25.41	8.19E+15	3.40E+15
76.36	3.81E+15	1.78E+15
152.27	2.21E+15	1.15E+15
305	1.19E+15	6.90E+14
509.09	6.85E+14	4.41E+14
761.36	4.63E+14	3.23E+14
1522.73	2.24E+14	1.74E+14

Figure 10. Silicon solar cells equivalent 1 MeV electron curves for the mission.
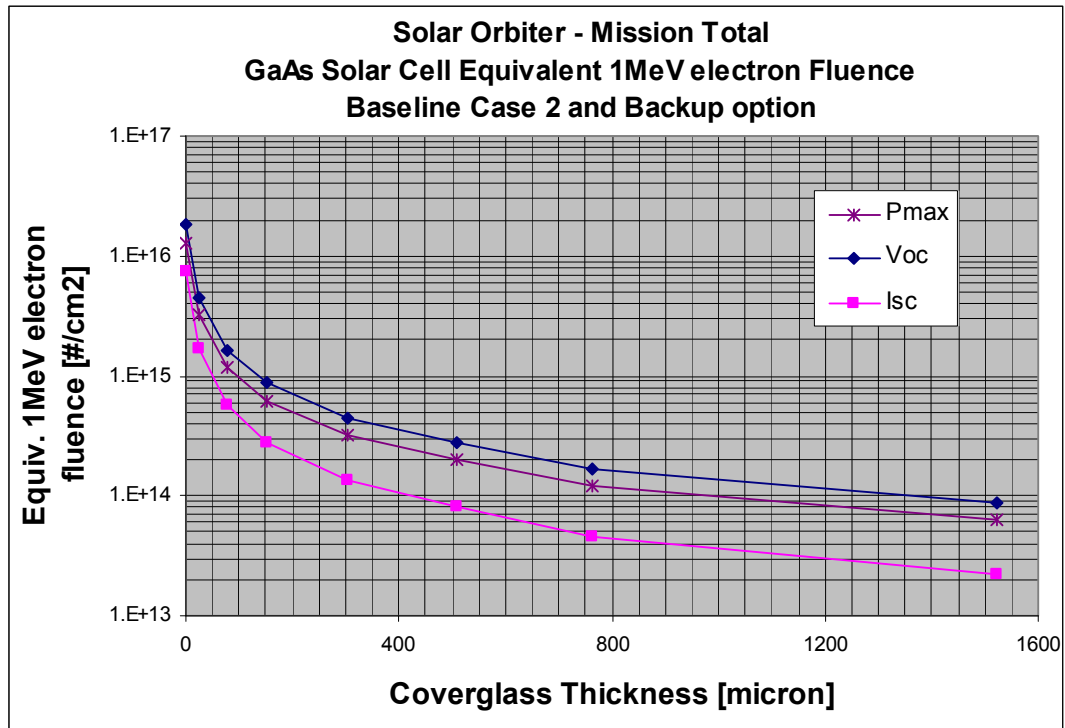
GaAs solar cells equivalent 1MeV electron fluence Mission total – 2017 Launch			
Cover Glass Thick (Microns)	PMAX	VOC	ISC
0	1.29E+16	1.81E+16	7.37E+15
25.41	3.21E+15	4.49E+15	1.67E+15
76.36	1.18E+15	1.65E+15	5.67E+14
152.27	6.19E+14	8.66E+14	2.79E+14
305	3.18E+14	4.47E+14	1.36E+14
509.09	2.01E+14	2.82E+14	8.14E+13
761.36	1.20E+14	1.69E+14	4.52E+13
1522.73	6.33E+13	8.88E+13	2.19E+13

Figure 11: GaAs solar cells equivalent 1 MeV electron curves for the mission.
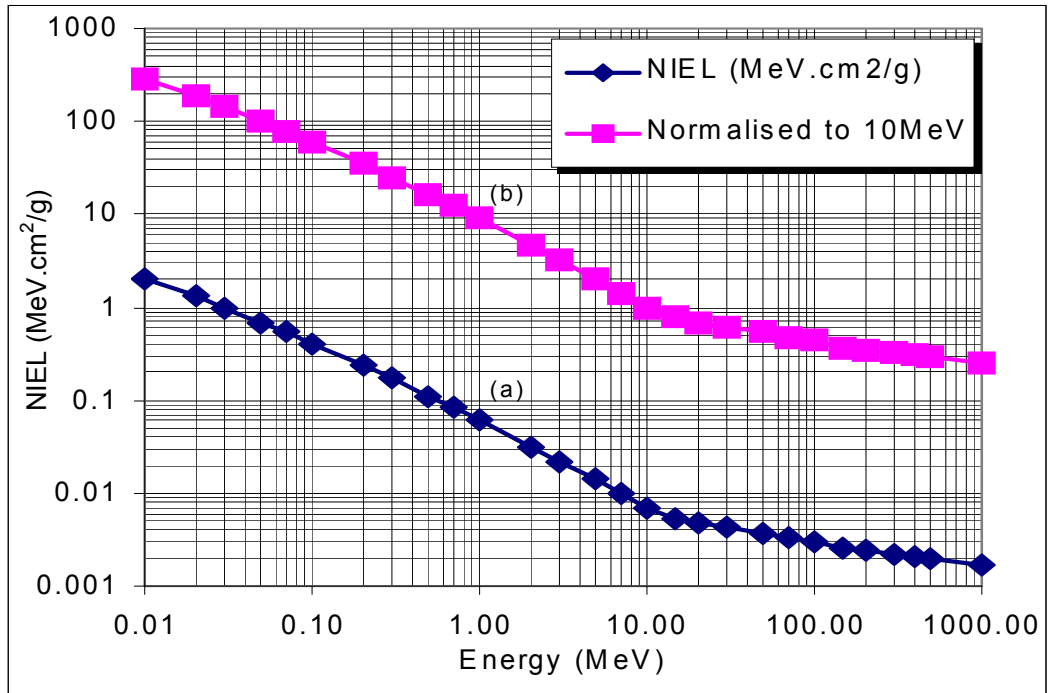
Figure 12 :NIEL curve: (a) energy lost by protons in non-ionizing interactions (bulk, displacement damage); (b) NIEL relative to 10MeV giving damage-equivalence of other energies.
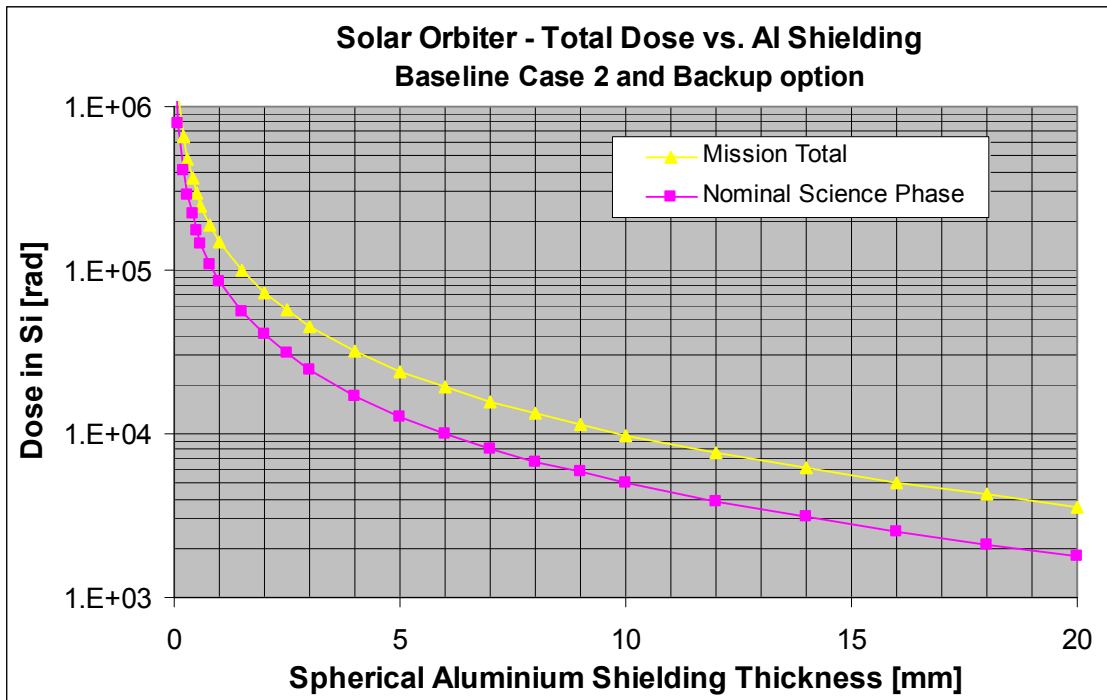
Figure 13: Non-Ionising Energy Loss equivalent 10 MeV Proton Fluence as a function of shielding thickness for the mission.

Aluminium shielding thickness [mm]	Non ionising energy loss equivalent 10MeV proton fluence [#/cm2]					
	Baseline Case2 and Backup		Baseline Case 3		Baseline Case 4	
	Mission Total	Nominal Science Phase	Mission Total	Nominal Science Phase	Mission Total	Nominal Science Phase
5.00E-02	6.82E+12	4.24E+12	6.50E+12	3.86E+12	7.22E+12	4.61E+12
1.00E-01	3.04E+12	1.92E+12	2.90E+12	1.75E+12	3.22E+12	2.09E+12
2.00E-01	1.56E+12	9.72E+11	1.49E+12	8.85E+11	1.65E+12	1.06E+12
3.00E-01	1.12E+12	6.90E+11	1.07E+12	6.30E+11	1.19E+12	7.52E+11
4.00E-01	8.77E+11	5.31E+11	8.35E+11	4.85E+11	9.28E+11	5.82E+11
5.00E-01	7.01E+11	4.18E+11	6.68E+11	3.84E+11	7.42E+11	4.61E+11
6.00E-01	5.92E+11	3.50E+11	5.64E+11	3.21E+11	6.26E+11	3.84E+11
8.00E-01	4.41E+11	2.55E+11	4.20E+11	2.35E+11	4.67E+11	2.82E+11
1.00E+00	3.59E+11	2.06E+11	3.42E+11	1.90E+11	3.80E+11	2.28E+11
1.50E+00	2.31E+11	1.29E+11	2.20E+11	1.19E+11	2.44E+11	1.43E+11
2.00E+00	1.78E+11	9.75E+10	1.69E+11	9.04E+10	1.88E+11	1.09E+11
2.50E+00	1.35E+11	7.32E+10	1.29E+11	6.80E+10	1.43E+11	8.16E+10
3.00E+00	1.13E+11	6.06E+10	1.08E+11	5.62E+10	1.19E+11	6.75E+10
4.00E+00	8.11E+10	4.28E+10	7.73E+10	3.97E+10	8.58E+10	4.77E+10
5.00E+00	6.17E+10	3.21E+10	5.87E+10	2.99E+10	6.53E+10	3.58E+10
6.00E+00	5.01E+10	2.59E+10	4.78E+10	2.42E+10	5.31E+10	2.91E+10
7.00E+00	4.19E+10	2.16E+10	3.99E+10	2.01E+10	4.44E+10	2.42E+10
8.00E+00	3.51E+10	1.79E+10	3.34E+10	1.67E+10	3.71E+10	2.01E+10
9.00E+00	3.07E+10	1.56E+10	2.92E+10	1.45E+10	3.25E+10	1.75E+10
1.00E+01	2.69E+10	1.36E+10	2.57E+10	1.27E+10	2.85E+10	1.53E+10
1.20E+01	2.11E+10	1.06E+10	2.01E+10	9.92E+09	2.23E+10	1.19E+10
1.40E+01	1.75E+10	8.78E+09	1.67E+10	8.19E+09	1.86E+10	9.89E+09
1.60E+01	1.44E+10	7.16E+09	1.37E+10	6.71E+09	1.53E+10	8.10E+09
1.80E+01	1.25E+10	6.19E+09	1.19E+10	5.78E+09	1.32E+10	6.98E+09
2.00E+01	1.05E+10	5.22E+09	1.00E+10	4.88E+09	1.12E+10	5.89E+09

Figure 14. Non-Ionising Energy Loss equivalent 10 MeV Proton Fluence as a function of shielding thickness for the mission.

4.7 References

[1] Hess W.N., "The Radiation Belt and Magnetosphere", Blaisdell Publ. Co.,1968

[2] Daly, E.J., "The Radiation Belts", Radiation Physics and Chemistry 43, 1, pp.1-18 (in Special Issue on Space Radiation Environment and Effects), 1994

[3] Vette J.I. "The AE-8 Trapped Electron Model Environment", NSSDC/WDC-A-R&S Report 91-24, NASA-GSFC (1991)

[4] Sawyer D.M. and Vette J.I., "AP8 Trapped Proton Environment For Solar Maximum and Solar Minimum", NSSDC WDC-A-R&S 76-06, NASA-GSFC (1976).

[5] ECSS-E-ST-10-04C, System Engineering, Space Environment Standard
WWW site: http://www.ecss.nl

[6]   Xapsos, M. A., G.P. Summers, J.L. Barth, E. G. Stassinopoulos and E.A. Burke, "Probability Model for Cumulative Solar Proton Event Fluences", IEEE Trans. Nucl. Sci., vol. 47, no. 3, June 2000, pp 486-490

[7]   Feynman, J., T. P. Armstrong, L. Dao-Gibner, and S. Silverman, New Interplanetary Proton Fluence Model, *J. Spacecraft and Rockets, 27*, 403, 1990.

[10]   King, J.H., "Solar Proton Fluences for 1977-1983 Space Missions", J. Spacecraft & Rockets 11, 401, (1974)

[11]   Mathews J. and Towheed S., OMNIWeb, http://nssdc.gsfc.nasa.gov/omniweb/ mathews@nssdc.gsfc.nasa.gov, Code 633, NASA GSFC, Greenbelt, MD 20771, USA

[12]   National Geophysical Data Center, "Space Environment Data from NOAA's GOES Satellites", National Geophysical Data Center, Code E/GC2, Dept. 946 325 Broadway Boulder Co 80303 3328 USA., also Space Physics Interactive Data Resource at http://www.ngdc.noaa.gov:8080/

[13]   A.J. Tylka et al. "CREME96: A Revision of the Cosmic Ray Effects on Micro-Electronics Code", IEEE Trans. Nucl. Sci. NS-44, 2150-2160 (1997).

[14]   Adams J.H., Silberberg R. and Tsao C.H., "Cosmic Ray Effects on Microelectronics, Part I: The Near-Earth Particle Environment", NRL Memorandum Report 4506, Naval Research Laboratory, Washington DC 20375-5000, USA (1981).

[15]   R.A. Nymmik, M.I. Panasyuk, T. I. Pervaja, and A.A. Suslov "A Model of Galactic Cosmic Ray Fluxes", by, Nucl. Tracks & Radiat. Meas, **20**, 427-429 (1992)

[16]   Seltzer S., 'SHIELDOSE: A Computer Code For Space Shielding Radiation Dose Calculations', NBS Technical Note 1116, National Bureau of Standards, May 1980 .

[17]   Petersen E.L., "Approaches to Proton Single-Event-Rate Calculation", IEEE Trans. Nucl. Sci. NS-43, 2 (special issue on Single Event Effects and the Space Environment), 496 (1996)

[18]   Pickel J.C., " Single-Event Effects Rate Prediction", IEEE Trans. Nucl. Sci. NS-43, 2 (special issue on Single Event Effects and the Space Environment), 483 (1996).

[19]   Tada H.Y., Carter J.R, Anspaugh B.E. & Downing R.G, " Solar Cell Radiation Handbook", 3rd Edition, JPL Publn. 82-69 (1982); Anspaugh B.E, "GaAs Solar Cell Radiation Handbook", JPL Publn. 96-9 (1996).

[20]   J. Sorensen, "An Engineering Specification of the Internal Charging", Proceeding of the Symposium on Environment Modelling for Space-based Applications, ESA-SP-392, Dec. 1996

[21]   Hopkinson G.R., Dale C.J. and Marshall P.W., "Proton Effects in Charge-Coupled Devices", IEEE Trans. Nucl. Sci. NS-43, 2 (special issue on Single Event Effects and the Space Environment), 614 (1996).

[23]   Nieminen P., "Spectral Input Code for Induced X-Ray Emission Calculations from Solar System Bodies", ESA Working Paper 2009, February 1999

[25]   Ziegler J.F., The Stopping and Range of Ions in Matter http://www.research.ibm.com/ionbeams/

[26]   "Topical Teams in the Life & Physical Sciences", R. Mueller-Mellin, P. Nieminen ESA SP-1281, pp 184-199

5

Particulates

5.1 Introduction

Every spacecraft in orbit is exposed to a certain flux of micrometeoroids. Spacecraft in Earth orbit encounter man-made space debris as well. Collisions with these particles will take place with hypervelocity speed.

Meteoroids are particles of natural origin. Nearly all meteoroids originate from asteroids or comets. The natural meteoroid flux represents, at any instant, a total of about 200 kg of mass within 2000 km of the Earth's surface [1]. Meteoroids that retain the orbit of their parent body can create periods of high flux and are called streams. Random fluxes with no apparent pattern are called sporadic.

Space debris is man-made. Space debris particles are mainly encountered in earth orbits below 2000 km altitudes and near the geostationary ring.

The damage caused by collisions with meteoroids and space debris will depend on the size, density, speed and direction of the impacting particle and on the shielding of the spacecraft. Submillimeter sized particles can cause pitting and cratering of outer surfaces and lead to degradation of optical, electrical, thermal, sealing or other properties. Larger particles can puncture outer surfaces and may cause damage to structure or equipment by penetration and spallation.

Flux models have been developed for both micrometeoroids and space debris. The resulting damage can be assessed through empirically derived design equations which give penetration capabilities, crater sizes, etc. as function of the particle parameters and target properties.

As the Solar Orbiter will spend only very limited time near Earth impacts from space debris particles can be neglected and in the following impacts from meteoroids only will be considered.

5.2 Analysis techniques

Meteoroid impacts are specified by statistical flux models. Meteoroid fluxes are usually specified as a time-averaged flux, F_r, to one side of a randomly tumbling surface. Flux is defined as number of intercepted objects per unit time and area. The relevant area for F_r is the actual outer surface area of a spacecraft element.

For spacecraft which fly with a fixed orientation, the directionality of the meteoroid fluxes should be taken into account. Most impacts from meteoroids will occur on forward facing surfaces.

The number of impacts, N, increases linearly with exposed area and with exposure time:

$$N = F \times A \times T$$

where F is the number of impacts per unit area, A is the total exposed area and T is the exposure time.

Fluence is the flux integrated over time.

Once N has been determined, the probability of exactly n impacts occurring in the corresponding time interval is given by Poisson statistics:

$$P_n = (N^n)/n! \cdot e^{-N}$$

The probability for no impacts, P_0 is thus given by:

$$P_0 = e^{-N}$$

For values of $N \ll 1$ the probability, Q, for at least one impact ($Q = 1 - P_0$) is equal to N:

$$Q = 1 - e^{-N} \approx 1 - (1 - N) = N$$

All these equations apply as well if the number of impacts, N, is replaced by the number of failures, NF, resulting from an impact.

5.3 Model presentation

The new ESA Interplanetary Meteoroid Engineering Model (ESA-IMEM) [2,3] is used to calculate the meteoroid fluences on the Solar Orbiter during the interplanetary orbit. This model uses astrophysical knowledge of the evolution of meteoroid orbits in order to interpolate actual data taken from Apollo lunar crater counts, in situ measurements by interplanetary spacecrafts, astronomical observations and radar meteor measurements. Calculated is the total average meteoroid fluence (sporadic + stream average) in terms of the integral fluence, N, which is the number of particles with mass m or larger per m² impacting a randomly-oriented flat plate under a viewing angle of 2π during the mission duration.

The model gives a yearly average. **Meteoroid streams** are included in an average sense.

5.4 Meteoroid fluences

Tables 1 give meteoroid fluences for the Solar Orbiter orbit as obtained from the model. Presented are the cumulative fluences (i.e. fluxes of particles of given size or larger integrated over the mission duration) The Tables give the number of impacts, N, /m²/mission from one side to a randomly oriented plate for a range of minimum particle sizes.

Table 1 gives the mission integrated fluences only. A more detailed analysis shows that the flux along the orbit varies by up to an order of magnitude between perihelion (where it is highest) and aphelion.

Meteoroids directionality

The results in Tables 1 are for a randomly oriented plate. The directionality caused by the relative orientation to the ecliptic and the spacecraft motion leads to a directional dependence. This directional dependence depends on the size of the meteoroids as well as on the location of the spacecraft in the solar system. At sun-distances below 1 AU the directional dependence is rather complex. Spacecraft in Earth orbit normally encounter highest meteoroid fluxes on ram pointing surfaces. For spacecraft in interplanetary space closer to the sun highest fluxes can occur on other surfaces. The flux on a specific spacecraft surface with given surface orientation and velocity vector can be calculated numerically from the ESA-IMEM model if required. For design purposes the same fluxes for all surfaces can be assumed.

Solar Orbiter Environmental Specification – Issue 3.0

Mass, m [g]	Diameter, D [cm (ρ = 2 g/cm³)]	Fluence, N Baseline Case 2 and Backup [/m² /9.5 years]	Fluence, N Baseline Case 3 [/m² /9.4 years]	Fluence, N Baseline Case 4 [/m² /10.2 years]
1.E-15	9.84E-6	4.1E+05	4.1E+05	4.4E+05
1.E-14	2.12E-5	1.1E+05	1.0E+05	1.1E+05
1.E-13	4.57E-5	3.5E+04	3.5E+04	3.8E+04
1.E-12	9.84E-5	1.4E+04	1.4E+04	1.6E+04
1.E-11	2.12E-4	6.2E+03	6.2E+03	6.7E+03
1.E-10	4.57E-4	2.6E+03	2.6E+03	2.8E+03
1.E-9	9.84E-4	1.1E+03	1.1E+03	1.2E+03
1.E-8	2.12E-3	4.4E+02	4.4E+02	4.7E+02
1.E-7	4.57E-3	1.1E+02	1.1E+02	1.2E+02
1.E-6	9.84E-3	1.3E+01	1.3E+01	1.4E+01
1.E-5	2.12E-2	3.2E-01	3.2E-01	3.5E-01
1.E-4	4.57E-2	2.3E-02	2.3E-02	2.5E-02
1.E-3	9.84E-2	1.3E-03	1.3E-03	1.4E-03
1.E-2	2.12E-1	6.8E-05	6.8E-05	7.3E-05
1.E-1	4.57E-1	3.3E-06	3.3E-06	3.5E-06
1.E+0	9.84E-1	1.6E-07	1.5E-07	1.7E-07

Table 1: Cumulative number of meteoroid impacts, N, per m² from 1 side to a randomly oriented surface for a range of minimum particle sizes as obtained by the ESA Interplanetary Meteoroid Engineering Model. The results are for the total duration of the Solar Orbiter mission. A density of ρ = 2.0 g/cm³ and spherical shape were used to convert masses to diameters.

Application guidelines

For intermediate sizes which are not explicitly given in Tables 1 an interpolation can be used.

Meteoroid density

Material densities for meteoroids range from about 0.15 – 8.0 g/cm³ . Values for average mass densities of meteoroids are:

Low: 1.0 g/cm³
Nominal: 2.0 g/cm³
High: 4.0 g/cm³

For analysis of effects the nominal value of 2.0 g/cm³ shall be used.

A spherical shape shall be assumed to convert particle masses and diameters.

Impact velocity and direction

Meteoroids impacting the Solar Orbiter will show a distribution of velocities ranging from below 10 km/s up to values larger than 100 km/s. Smaller particles have higher average impact velocities than larger particles. The average impact velocity (averaged over meteoroid type, i.e. asteroidal and cometary, as well as over mass) varies from just below 20 km/s at 1 AU to over 50 km/s at the perihelion.

For the assessment of impact effects a constant velocity of 45 km/s shall be used.

An average impact angle of 45 degrees from the surface normal shall be used.

5.5 Model uncertainties

According to [1] uncertainties in the meteoroid models near Earth mainly result from uncertainties in particle densities and masses. Near Earth fluxes for meteoroids larger than 10^{-6} g are well defined, but the associated masses are quite uncertain. The mass density of meteoroids spans a wide range, from about 0.15 g/cm^3 to values as large as 8 g/cm^3. At a set mass this implies an uncertainty in the flux of a factor 0.1 to 10. For meteoroids smaller than 10^{-6} g flux uncertainties at a given mass are estimated to be a factor of 0.33 to 3. The uncertainties in meteoroid fluences at other distances from the sun than 1 AU is larger still but can at present not be quantified.

5.6 Damage assessment

In this section a brief general overview of damage assessment criteria and procedures is given. For each individual project the damage assessment has to be tailored according to the specific conditions and requirements (e.g. shielding, damage criteria, required reliability, etc.). Any damage assessment depends to a large extent on the relevant failure criteria. Possible failure criteria include:

- cratering (sensor degradation, window blinding, surface erosion)
- larger craters (sealing problems, short circuits on solar arrays)
- impact generated plasma (interference, discharge triggering)
- wall penetration (damage, injury, loss of liquid or air)
- burst, rupture (pressurised parts)
- structural damage

For a quantitative damage and risk assessment, so-called damage or design equations for the given shielding configuration are needed. They give shielding thresholds or hole sizes for given impacting particle parameters and failure mode. One of the most widely used damage equation gives the threshold thickness for penetration of single metal plates (thin plate formula):

$$t = k_m \, m^{0.352} \, \rho^{0.167} v^{0.875}$$

where:

t: threshold thickness for penetration [cm]

k_m: material constant, 0.55 for Aluminium

m: mass of projectile [g]

ρ: density of projectile [g/cm^3]

v: normal impact velocity component of projectile [km/s]

A puncture occurs whenever the threshold thickness for an impacting particle with given mass, density and velocity exceeds the shielding thickness of the surface under consideration. Finding a realistic damage equation for a given shielding configuration can be problematic. The translation of a failure mode to a damage equation can be difficult. Many damage equations for different types of shields and for different velocity regimes have been developed. A comprehensive list of available damage equations for the most commonly used shielding types and surface materials is given in [4]. However, for most materials, compounds, and shielding concepts no specific damage equation is available. Specific impact tests for sensitive subsystems are recommended for a reliable assessment of the impact risk.

Once a damage equation for a given subsystem, shielding configuration and failure mode has been identified a simplified risk assessment proceeds as follows:

Using the damage equation, shielding thickness and impact parameters specified above (density, velocity, impact angle) the critical particle size for the failure (e.g. penetration or crater larger than given size) is calculated.

For this critical particle size the failure fluences, NF, are obtained from Table 1 after multiplication by the total surface area.

From NF the probabilities for no failure or failure are calculated according to the equations in 5.2.

In most cases such a simplified analysis with fixed impact parameters will be sufficient. A more detailed analysis which considers the full distribution of impact velocities and angles can only be performed with the help of more sophisticated numerical tools.

5.9 References

[1]   Anderson B.J., "Natural Orbital Environment Guidelines for Use in Aerospace Vehicle Development", by:, editor and R.E. Smith, compiler; NASA TM 4527, chapter 7, June 1994

[2]   V. Dikarev, R. Jehn and E. Grün, "Towards a New Model of the Interplanetary Meteoroid Environment", Advances in Space Research, Vol. 29, No. 8, pp 1171-1175, 2002.

[3]   W.J. Baggaley, V. Dikarev, E. Grün and D.P. Galligan, "Update of the interplanetary meteoroid model to predict fluxes on spacecraft",
Final Report Contract No. 13809/99/D/CS, ESA, 2002.

[4]   Inter Agency Debris Committee- Protection Manual, in preparation, 2003

6

Contamination

6.1 Introduction

This chapter deals with the induced molecular and particulate (solid or liquid) environment in the vicinity of and created by the presence of the Solar Orbiter in its orbit. It is meant mainly to aid in the definition of the contamination environment (foreign or unwanted matter that can affect or degrade the performance of any component when being in line of sight with that component or when residing onto that component). The relevant computer models and tools are also presented.

Due to the specific aspects of the mission, the contamination environment of Solar Orbiter can be expected to be particular severe. The principle spacecraft engineering concerns for the Solar Orbiter due to contamination are outlined in Table 1. Critical surfaces like radiators and reflectors as well as optics need special attention.

Table 1: Main engineering concerns for the Solar Orbiter due to contamination

Mission Aspect	Problem
High temperatures and temperature variations	Increased outgassing
High fluxes UV, e^- ,p^+	Increased degradation of materials Increased photo-deposition Increased carbonisation, discolouring, darkening

The quantitative modelling of the contamination environment is very complex. This is due to the high number of materials involved, with a variability of outgassing characteristics. Furthermore, there are interactions of the outgassing products with surfaces, residual gas and with other environmental parameters such as solar radiation.

The contamination analysis, which necessarily is very much dependent of a specific application, cannot be more detailed in this specification. ESA PSS-01-201 [1] defines amongst others the requirements to be followed and guidelines to be taken into account in order to control the particulate and molecular contamination within the specified limits during a mission.

It is the responsibility of the user:

- to estimate the sensitivity of his system/equipment with regard to contamination
- to identify the contamination sources on his experiment
- to evaluate with all appropriate means the expected contamination levels/quantities present in critical areas, taking into account the mechanisms of transport and fixation of contaminants.

6.2 Molecular contamination

6.2.1 Sources of molecular contamination

Outgassing of Organic Materials

Outgassing of organic materials can be approached as a surface evaporation combined with a diffusion for bulk contaminant species. These species can be either initially present components, or decomposition products.

Initially present outgassing species can be:

- water
- solvents
- additives
- uncured monomeric material
- lubricants
- ground contamination species, due to e.g. processes, test, storage, handling, pre-launch and launch.

Outgassing rates are usually given in mass of molecular species evolving from a material per unit time and unit surface area [g.cm^{-2}.s^{-1}] (other units are also possible, such as relative mass unit per time unit : [g .g^{-1}.s^{-1}], [% s^{-1}] or [%.s^{-1}.cm^{-2}]).

The decomposition products are due to exposure of molecular materials to other environments, such as:

- thermal
- solar radiation, electromagnetic and charged particles
- impacts by micrometeoroids or debris
- Electrical discharges and arcing

These products consist of lower molecular weight (higher volatility) species than the original species.

Plumes

Plume species can result from combustion, unburned propellant vapours, incomplete combustion products, sputtered material and other degradation products from a propulsion or attitude control system and its surroundings swept along with the jet.

Plumes can also be produced by dumps of gaseous and liquid waste materials of the environment control and life support systems in manned spacecraft or by leaks in systems or internal payloads. Overboard disposal of materials will cause increased molecular column densities and may cause molecular deposition. Plumes can consist of gaseous (molecular) species, liquid droplets and solid particles.

Contamination of surfaces not in direct view is possible due to ambient scattering (collisions with other residual atmosphere species), self scattering (collisions with other identical or different contaminant species) or ionisation of the molecules under radiation, e.g. UV or particles, and subsequent attraction to a charged surface

Pyrotechnics and release mechanisms

During operation of pyrotechnics or other release mechanisms gases can evolve.

Secondary sources

A surface can act as a secondary source if an incoming contaminant molecule will reflect (not accommodate stick or condense on the surface) or if it has a limited residence time on that surface. Secondary sources can for example be solar panels having a higher temperature than the surrounding surfaces.

6.2.2 Transport mechanisms

Apart from the direct flux there are different transport mechanisms by which a contaminant molecule can reach a surface. Surface accommodation occurs when a molecule becomes attached to a surface long enough to come into a thermal equilibrium with that surface (an accommodation coefficient can be defined as a measure for the amount of energy transfer between the contaminant molecule and the surface). It is useful to define the concept of a sticking coefficient as the probability that a molecule, colliding with a surface, will stay onto that surface for a time long compared to the phenomena under investigation. The sticking coefficient is a function of such parameters as contamination/surface material pairing, temperature, photo-polymerisation, reactive interaction with atomic oxygen.

Reflection on surface

A molecule will reflect on a surface when the accommodation coefficient during a collision is zero, i.e. when there is no energy transfer between the molecule and the surface during that collision. A reflection of a molecule is always specular, although this will be dependent on surface roughness, RMS)

Re-evaporation from surface

A molecule having a non-zero residence time can re-evaporate from a surface. Re-evaporation is diffuse, i.e. the molecule is leaving the surface following a Lambertian distribution law.

Migration on surface

A molecule accommodated on a surface can migrate over that surface.

Collision with residual (natural) atmosphere

The contamination environment shall take into account the collision between the contamination species and the residual atmosphere. This interaction results in an ambient scattering of the contamination species, and can sometimes lead to an increase in the local pressure.

Collision with other outgassed molecules

The contamination environment shall take into account the collision between two contamination molecules. This interaction results in self-scattering of the contamination species.

Ionisation by other environmental parameters

A molecule can be ionised due to interaction with (V)UV or charged particles (electrons, protons, ions) and subsequently be attracted by a charged surface

Permanent Molecular Deposition (PMD)

Molecular matter can permanently stick onto a surface (non-volatile under the given circumstances) as a result of reaction with surface material, UV-irradiation or residual atmosphere induced reactions (e.g. polymerisation, formation of inorganic oxides).

6.3 Particulate contamination

6.3.1 Sources of particulate contamination

Sources inherent to materials

- Particles originating from manufacturing (machining, sawing), handling (e.g. for brittle materials such as certain paints) or wear (friction)
- Degradation of binder under different environments (e.g. UV) resulting in loose filler
- Crack formation and subsequent flaking as a result of thermal cycling

Sources external to materials

- Dust particles can be caused by atmospheric fall-out (dust) during assembly, integration and storage or by human sources during such activities (hair, skin flakes, lints or fibres from garments...)
- Particles can be produced during spacecraft propulsion or attitude control operations, the functioning of moving parts (such as shutters).
- Particles can result from micrometeoroid or debris impacts on materials

6.3.2 Transport mechanisms

(Acoustic) vibrations

Vibrations due to launch, (attitude control) manoeuvring, docking, Pyrotechnic shocks can cause particles to migrate from one surface to another.

Electrostatic attraction

Particles can be charged due to their interaction with ambient plasma, or photo emission and subsequently attracted by electrically-charged surfaces.

Other mechanisms

For specific missions other mechanism can play a non negligible role, such as:

- Radiation pressure due to solar radiation

6.4 Effect of contamination

The primary concerns of contamination are related to the degradation of spacecraft elements or sub-system performances due to the presence of :

- deposited species onto a critical surface:
  - (thermo-)optical properties, such as transmission, reflection, absorption, scattering,
  - tribological properties, outgassing of lubricant, friction due to particles
  - electrical properties, such as surface conductivity, secondary emission and photo-emission.
- glow or other surface/gas reactions
- free flying species in the field of view of sensors:
  - light scattering (star trackers)
  - light absorption
  - background increase (natural environment analysis)

The effect of a contamination can be altered by the exposure to other environmental parameters, e.g. UV can increase the absorption due to photo-degradation (darkening) of the deposited contaminant.

6.5 Models

Worst case outgassing modelling are usually based on screening thermal vacuum test (VCM-test) to determine the outgassing properties of materials. The test is described in ECSS-Q-70-02 and ASTM-E595-90 [2] [3]. The test results are:

- **TML** -- Total Mass Loss (sum of condensable and non-condensable material), measured ex-situ as a difference of mass before and after exposure to a vacuum under the conditions specified in the outgassing test.
- **RML** -- Recovered Mass Loss (difference between the initial mass and the mass after re-climatisation after the vacuum test, showing the amount on non-water products in the total mass loss).
- **CVCM** -- Collected Volatile Condensable Material (Low Vapour Pressure, condensable material), measured ex-situ on a collector plate after exposure (to a vacuum) under the conditions specified in the outgassing test.

TML, RML and CVCM are normally expressed in % of the initial mass of the material.

More sophisticated outgassing/condensation models will take into account the data of outgassing or mass flow rates, surface accommodation and sticking coefficients as obtained by e.g. the VBQC-test [4] or the ASTM E-1559 test [5].

For the Solar Orbiter, the outgassing testing and modelling must take into account the special aspects of the mission. In particular the 125°C of the nominal VCM-test is probably too low to be representative for the real environment that will be seen by some parts of the spacecraft (there is no real knowledge on the acceleration of the phenomena at the expected very high temperatures).

6.5.1 Outgassing sources

For a material that outgassses at a constant rate, independently of the quantity present, such as e.g. during evaporation or sublimation from a bulk, the process can be described as a zero order reaction.

$$dm/dt = k$$

with:

dm/dt outgassing rate in $g \cdot cm^{-2} \cdot s^{-1}$

k   reaction constant

The weight-loss through evaporation, at a temperature T is given by [6]

$dm/dt = 0.04375 \cdot P_s \cdot (M/T)^{1/2}$

with:

P_s Vapour Pressure in mbar

dm/dt weight-loss per unit area in $g \cdot cm^{-2} \cdot s^{-1}$

M   Molecular mass

T   Temperature in K

The outgassing is often described as a first order reaction [7], i.e. the material outgasses at a rate that is proportional to the mass available, and using Arrhenius law for the temperature dependency. Important parameters for the outgassing rate are temperature, exposed surface area (or the surface available for evaporation), surface morphology, dimensions of the material (characteristic dimension, thickness).

$dm/dt = -m/\tau$

with τ being a temperature dependent time constant of the outgassing phenomenon. Integration gives:

$m = m_0 \cdot \exp(-t/\tau)$

Assuming the Arrhenius relation to be valid

$\tau = \tau_0 \exp(-E/RT)$

it is possible to determine the outgassing as function of temperature.

The mass loss can be expressed as

$m_{loss} = m_0 \cdot m = m_0 \cdot (1 - \exp(-t/\tau))$

Plumes

Evaluation of plumes of thrusters or vents is often described by specific application related models. Parametric descriptions of plumes constitute an interesting alternative to spacecraft designers.

The mass flux Φ of a plume can be expressed in the most generic form

$\Phi(r, \Theta) = f(r, \Theta, dm/dt)$

with

$\Phi(r, \Theta)$ flux at a given position from the vent

r   radial distance from the vent

Θ angle from the centerline of the vent

dm/dt Mass flow from the vent

where moreover the function f will depend on the plume type. However this formula can in general be reduced in a good approximation to the product

$\Phi(r, \Theta) = A \cdot (dm/dt) \cdot f_1(\Theta) \cdot r^{-2}$

where A is a normalisation coefficient.

For a thruster, the function f_1 is peaked around $\Theta=0$ and can be expressed as a sum of decreasing exponentials [8] or as a (high) power law of $\cos(\Theta)$ or both [9]. It is in some extent specific of each thruster.

Plumes from vents are more standard and the f_1 function can consequently be fixed : the mass flux is approximated by the following engineering model

$\Phi(r, \Theta) = ((n+1)/(2\pi)) \cdot (dm/dt) \cdot \cos^n(\Theta) \cdot r^{-2}$

where $1 \leq n \leq 2$ are typical values used for design. The divergence is larger than the one of thrusters.

6.5.2 Transport of molecular contaminants

Transport between surfaces

This section only deals with the methods and models for transport of neutral molecules. There is no available model of ion transport devoted to contamination.

Three levels of complexity and accuracy in modelling the transport of neutral molecular contaminants can be distinguished.

Simplest view factors

This model simulates collisionless transport. In such a case the fraction of contaminants coming from surface j to surface i is given by the view factor V_{ij} of surface i seen from surface j (including the cosine factor coming from lambertian emission law). These view factors are similar to the ones of radiative thermal analysis. They can be computed geometrically or by Monte-Carlo ray tracing. The incident mass on a surface i is then given by

$$S_j\, V_{ij} \cdot dm_j/dt$$

where j runs over all surfaces and dm_j/dt denotes the outgassing mass rate of surface j.

Simplified Monte-Carlo

Collisions of contaminants are simulated in a simplified way, the density and speed of possible partners for molecular collisions are given a priori:

- for ambient scatter, the ambient density and speed are easily known, but wakes (or 'shades') are usually not treated,
- for self-scatter, the contaminant density is very simplified and usually taken proportional to $1/r^2$ and with spherical symmetry.

This simplifying assumption has a very interesting consequence: the fraction of contaminants coming onto surface i from surface j is still a constant (depending on assumed densities) that can be called an effective view factor. It results from the simple view factor for collisionless processes diminished by the fraction of scattered molecules and increased by molecules outgassed in other directions but redirected to surface i due to collisions. The deposition rate is then computed similarly to using simple viewfactors.

This method is usually limited to one collision per molecule because the uncertainties due to the densities given a priori increase with collision number. This effective view factors can conveniently be computed by Monte-Carlo ray-tracing method.

Both methods can include other contaminant sources such as vents and plumes. The view factors are then replaced by interception factors.

True Monte-Carlo (Direct Simulation Monte-Carlo DSMC)

It computes multiple collisions in a realistic way. The collision probabilities are computed auto-coherently from the densities given by the simulation. This method is far more time consuming and requires more work for programming (in particular it requires a meshing of volume and not only of spacecraft surfaces).

Either method can be better suited, depending on the spacecraft configuration. A potential contamination of a sensitive protected surface through multiple collisions shall require a precise DSMC simulation. In simpler cases, when contamination essentially happens in line-of-sight, it shall be more appropriate to use the less time-consuming methods.

Surface transport

Reflections on surfaces and re-evaporation are easy to implement and are usually included in models, the latter (re-evaporation) often as part of the outgassing process. Migrations on surfaces on the contrary are complex processes and there is no commercial available model.

Transport of particles

As mentioned earlier particulate transport is governed by several phenomena:

- solar radiation pressure
- particulate charging and subsequent electrostatic effects

The first may be computed by methods similar to spacecraft orbit computing, whereas the second requires specific modelling to assess particulate charging in a plasma and potential map around spacecraft.

A last aspect of particulate transport is their interaction with walls. Sticking and accommodation coefficients are however very difficult to assess.

Most particulate contamination models remain in the field of research. Very few of them seem to be transferable to other users.

6.6 Specific Requirements

The external contamination requirements are based on the criticality of the mission, i.e. the sensitivity of systems (thermal blankets, solar arrays, radiators, star trackers etc.) as well as payload (optical sensors, cameras, spectrometers etc.) to contamination. When considering the effect of the contamination is has to be taken into account that due to the reduced distance to the sun there will be an increased photo-induced condensation and polymerisation (or fixation) of organic components onto surfaces as well as higher UV degradation rate of these components.

Some tentative overall external contamination requirements for the Solar Orbiter spacecraft can be derived from previous specifications for other scientific projects like the external contamination control requirements for the Soho. The requirements shall be such that the deposition of organic contaminants will not exceed the following level (integrated over the entire mission):

- Total molecular deposition of 100 Ångstrøm (this correspond to some $10^{-6}g/cm^2$ or about 300ng/cm^2/year).

The requirement is intended to be achievable at minimum cost if considered early in the design, and reflect the maximum level that can be tolerated. Within the overall limit, the various spacecraft elements can be assigned contamination allocations not to be exceeded. It is important for each element not to exceed the limit in order not to cause unacceptable degradation of the overall spacecraft thermal control and power production performance. Payloads (or the proximity of such) with e.g. cryogenic (or relatively cold sensitive surfaces) or optics (UV, visible) can pose more stringent requirements.

In order to achieve this the following guidelines shall be observed:

- Any material proposed for use and which will be exposed to space vacuum should, at a minimum, pass the outgassing requirements TML≤1% and CVCM≤0.1% when tested according to ECSS-Q-70-02 or ASTM-E595 (see section 7.5).

- Where possible, materials should be selected from ESA or NASA approved lists for space proven materials, such as ESA-PSS-1-701 (even in such cases an outgassing test may be required, depending on the criticality of the processes involved, batch to batch variability, etc.).

- In specific cases a dynamic outgassing test, such as the ESA VBQC-test or the ASTM-E1559 (see section 7.5) is required. This should, at a minimum, be done if the material used covers a surface area larger than 1000 cm^2 (this also includes any MLI materials used).

6.7 Existing Tools and Databases

Several computer codes dedicated to spacecraft contamination exist. Most of them are simulation tools at system level, but some are devoted to thruster plume modelling. Some also contain integrated (limited) data bases.

The main field of applicability of the codes is external contamination in LEO or GEO orbit. However, some programs, have limited transport modelling capabilities (simple or improved view factors only), and will give poor results in cases when return-flux through self-scatter is important.

Many the tools are also capable of analysing semi-enclosed. Here again, some codes can be limited due to too poor transport modelling in case of high pressures. A difference with external

contamination computing for which collisional return flux may often be the main contamination process (for surfaces not in direct view), is that in closed systems direct surface to surface collisionless transport (with possible surface reflections) is most of the time the dominant process. Except for really high pressures such as 10^{-3} hPa (and thus decimetric mean free path), which may be found in semi enclosed systems yet.

For a description of available tools see [10]

Some tools include data bases about contamination effects. References to some other important data bases created independent from the tools, are found in literature:

- A data base was created by Boeing Aerospace & Electronics in 1986-1988 for Air Force Wright Research and Development Centre [11]. Its availability to non-Americans is not reported. It is a very important work resulting from the collection of over 3000 sources and covering most of contamination fields.

- The Plume Contamination Database (PCD) was developed by MMS for ESTEC, using ORACLE [10]. It is foreseen to be progressively filled by ESTEC contractors and presently essentially contains measurements made at TUHH [12]. It should be available from ESA/ESTEC to the European space community.

- A materials outgassing contamination and effects data base [13] (obtained using the NASA ASTM-E-1559 standard) is being created by the NASA Space Environmental Effects (SEE) Program office. Data is being accumulated from both national and international sources (including ESA). Once established, the data will be available to the entire community.

These data bases can be used to assess contamination effects from contaminant deposit and column densities computed by the models described in the previous section.

6.9 References

[1] ESA PSS-01-201: Contamination and Cleanliness Control
(to be replaced by ECSS-Q-70-01 in the near future).

[2] ECSS-Q-70-02: A thermal vacuum test for the screening of space Materials.(former ESA PSS-01-702)

[3] ASTM E-595 Method for Total Mass Loss and Collected Volatile Condensable Materials from outgassing in a vacuum environment.

[4] Van Eesbeek M. and A. Zwaal "Outgassing and contamination model based on residence time", ESA SP232, Proc. of the 3rd European Symp. on spacecraft materials in a space environment, Noordwijk, The Netherlands, 1-4 Oct 1985.

[5] ASTM E-1559 Method for contamination outgassing characteristics of space materials

[6] Dushman S., "Scientific Foundations of Vacuum Technique"; Wiley & Sons, Inc, New-York-London

[7] Scialdone J.: "Characterisation of the outgassing of spacecraft materials"; SPIE Vol. 287 Shuttle Optical Environment; 1981

[8] Trinks H.: "Exhaust Plume Databook Update Version No 3 / ESA/ESTEC Contract 7590/87/NL/TP"

[9] Simons G.A.: "Effect of Nozzle Boundary Layers on Rocket Exhaust Plumes", AIAA Journal, Tech. Notes, vol.10, No 11, 1972, pp. 1534-1535

[10] ECSS-E-ST-10-04C, System Engineering, Space Environment Standard
WWW site: http://www.ecss.nl

[11] Thorton M., Gilbert C., Spacecraft Contamination Data Base, SPIE Vol. 1329, 1990

[12] Trinks H., Surface Effet Data Handbook (SEDH III)

[13]   Wood B. E., Green B. D., Uy O. M., Cain R. P., Yung S. K., Satellite Contamination and Materials Outgassing Effects Databases, 8th Int. Symp. Materials in a Space Environment Arachon, June 2000

A

Annual Expected Number of Solar Proton Events above a given > 10 MeV Fluence Threshold

A.1 Introduction

Following the work of Feynman et al. (1993) [1], the distribution of solar proton events follows a Poisson distribution. Consequently, the probability of observing n events in a time τ can be represented as follows:

$$p(n, w\tau) = e^{-w\tau} \frac{(w\tau)^n}{n!}$$

(1)

Where w is the average number of events seen per year.

In addition, the distribution of the event intensities can be represented as a log-normal distribution. If the fluence of a particular event is written f_p, then $f_p = 10^F$ and it follows that:

$$f(F) = \frac{1}{\left(\sqrt{2\pi}\sigma\right)} e^{\left[-(F-\mu)^2 / 2\sigma^2\right]}$$

(2)

Where μ and σ are the mean and standard deviation of the distribution of the $\log_{10}$ of the fluence values respectively.

A good approximation of the expected number of events during τ with fluence exceeding 10^F is given by:

$$K = w\tau \int_F^\infty f(F)df = w\tau \frac{1}{2}\left(1 - erf\left((F-\mu) / \sqrt{2}\sigma\right)\right)$$

(3)

where: $\qquad erf(x) = \frac{2}{\sqrt{\pi}} \int_0^x e^{-t^2} dt$

Figure 1 illustrates K as a function of F for >10MeV proton data at 1AU. This figure uses values of τ =1 year, and w, μ, τ and σ defined by Feynman et al (1993) together with a recent update published by Rosenqvist et al (2005) [2].
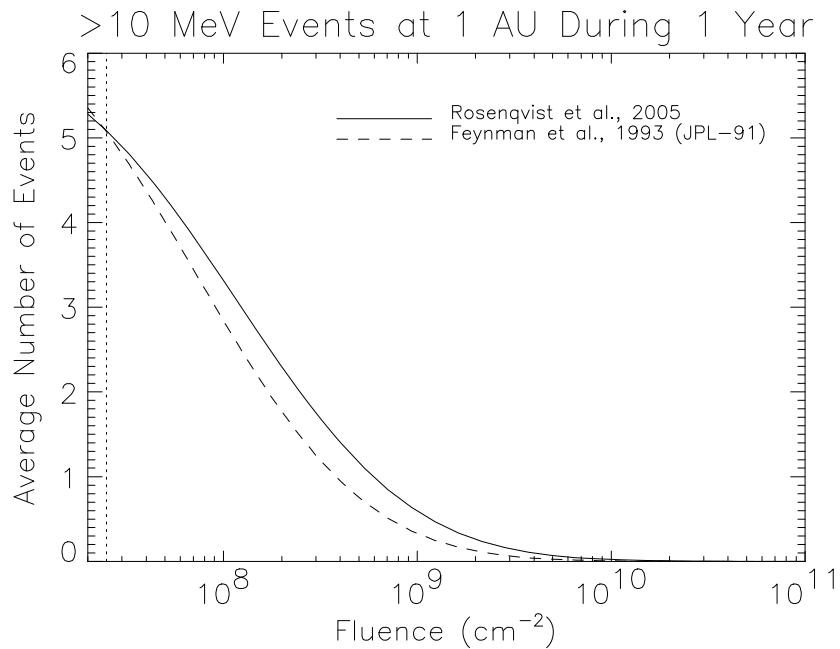
Figure 1. Expected number of solar proton events per year exceeding a given >10MeV fluence at 1AU. JPL-91 values are based on solar active years between 1973 and 1991 whereas Rosenqvist et al. values are based on active years between 1974 and 2002.

The dotted vertical line illustrates the approximate cosmic ray yearly background fluence. This is purely illustrative and it should be noted that the energies are mainly in the GeV range.

The X-axis of the above figure starts at 2×10^7 particles.cm^{-2}. This is because for smaller fluences, the distribution of events is not seen to follow a log-normal distribution.

The panels in Figure 2 provide an estimate of the averaged number of solar proton events per year as a function of fluence exceeded by each event at 1AU for a range of values of integral proton fluence and based on the Feynman model.
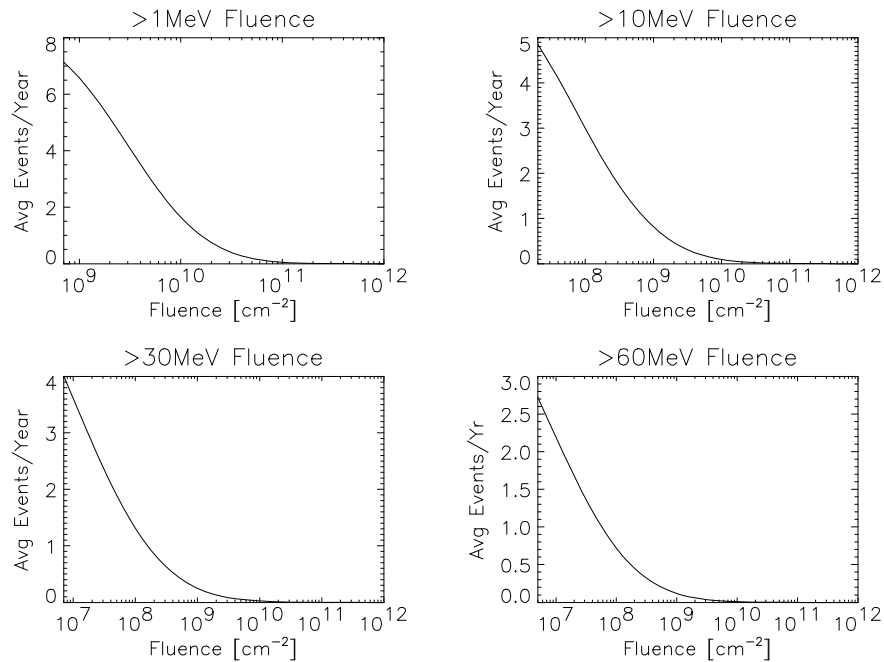
Figure 2: averaged number of solar proton events per year as a function of fluence exceeded by each event. Data assumes the observer is located at 1AU and is based on the statistical model employed by Feynman et al (1993). Plots are produced for >1MeV, >10MeV, >30MeV and >60 MeV proton fluence respectively. The X-axis cutoff in each case is determined from the point below which the distribution of measured event fluences in the given energy range deviates from a log-normal distribution. These are $7x10^8$, $2x10^7$, $7x10^6$ and $5x10^6$ cm^{-2} respectively. The data are based on solar active years between 1973 and 1991.

A.2 References

[1] Feynman J, G. Spitale and J. Wang, 1993, *Interplanetary Proton Fluence Model: JPL 1991*, JGR, Vol 98, A8, p13281-13294

[2] Rosenqvist L., A. Hilgers, H. Evans, E. Daly, M. Hapgood, R. Stamper, R. Zwickl, S. Bourdarie, D. Boscher, 2005, *Toolkit for Updating Interplanetary Proton Cumulated Fluence Models*, Journal of Spacecraft and Rockets

B

Data for specific solar particle events

B.1 Introduction

This appendix presents the particle spectra and total ionising doses for some specific severe solar particle events. The selected events are listed in table 1. They comprise the severe event of August 1972 plus the 5 "worst" events from the list in [1] covering the period from 1976 until the present.

Table 1: Solar Particle Events

	Proton Flux [pfu>10MeV] *)
August 1972	n.a.
October 1989	40000
March 1991	43000
July 2000	24000
November 2001	31700
October 2003	29500

*) 1 pfu = 1 p cm^{-2} sr^{-1} s^{-1}

B.2 Figures
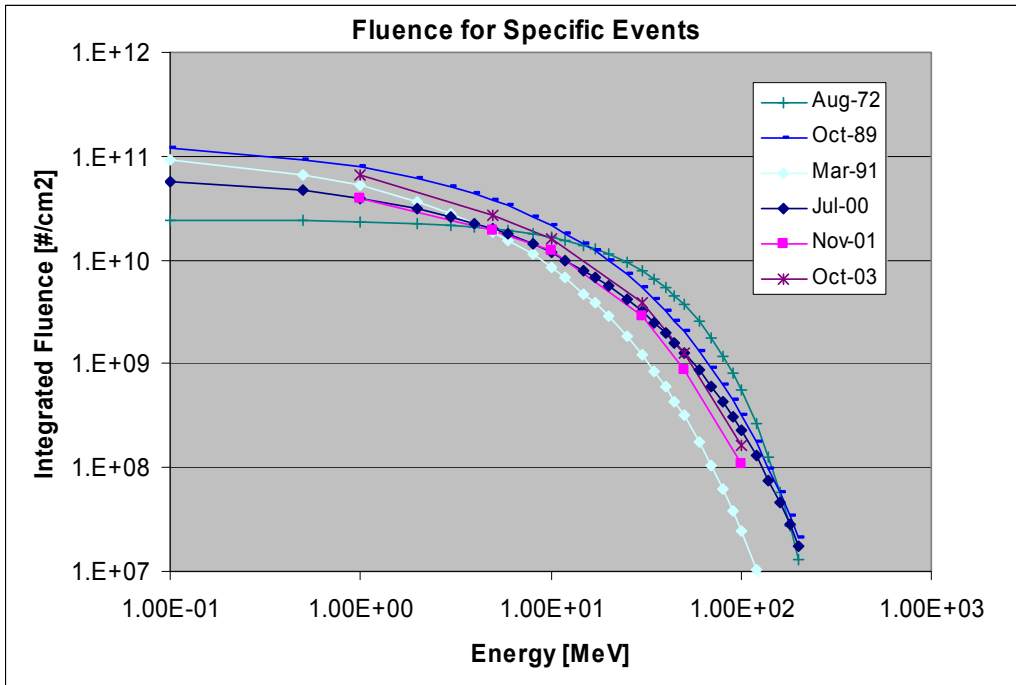
Figure 1: Integrated Solar Proton Fluence for selected solar particle events
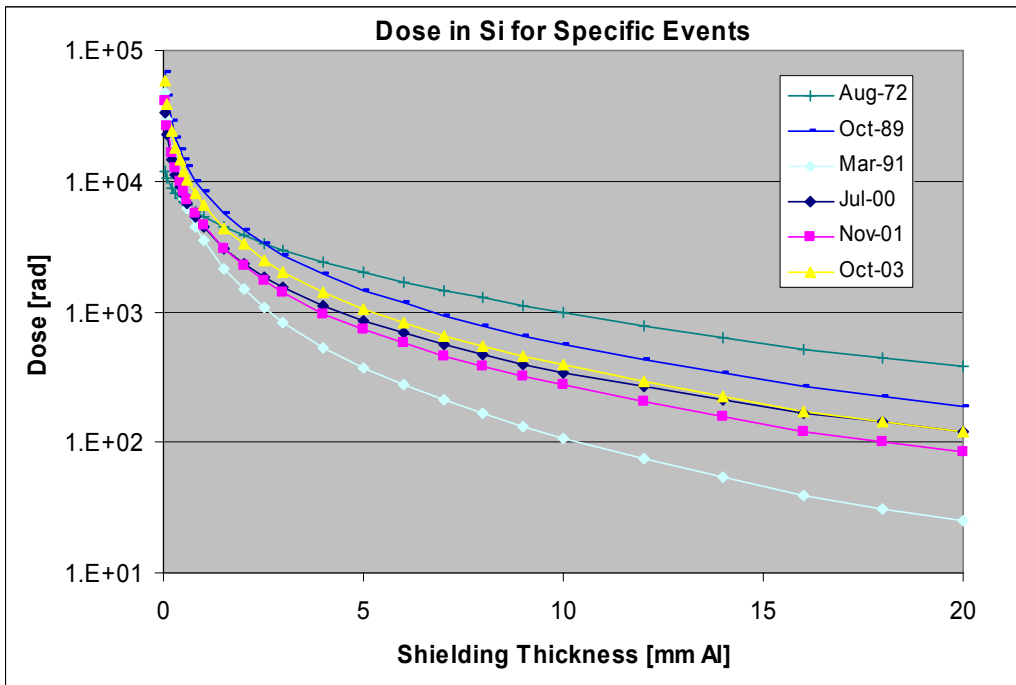
Figure 2: Total Ionising dose for selected solar particle events

Energy [MeV]	Integrated Proton Fluence for selected solar particle events [#/cm2]					
	Aug-72	Oct-89	Mar-91	Jul-00	Nov-01	Oct-03
1.00E-01	2.44E+10	1.18E+11	9.16E+10	5.78E+10	n.a.	n.a.
5.00E-01	2.40E+10	9.34E+10	6.63E+10	4.65E+10	n.a.	n.a.
1.00E+00	2.36E+10	7.85E+10	5.20E+10	3.95E+10	3.93E+10	6.59E+10
2.00E+00	2.27E+10	6.14E+10	3.69E+10	3.14E+10	n.a.	n.a.
3.00E+00	2.19E+10	5.08E+10	2.83E+10	2.63E+10	n.a.	n.a.
4.00E+00	2.11E+10	4.33E+10	2.27E+10	2.26E+10	n.a.	n.a.
5.00E+00	2.03E+10	3.76E+10	1.86E+10	1.98E+10	1.93E+10	2.73E+10
6.00E+00	1.95E+10	3.31E+10	1.56E+10	1.76E+10	n.a.	n.a.
8.00E+00	1.81E+10	2.64E+10	1.14E+10	1.42E+10	n.a.	n.a.
1.00E+01	1.68E+10	2.17E+10	8.61E+09	1.18E+10	1.24E+10	1.57E+10
1.20E+01	1.56E+10	1.81E+10	6.69E+09	9.98E+09	n.a.	n.a.
1.50E+01	1.39E+10	1.42E+10	4.75E+09	7.93E+09	n.a.	n.a.
1.70E+01	1.29E+10	1.22E+10	3.85E+09	6.89E+09	n.a.	n.a.
2.00E+01	1.15E+10	9.87E+09	2.87E+09	5.66E+09	n.a.	n.a.
2.50E+01	9.54E+09	7.18E+09	1.84E+09	4.20E+09	n.a.	n.a.
3.00E+01	7.90E+09	5.38E+09	1.23E+09	3.20E+09	2.92E+09	3.86E+09
3.50E+01	6.54E+09	4.12E+09	8.47E+08	2.49E+09	n.a.	n.a.
4.00E+01	5.42E+09	3.21E+09	5.98E+08	1.97E+09	n.a.	n.a.
4.50E+01	4.49E+09	2.54E+09	4.31E+08	1.58E+09	n.a.	n.a.
5.00E+01	3.71E+09	2.03E+09	3.15E+08	1.28E+09	8.84E+08	1.26E+09
6.00E+01	2.55E+09	1.34E+09	1.76E+08	8.67E+08	n.a.	n.a.
7.00E+01	1.75E+09	9.07E+08	1.03E+08	6.03E+08	n.a.	n.a.
8.00E+01	1.20E+09	6.31E+08	6.18E+07	4.29E+08	n.a.	n.a.
9.00E+01	8.21E+08	4.48E+08	3.82E+07	3.11E+08	n.a.	n.a.
1.00E+02	5.63E+08	3.23E+08	2.42E+07	2.29E+08	1.07E+08	1.62E+08

Figure 3: Integrated proton fluence for selected solar particle events (n.a. - not available)

Aluminium shielding thickness [mm]	Total Ionising dose for selected solar particle events [rad]					
	Aug-72	Oct-89	Mar-91	Jul-00	Nov-01	Oct-03
5.00E-02	1.17E+04	6.72E+04	4.81E+04	3.31E+04	4.08E+04	5.90E+04
1.00E-01	1.04E+04	4.50E+04	2.95E+04	2.25E+04	2.67E+04	3.86E+04
2.00E-01	8.92E+03	2.85E+04	1.68E+04	1.45E+04	1.66E+04	2.40E+04
3.00E-01	8.05E+03	2.16E+04	1.19E+04	1.11E+04	1.25E+04	1.80E+04
4.00E-01	7.44E+03	1.76E+04	9.14E+03	9.11E+03	1.00E+04	1.45E+04
5.00E-01	6.95E+03	1.48E+04	7.39E+03	7.75E+03	8.35E+03	1.20E+04
6.00E-01	6.53E+03	1.28E+04	6.15E+03	6.74E+03	7.17E+03	1.03E+04
8.00E-01	5.86E+03	1.00E+04	4.51E+03	5.33E+03	5.60E+03	8.06E+03
1.00E+00	5.34E+03	8.23E+03	3.50E+03	4.41E+03	4.56E+03	6.57E+03
1.50E+00	4.40E+03	5.59E+03	2.13E+03	3.05E+03	3.05E+03	4.38E+03
2.00E+00	3.81E+03	4.24E+03	1.49E+03	2.34E+03	2.28E+03	3.27E+03
2.50E+00	3.30E+03	3.30E+03	1.08E+03	1.84E+03	1.73E+03	2.49E+03
3.00E+00	2.92E+03	2.69E+03	8.27E+02	1.52E+03	1.39E+03	1.99E+03
4.00E+00	2.37E+03	1.92E+03	5.33E+02	1.10E+03	9.69E+02	1.39E+03
5.00E+00	1.98E+03	1.46E+03	3.74E+02	8.50E+02	7.28E+02	1.04E+03
6.00E+00	1.69E+03	1.16E+03	2.75E+02	6.81E+02	5.71E+02	8.16E+02
7.00E+00	1.45E+03	9.40E+02	2.09E+02	5.58E+02	4.61E+02	6.58E+02
8.00E+00	1.27E+03	7.89E+02	1.66E+02	4.73E+02	3.86E+02	5.50E+02
9.00E+00	1.11E+03	6.58E+02	1.31E+02	3.98E+02	3.20E+02	4.57E+02
1.00E+01	9.77E+02	5.63E+02	1.07E+02	3.43E+02	2.72E+02	3.88E+02
1.20E+01	7.88E+02	4.32E+02	7.49E+01	2.67E+02	2.05E+02	2.92E+02
1.40E+01	6.33E+02	3.35E+02	5.35E+01	2.10E+02	1.56E+02	2.21E+02
1.60E+01	5.17E+02	2.67E+02	3.96E+01	1.69E+02	1.22E+02	1.74E+02
1.80E+01	4.38E+02	2.22E+02	3.10E+01	1.42E+02	1.01E+02	1.43E+02
2.00E+01	3.77E+02	1.89E+02	2.49E+01	1.22E+02	8.50E+01	1.21E+02

Figure 4: Total Ionising dose for selected solar particle events

B.3 References

[1]   NOAA Space Environment Centre Event List 1976-present :
        http://umbra.nascom.nasa.gov/SEP/seps.html

C

Energetic particle spectra and NIEL for individual ions

C.1 Introduction

The high energy radiation environment consists of a variety of particle species, including protons and heavy ions from solar particle events and galactic cosmic radiation. The particles interact with matter in different ways depending on energy, particle type and the target material it interacts with. For the prediction of the induced degradation it is generally sufficient to consider the deposition of non-ionising energy by the impinging particles and the produced secondaries. It has been experimentally shown that in general the displacement damage induced in a device is proportional to the deposited non-ionising energy - NIEL (non-ionising energy loss).

The NIEL is strongly dependent on the particle type and to a lesser extent on the target material. Heavier ions causes far more damage per nucleon for the same particle energy than lighter ones.

C.2 Energy and LET spectra

In figure 1 to 4 is shown the predicted unshielded energy spectre for selected individual ions for the Solar Orbiter mission for 4 environments: the nominal solar minimum cosmic ray flux; the average flux for a "worst week" of a large SEPE; the average flux for a "worst day" of a large SEPE and the peak flux from a large SEPE. The predictions are performed with the CREME96 model [1]. The nominal solar minimum flux corresponds to 1AU (providing a worst case). The other fluxes are scaled according to the inverse square law giving a peak value (see table 1 of Chapter 1 – this means a factor 12.7 has been applied to the 1AU predictions). Figure 5 to 8 show the predicted LET spectre for individual ions or ion ranges for the Solar Orbiter mission for the same 4 environments assuming a 1g/cm² shielding and applying the same scaling principles. Figure 9 to 44 show the same data as in the plot in tabular form.

C.3 Non-ionising energy loss (NIEL) data

For assessing the damage due to individual ions to CCDs and other electro-optical components susceptible to displacement damage the corresponding NIEL function for the target material in question is required. For protons extensive data is available. Figure 45 shows the proton NIEL for various target materials [2]. It is seen that, except for the very high and very low energies, there only modest difference between the different target materials. It should be remarked that the lower energies (below about 1MeV) are of little importance for spacecraft electronic components because of the insignificant range of the particles (less than about 10μm). For Alphas similar data can be found in [3]. Figure 46 shows the Alpha NIEL for some specific target materials together with the proton NIEL for Si of figure 45. It is seen that the Alpha NIEL is generally slightly more than an order of magnitude higher than the proton NIEL, but vary very little from material to material. For heavier ions some analytical data can be found in [4]. Figure 47 show the predicted NIEL in Silicium for some selected ions from [4]. It is seen that the peak NIEL for instance for Gold is more than 3 orders of magnitude higher than that for protons. In addition to Si, some other target materials are also investigated in [4], namely GaAs, InP and SiC. Their general behaviour is very similar to Si and the

resulting NIEL almost identical. In figure 48 the NIEL from the different data sources is compared. It is seen that the analytical approach applied in [4] predicts lower NIEL than the other publications. The main the reason is that the analytical approach does not include certain effects important at high energies. It is recommended to apply the worst case (e.g.for proton the one from [2]). Figure 49 to 54 show the same NIEL data as in the plot in tabular form.

C.4 References

[1]   A.J. Tylka et al. "CREME96: A Revision of the Cosmic Ray Effects on Micro-Electronics Code", IEEE Trans. Nucl. Sci. NS-44, 2150-2160 (1997).

[2]   Inso Jun et al. "Proton Nonionizing Energy Loss (NIEL) for Device Applications", IEEE Trans. Nucl. Sci. Vol 50, No 6, Dec 2003

[3]   Inso Jun et al. "Alpha Particle Nonionizing Energy Loss (NIEL)", IEEE Trans. Nucl. Sci Vol 51, No 6, Dec 2004.

[4]   S.R. Messenger et al. "NIEL for Heavy Ions: An Analytic Approach", IEEE Trans. Nucl. Sci. Vol 50, No 6, Dec 2003.

C.5 Figures
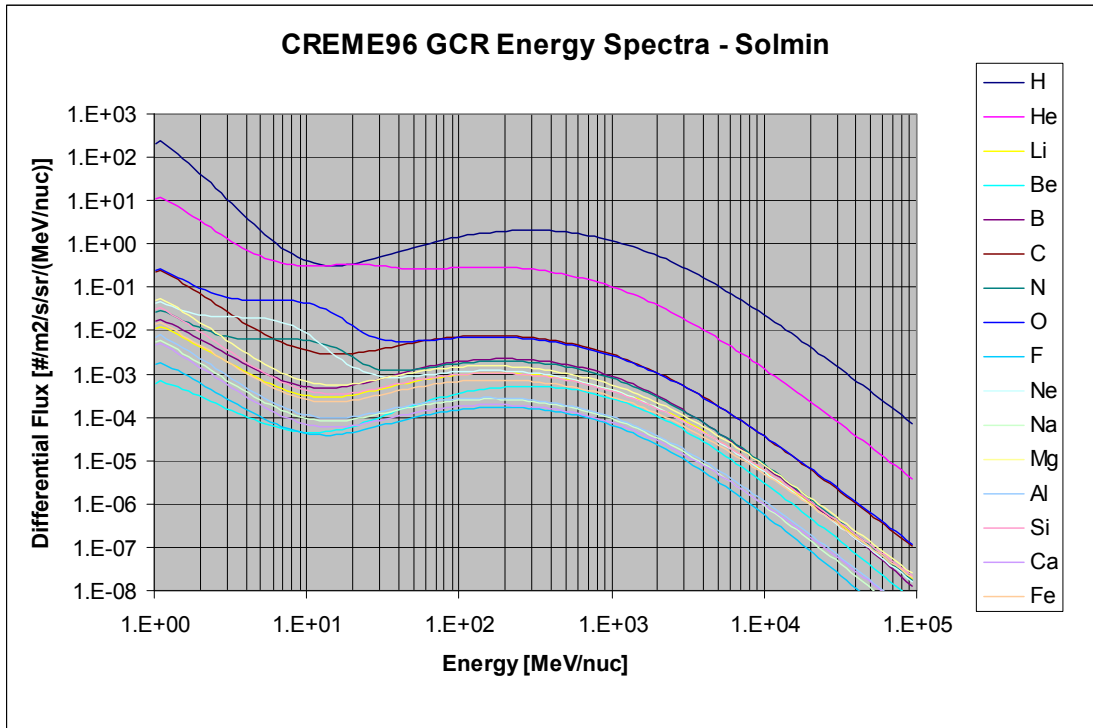
Figure 1. CREME96 Galactic Cosmic Ray Energy Spectra for solar minimum conditions and nominal (quiet) activity.
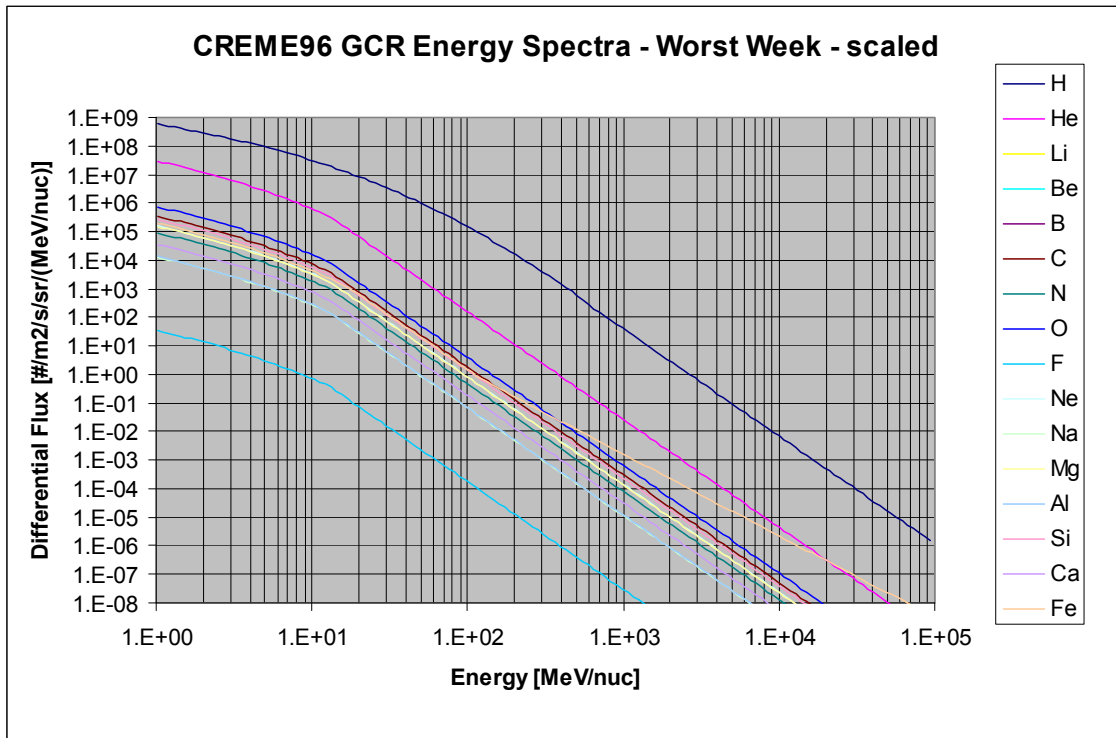
Figure 2. CREME96 Galactic Cosmic Ray Energy Spectra for the worst week of a large SEPE (scaled)
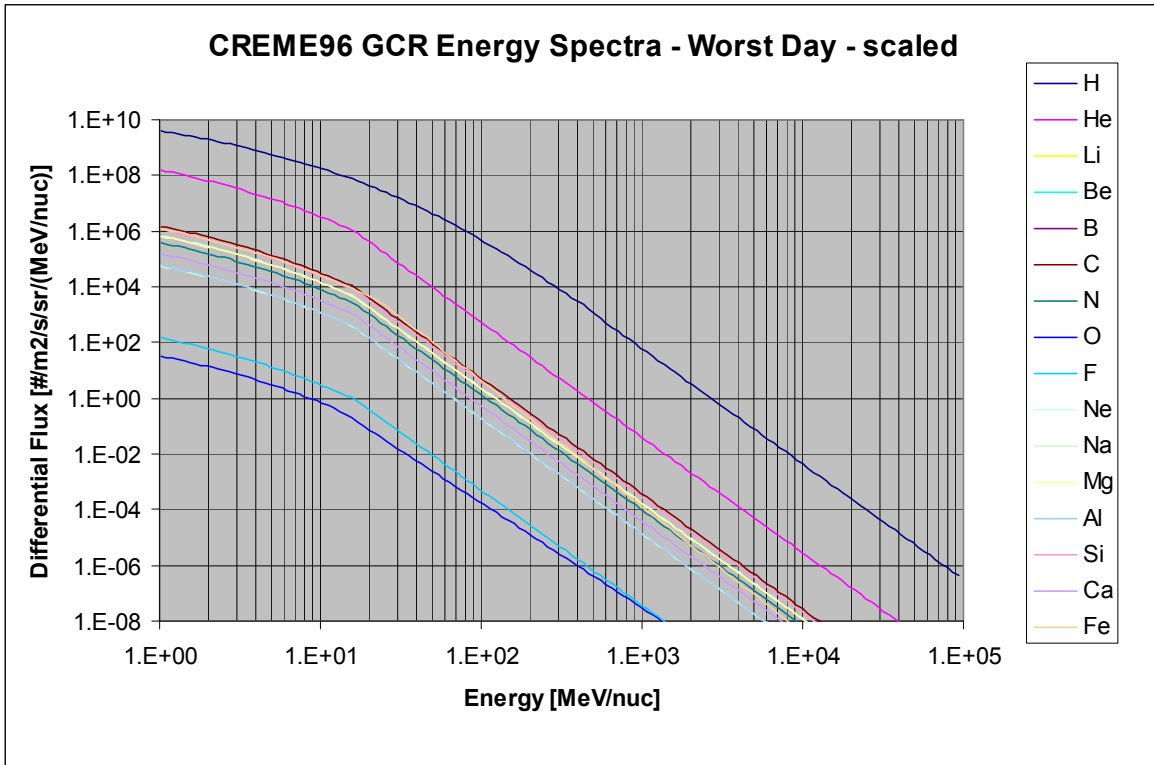
**Figure 3. CREME96 Galactic Cosmic Ray Energy Spectra
for the worst day of a large SEPE (scaled)**
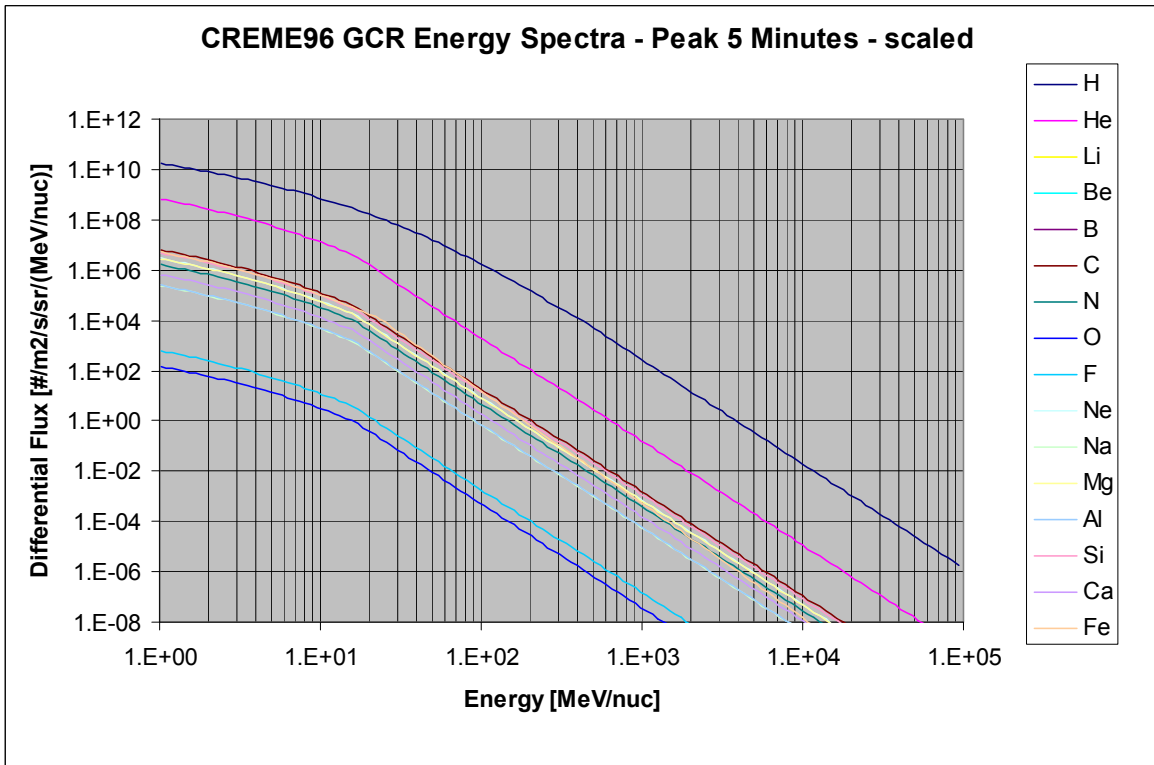
**Figure 4. CREME96 Galactic Cosmic Ray Energy Spectra
for the peak 5 min of a large SEPE (scaled)**

Figure 5. CREME96 Galactic Cosmic Ray LET Spectra for Solar minimum conditions and nominal (quiet) activity.
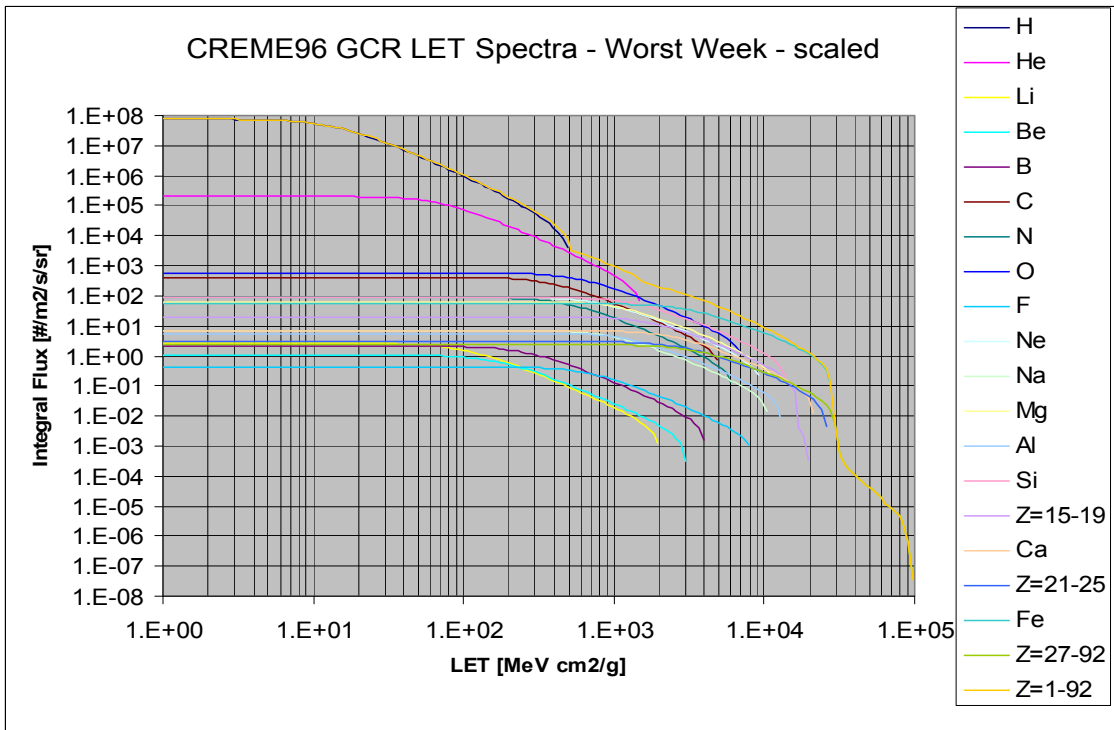
Figure 6. CREME96 Galactic Cosmic Ray LET Spectra for the worst week of a large SEPE (scaled)
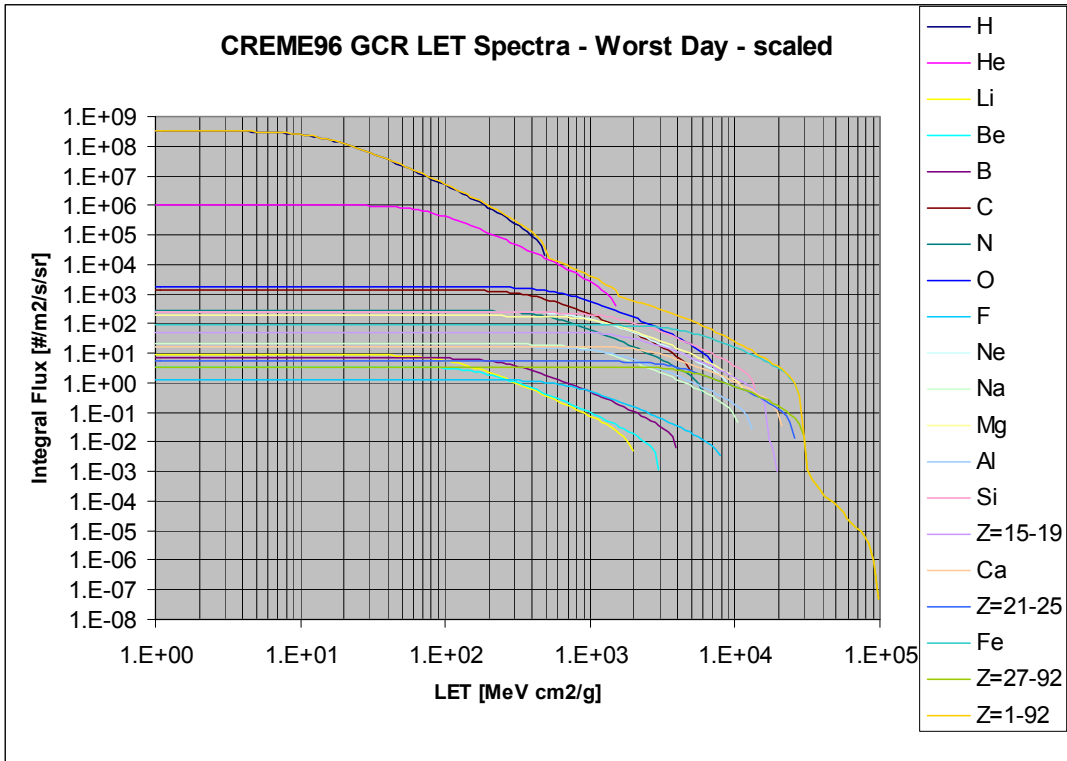
Figure 7. CREME96 Galactic Cosmic Ray LET Spectra for the worst day of a large SEPE (scaled)
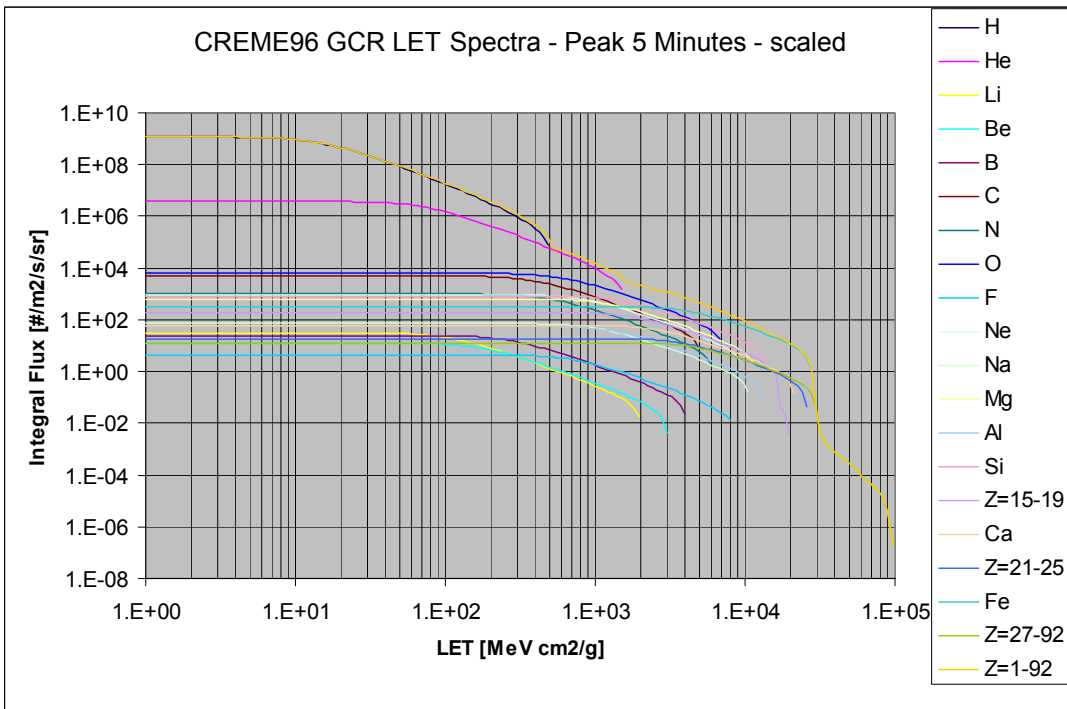
Figure 8. CREME96 Galactic Cosmic Ray LET Spectra for the peak 5 min of a large SEPE (scaled)

Particle Energy [MeV/nuc]	Solar Orbiter – CREME96 GCR Spectra - Solmin Differential Flux [#/m2/sec/sr/(MeV/nuc)]			
	H (Z=1)	He (Z=2)	Li (Z=3)	Be (Z=4)
1.02E+00	2.07E+02	1.14E+01	1.14E-02	6.08E-04
1.30E+00	1.48E+02	8.72E+00	9.35E-03	5.56E-04
1.67E+00	7.20E+01	5.08E+00	5.93E-03	3.93E-04
2.14E+00	3.31E+01	2.90E+00	3.69E-03	2.71E-04
2.75E+00	1.46E+01	1.65E+00	2.26E-03	1.85E-04
3.52E+00	6.34E+00	9.59E-01	1.39E-03	1.26E-04
4.51E+00	2.79E+00	5.97E-01	8.78E-04	8.84E-05
5.78E+00	1.31E+00	4.19E-01	5.81E-04	6.49E-05
7.42E+00	6.88E-01	3.40E-01	4.15E-04	5.14E-05
9.51E+00	4.32E-01	3.14E-01	3.29E-04	4.53E-05
1.22E+01	3.34E-01	3.16E-01	2.93E-04	4.49E-05
1.56E+01	3.14E-01	3.28E-01	2.94E-04	5.02E-05
2.00E+01	3.47E-01	3.35E-01	3.27E-04	6.21E-05
2.57E+01	4.22E-01	3.28E-01	3.89E-04	8.24E-05
3.29E+01	5.41E-01	3.04E-01	4.77E-04	1.13E-04
4.22E+01	7.03E-01	2.74E-01	5.83E-04	1.54E-04
5.41E+01	9.05E-01	2.59E-01	6.99E-04	2.05E-04
6.94E+01	1.13E+00	2.66E-01	8.13E-04	2.63E-04
8.89E+01	1.36E+00	2.81E-01	9.13E-04	3.27E-04
1.14E+02	1.59E+00	2.94E-01	9.90E-04	3.89E-04
1.46E+02	1.79E+00	2.99E-01	1.03E-03	4.45E-04
1.87E+02	1.96E+00	2.93E-01	1.05E-03	4.88E-04
2.40E+02	2.07E+00	2.78E-01	1.02E-03	5.13E-04
3.08E+02	2.10E+00	2.56E-01	9.63E-04	5.17E-04
3.95E+02	2.02E+00	2.27E-01	8.78E-04	4.99E-04
5.06E+02	1.87E+00	1.95E-01	7.71E-04	4.59E-04
6.49E+02	1.65E+00	1.60E-01	6.49E-04	4.00E-04
8.32E+02	1.39E+00	1.27E-01	5.22E-04	3.30E-04
1.07E+03	1.12E+00	9.62E-02	4.01E-04	2.57E-04
1.37E+03	8.63E-01	6.96E-02	2.93E-04	1.89E-04
1.75E+03	6.35E-01	4.81E-02	2.05E-04	1.31E-04
2.25E+03	4.46E-01	3.19E-02	1.37E-04	8.62E-05
2.88E+03	2.99E-01	2.03E-02	8.79E-05	5.41E-05
3.69E+03	1.92E-01	1.24E-02	5.44E-05	3.25E-05
4.74E+03	1.19E-01	7.39E-03	3.25E-05	1.88E-05
6.07E+03	7.08E-02	4.27E-03	1.89E-05	1.05E-05
7.78E+03	4.10E-02	2.40E-03	1.08E-05	5.75E-06
9.98E+03	2.32E-02	1.33E-03	5.99E-06	3.07E-06
1.28E+04	1.28E-02	7.19E-04	3.28E-06	1.61E-06
1.64E+04	6.95E-03	3.84E-04	1.77E-06	8.29E-07
2.10E+04	3.72E-03	2.03E-04	9.44E-07	4.22E-07
2.70E+04	1.97E-03	1.06E-04	5.00E-07	2.13E-07
3.46E+04	1.03E-03	5.52E-05	2.63E-07	1.07E-07
4.43E+04	5.35E-04	2.85E-05	1.37E-07	5.31E-08
5.68E+04	2.76E-04	1.46E-05	7.13E-08	2.63E-08
7.28E+04	1.42E-04	7.50E-06	3.69E-08	1.30E-08
9.33E+04	7.27E-05	3.83E-06	1.91E-08	6.38E-09

Figure 9. CREME96 Galactic Cosmic Ray Energy Spectra for solar minimum conditions and nominal (quiet) activity.

Particle Energy [MeV/nuc]	Solar Orbiter – CREME96 GCR Spectra - Solmin Differential Flux [#/m2/sec/sr/(MeV/nuc)]			
	B (Z=5)	C (Z=6)	N (Z=7)	O (Z=8)
1.02E+00	1.66E-02	2.29E-01	2.73E-02	2.53E-01
1.30E+00	1.39E-02	1.78E-01	2.27E-02	2.01E-01
1.67E+00	8.92E-03	1.05E-01	1.50E-02	1.27E-01
2.14E+00	5.58E-03	6.00E-02	1.04E-02	8.51E-02
2.75E+00	3.45E-03	3.39E-02	7.83E-03	6.33E-02
3.52E+00	2.13E-03	1.92E-02	6.67E-03	5.39E-02
4.51E+00	1.35E-03	1.12E-02	6.34E-03	5.12E-02
5.78E+00	8.98E-04	6.95E-03	6.41E-03	5.11E-02
7.42E+00	6.46E-04	4.71E-03	6.47E-03	4.99E-02
9.51E+00	5.16E-04	3.57E-03	6.17E-03	4.48E-02
1.22E+01	4.69E-04	3.03E-03	5.27E-03	3.50E-02
1.56E+01	4.80E-04	2.85E-03	3.86E-03	2.27E-02
2.00E+01	5.47E-04	2.95E-03	2.41E-03	1.27E-02
2.57E+01	6.70E-04	3.30E-03	1.50E-03	7.65E-03
3.29E+01	8.48E-04	3.90E-03	1.20E-03	6.00E-03
4.22E+01	1.07E-03	4.66E-03	1.20E-03	5.59E-03
5.41E+01	1.32E-03	5.49E-03	1.32E-03	5.75E-03
6.94E+01	1.59E-03	6.29E-03	1.49E-03	6.19E-03
8.89E+01	1.83E-03	6.96E-03	1.68E-03	6.67E-03
1.14E+02	2.03E-03	7.43E-03	1.84E-03	7.04E-03
1.46E+02	2.17E-03	7.65E-03	1.95E-03	7.20E-03
1.87E+02	2.23E-03	7.59E-03	1.99E-03	7.12E-03
2.40E+02	2.20E-03	7.27E-03	1.96E-03	6.80E-03
3.08E+02	2.08E-03	6.73E-03	1.85E-03	6.29E-03
3.95E+02	1.90E-03	6.02E-03	1.68E-03	5.62E-03
5.06E+02	1.66E-03	5.19E-03	1.47E-03	4.86E-03
6.49E+02	1.38E-03	4.31E-03	1.23E-03	4.04E-03
8.32E+02	1.09E-03	3.43E-03	9.77E-04	3.22E-03
1.07E+03	8.17E-04	2.61E-03	7.39E-04	2.46E-03
1.37E+03	5.80E-04	1.89E-03	5.32E-04	1.79E-03
1.75E+03	3.90E-04	1.31E-03	3.63E-04	1.25E-03
2.25E+03	2.50E-04	8.71E-04	2.37E-04	8.37E-04
2.88E+03	1.53E-04	5.55E-04	1.48E-04	5.38E-04
3.69E+03	8.95E-05	3.41E-04	8.83E-05	3.34E-04
4.74E+03	5.06E-05	2.03E-04	5.11E-05	2.00E-04
6.07E+03	2.77E-05	1.17E-04	2.86E-05	1.17E-04
7.78E+03	1.48E-05	6.59E-05	1.56E-05	6.65E-05
9.98E+03	7.70E-06	3.63E-05	8.34E-06	3.71E-05
1.28E+04	3.94E-06	1.97E-05	4.37E-06	2.04E-05
1.64E+04	1.98E-06	1.05E-05	2.25E-06	1.10E-05
2.10E+04	9.88E-07	5.57E-06	1.15E-06	5.88E-06
2.70E+04	4.87E-07	2.91E-06	5.81E-07	3.12E-06
3.46E+04	2.38E-07	1.51E-06	2.91E-07	1.64E-06
4.43E+04	1.16E-07	7.81E-07	1.45E-07	8.57E-07
5.68E+04	5.59E-08	4.02E-07	7.18E-08	4.46E-07
7.28E+04	2.69E-08	2.06E-07	3.54E-08	2.31E-07
9.33E+04	1.29E-08	1.05E-07	1.74E-08	1.19E-07

Figure 10. CREME96 Galactic Cosmic Ray Energy Spectra for solar minimum conditions and nominal (quiet) activity.

Particle Energy [MeV/nuc]	Solar Orbiter – CREME96 GCR Spectra - Solmin Differential Flux [#/m2/sec/sr/(MeV/nuc)]			
	F (Z=9)	Ne (Z=10)	Na (Z=11)	Mg (Z=12)
1.02E+00	1.67E-03	4.23E-02	5.31E-03	5.06E-02
1.30E+00	1.37E-03	3.63E-02	4.21E-03	3.90E-02
1.67E+00	8.65E-04	2.71E-02	2.55E-03	2.29E-02
2.14E+00	5.32E-04	2.26E-02	1.51E-03	1.31E-02
2.75E+00	3.22E-04	2.09E-02	8.77E-04	7.35E-03
3.52E+00	1.95E-04	2.04E-02	5.11E-04	4.13E-03
4.51E+00	1.21E-04	1.99E-02	3.05E-04	2.38E-03
5.78E+00	7.92E-05	1.82E-02	1.91E-04	1.44E-03
7.42E+00	5.59E-05	1.45E-02	1.30E-04	9.48E-04
9.51E+00	4.39E-05	9.57E-03	9.81E-05	6.94E-04
1.22E+01	3.92E-05	5.11E-03	8.44E-05	5.81E-04
1.56E+01	3.97E-05	2.53E-03	8.23E-05	5.52E-04
2.00E+01	4.47E-05	1.49E-03	8.95E-05	5.88E-04
2.57E+01	5.42E-05	1.04E-03	1.05E-04	6.76E-04
3.29E+01	6.81E-05	8.56E-04	1.27E-04	8.06E-04
4.22E+01	8.53E-05	8.41E-04	1.55E-04	9.63E-04
5.41E+01	1.05E-04	9.06E-04	1.84E-04	1.13E-03
6.94E+01	1.25E-04	9.99E-04	2.12E-04	1.28E-03
8.89E+01	1.43E-04	1.09E-03	2.36E-04	1.41E-03
1.14E+02	1.57E-04	1.16E-03	2.53E-04	1.50E-03
1.46E+02	1.67E-04	1.19E-03	2.62E-04	1.53E-03
1.87E+02	1.70E-04	1.18E-03	2.60E-04	1.51E-03
2.40E+02	1.67E-04	1.13E-03	2.50E-04	1.45E-03
3.08E+02	1.57E-04	1.04E-03	2.31E-04	1.33E-03
3.95E+02	1.43E-04	9.32E-04	2.06E-04	1.19E-03
5.06E+02	1.24E-04	8.04E-04	1.77E-04	1.03E-03
6.49E+02	1.03E-04	6.66E-04	1.46E-04	8.54E-04
8.32E+02	8.08E-05	5.30E-04	1.14E-04	6.81E-04
1.07E+03	6.04E-05	4.02E-04	8.55E-05	5.19E-04
1.37E+03	4.28E-05	2.92E-04	6.09E-05	3.79E-04
1.75E+03	2.88E-05	2.02E-04	4.13E-05	2.64E-04
2.25E+03	1.84E-05	1.34E-04	2.67E-05	1.76E-04
2.88E+03	1.12E-05	8.54E-05	1.66E-05	1.13E-04
3.69E+03	6.59E-06	5.24E-05	9.88E-06	7.02E-05
4.74E+03	3.73E-06	3.12E-05	5.69E-06	4.21E-05
6.07E+03	2.04E-06	1.80E-05	3.18E-06	2.46E-05
7.78E+03	1.09E-06	1.01E-05	1.73E-06	1.40E-05
9.98E+03	5.68E-07	5.59E-06	9.24E-07	7.80E-06
1.28E+04	2.91E-07	3.03E-06	4.84E-07	4.27E-06
1.64E+04	1.46E-07	1.62E-06	2.49E-07	2.31E-06
2.10E+04	7.29E-08	8.55E-07	1.27E-07	1.24E-06
2.70E+04	3.59E-08	4.47E-07	6.42E-08	6.54E-07
3.46E+04	1.76E-08	2.32E-07	3.21E-08	3.44E-07
4.43E+04	8.54E-09	1.20E-07	1.60E-08	1.80E-07
5.68E+04	4.13E-09	6.17E-08	7.93E-09	9.35E-08
7.28E+04	1.99E-09	3.16E-08	3.91E-09	4.85E-08
9.33E+04	9.54E-10	1.61E-08	1.92E-09	2.50E-08

Figure 11. CREME96 Galactic Cosmic Ray Energy Spectra for solar minimum conditions and nominal (quiet) activity.

| Particle Energy [MeV/nuc]	Solar Orbiter – CREME96 GCR Spectra - Solmin Differential Flux [#/m2/sec/sr/(MeV/nuc)]			
	Al (Z=13)	Si (Z=14)	Ca (Z=20)	Fe (Z=26)
1.02E+00	7.25E-03	3.05E-02	4.56E-03	1.37E-02
1.30E+00	5.67E-03	2.36E-02	3.58E-03	1.09E-02
1.67E+00	3.39E-03	1.39E-02	2.13E-03	6.62E-03
2.14E+00	1.97E-03	7.96E-03	1.24E-03	3.94E-03
2.75E+00	1.13E-03	4.49E-03	7.06E-04	2.31E-03
3.52E+00	6.50E-04	2.53E-03	4.03E-04	1.36E-03
4.51E+00	3.83E-04	1.46E-03	2.35E-04	8.18E-04
5.78E+00	2.36E-04	8.87E-04	1.45E-04	5.17E-04
7.42E+00	1.58E-04	5.84E-04	9.65E-05	3.53E-04
9.51E+00	1.18E-04	4.29E-04	7.18E-05	2.69E-04
1.22E+01	1.00E-04	3.61E-04	6.11E-05	2.32E-04
1.56E+01	9.65E-05	3.45E-04	5.91E-05	2.27E-04
2.00E+01	1.04E-04	3.69E-04	6.40E-05	2.47E-04
2.57E+01	1.20E-04	4.28E-04	7.50E-05	2.89E-04
3.29E+01	1.45E-04	5.14E-04	9.12E-05	3.51E-04
4.22E+01	1.74E-04	6.21E-04	1.11E-04	4.25E-04
5.41E+01	2.05E-04	7.33E-04	1.33E-04	5.04E-04
6.94E+01	2.34E-04	8.42E-04	1.54E-04	5.81E-04
8.89E+01	2.59E-04	9.34E-04	1.72E-04	6.48E-04
1.14E+02	2.76E-04	1.00E-03	1.86E-04	6.97E-04
1.46E+02	2.83E-04	1.03E-03	1.93E-04	7.24E-04
1.87E+02	2.80E-04	1.03E-03	1.94E-04	7.26E-04
2.40E+02	2.68E-04	9.89E-04	1.87E-04	7.04E-04
3.08E+02	2.47E-04	9.21E-04	1.75E-04	6.61E-04
3.95E+02	2.21E-04	8.29E-04	1.57E-04	6.01E-04
5.06E+02	1.90E-04	7.21E-04	1.37E-04	5.28E-04
6.49E+02	1.57E-04	6.04E-04	1.14E-04	4.46E-04
8.32E+02	1.24E-04	4.86E-04	9.13E-05	3.61E-04
1.07E+03	9.36E-05	3.74E-04	6.97E-05	2.80E-04
1.37E+03	6.74E-05	2.75E-04	5.08E-05	2.07E-04
1.75E+03	4.63E-05	1.94E-04	3.53E-05	1.47E-04
2.25E+03	3.04E-05	1.31E-04	2.35E-05	9.99E-05
2.88E+03	1.92E-05	8.49E-05	1.50E-05	6.53E-05
3.69E+03	1.17E-05	5.32E-05	9.21E-06	4.12E-05
4.74E+03	6.85E-06	3.23E-05	5.48E-06	2.52E-05
6.07E+03	3.91E-06	1.90E-05	3.16E-06	1.50E-05
7.78E+03	2.18E-06	1.10E-05	1.78E-06	8.72E-06
9.98E+03	1.19E-06	6.18E-06	9.84E-07	4.97E-06
1.28E+04	6.36E-07	3.43E-06	5.34E-07	2.79E-06
1.64E+04	3.36E-07	1.88E-06	2.85E-07	1.54E-06
2.10E+04	1.75E-07	1.02E-06	1.51E-07	8.43E-07
2.70E+04	9.06E-08	5.44E-07	7.89E-08	4.57E-07
3.46E+04	4.65E-08	2.90E-07	4.10E-08	2.46E-07
4.43E+04	2.37E-08	1.53E-07	2.12E-08	1.32E-07
5.68E+04	1.20E-08	8.07E-08	1.09E-08	7.02E-08
7.28E+04	6.08E-09	4.24E-08	5.57E-09	3.73E-08
9.33E+04	3.07E-09	2.22E-08	2.84E-09	1.97E-08

Figure 12. CREME96 Galactic Cosmic Ray Energy Spectra for solar minimum conditions and nominal (quiet) activity.

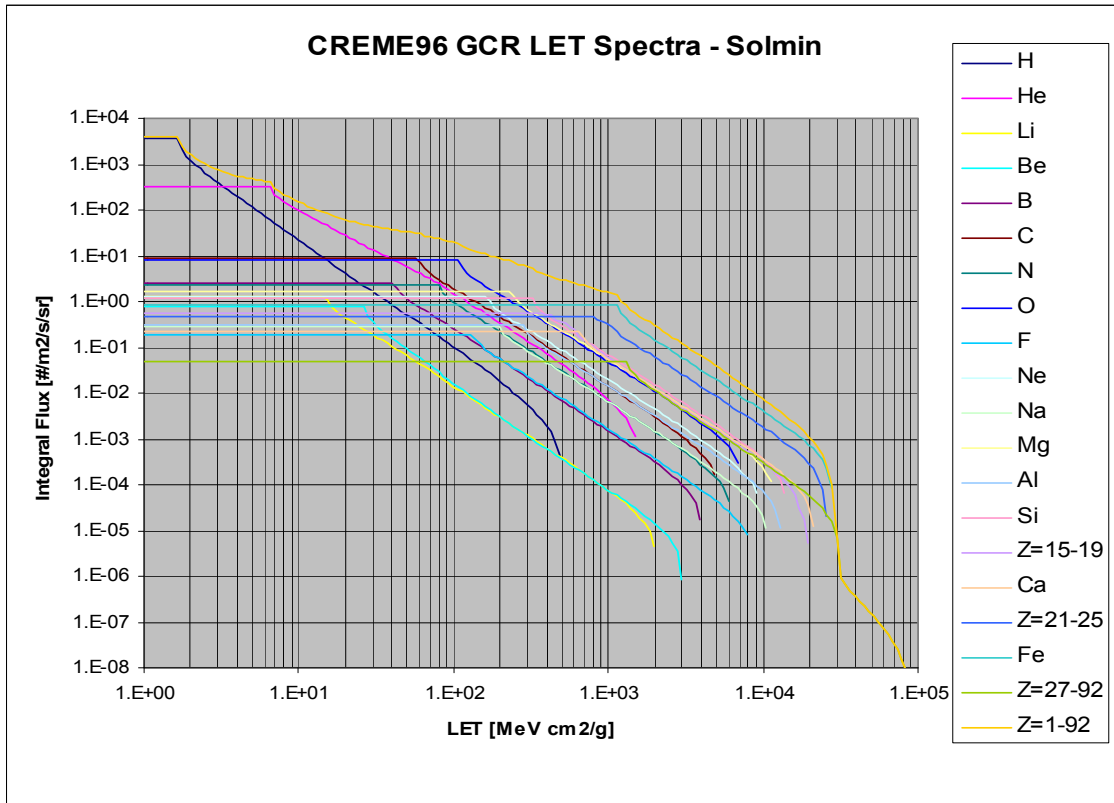| Particle Energy [MeV/nuc]	Solar Orbiter – CREME96 GCR Spectra – Worst Week Differential Flux [#/m2/sec/sr/(MeV/nuc)]			
	H (Z=1)	He (Z=2)	Li (Z=3)	Be (Z=4)
1.02E+00	5.80E+08	2.93E+07	1.14E-02	6.08E-04
1.30E+00	4.56E+08	2.16E+07	9.35E-03	5.56E-04
1.67E+00	3.52E+08	1.56E+07	5.93E-03	3.93E-04
2.14E+00	2.68E+08	1.09E+07	3.69E-03	2.71E-04
2.75E+00	2.01E+08	7.49E+06	2.26E-03	1.85E-04
3.52E+00	1.47E+08	4.98E+06	1.39E-03	1.26E-04
4.51E+00	1.05E+08	3.21E+06	8.78E-04	8.84E-05
5.78E+00	7.39E+07	2.01E+06	5.81E-04	6.49E-05
7.42E+00	5.07E+07	1.21E+06	4.15E-04	5.14E-05
9.51E+00	3.38E+07	7.06E+05	3.29E-04	4.53E-05
1.22E+01	2.18E+07	3.96E+05	2.93E-04	4.49E-05
1.56E+01	1.37E+07	1.68E+05	2.94E-04	5.02E-05
2.00E+01	8.37E+06	6.57E+04	3.27E-04	6.21E-05
2.57E+01	4.93E+06	2.58E+04	3.89E-04	8.24E-05
3.29E+01	2.81E+06	1.01E+04	4.77E-04	1.13E-04
4.22E+01	1.54E+06	3.96E+03	5.83E-04	1.54E-04
5.41E+01	8.17E+05	1.55E+03	6.99E-04	2.05E-04
6.94E+01	4.17E+05	6.08E+02	8.13E-04	2.63E-04
8.89E+01	2.06E+05	2.39E+02	9.13E-04	3.27E-04
1.14E+02	9.78E+04	9.35E+01	9.90E-04	3.89E-04
1.46E+02	4.50E+04	3.67E+01	1.03E-03	4.45E-04
1.87E+02	2.01E+04	1.44E+01	1.05E-03	4.88E-04
2.40E+02	8.66E+03	5.64E+00	1.02E-03	5.13E-04
3.08E+02	3.66E+03	2.21E+00	9.63E-04	5.17E-04
3.95E+02	1.50E+03	8.67E-01	8.78E-04	4.99E-04
5.06E+02	5.79E+02	3.40E-01	7.71E-04	4.59E-04
6.49E+02	2.01E+02	1.33E-01	6.49E-04	4.00E-04
8.32E+02	7.90E+01	5.23E-02	5.22E-04	3.30E-04
1.07E+03	3.10E+01	2.04E-02	4.01E-04	2.57E-04
1.37E+03	1.22E+01	8.04E-03	2.93E-04	1.89E-04
1.75E+03	4.79E+00	3.15E-03	2.05E-04	1.31E-04
2.25E+03	1.88E+00	1.24E-03	1.37E-04	8.62E-05
2.88E+03	7.39E-01	4.84E-04	8.79E-05	5.41E-05
3.69E+03	2.91E-01	1.91E-04	5.44E-05	3.25E-05
4.74E+03	1.14E-01	7.44E-05	3.25E-05	1.88E-05
6.07E+03	4.48E-02	2.92E-05	1.89E-05	1.05E-05
7.78E+03	1.77E-02	1.15E-05	1.08E-05	5.75E-06
9.98E+03	6.91E-03	4.50E-06	5.99E-06	3.07E-06
1.28E+04	2.72E-03	1.77E-06	3.28E-06	1.61E-06
1.64E+04	1.07E-03	6.91E-07	1.77E-06	8.29E-07
2.10E+04	4.19E-04	2.71E-07	9.44E-07	4.22E-07
2.70E+04	1.65E-04	1.06E-07	5.00E-07	2.13E-07
3.46E+04	6.46E-05	4.17E-08	2.63E-07	1.07E-07
4.43E+04	2.54E-05	1.64E-08	1.37E-07	5.31E-08
5.68E+04	9.98E-06	6.40E-09	7.13E-08	2.63E-08
7.28E+04	3.92E-06	2.51E-09	3.69E-08	1.30E-08
9.33E+04	1.54E-06	9.84E-10	1.91E-08	6.38E-09

Figure 13. CREME96 Galactic Cosmic Ray Energy Spectra for the worst week of a large SEPE (scaled)

Particle Energy [MeV/nuc]	Solar Orbiter – CREME96 GCR Spectra – Worst Week Differential Flux [#/m2/sec/sr/(MeV/nuc)]			
	B (Z=5)	C (Z=6)	N (Z=7)	O (Z=8)
1.02E+00	1.66E-02	3.43E+05	8.78E+04	7.28E+05
1.30E+00	1.39E-02	2.53E+05	6.46E+04	5.36E+05
1.67E+00	8.92E-03	1.82E+05	4.66E+04	3.86E+05
2.14E+00	5.58E-03	1.28E+05	3.28E+04	2.72E+05
2.75E+00	3.45E-03	8.74E+04	2.24E+04	1.85E+05
3.52E+00	2.13E-03	5.80E+04	1.49E+04	1.23E+05
4.51E+00	1.35E-03	3.75E+04	9.61E+03	7.96E+04
5.78E+00	8.98E-04	2.34E+04	6.01E+03	4.98E+04
7.42E+00	6.46E-04	1.41E+04	3.63E+03	3.01E+04
9.51E+00	5.16E-04	8.24E+03	2.11E+03	1.75E+04
1.22E+01	4.69E-04	4.62E+03	1.18E+03	9.82E+03
1.56E+01	4.80E-04	1.96E+03	5.00E+02	4.15E+03
2.00E+01	5.47E-04	7.66E+02	1.96E+02	1.63E+03
2.57E+01	6.70E-04	3.00E+02	7.70E+01	6.38E+02
3.29E+01	8.48E-04	1.18E+02	3.01E+01	2.50E+02
4.22E+01	1.07E-03	4.61E+01	1.18E+01	9.80E+01
5.41E+01	1.32E-03	1.80E+01	4.64E+00	3.85E+01
6.94E+01	1.59E-03	7.10E+00	1.82E+00	1.51E+01
8.89E+01	1.83E-03	2.78E+00	7.12E-01	5.92E+00
1.14E+02	2.03E-03	1.09E+00	2.79E-01	2.32E+00
1.46E+02	2.17E-03	4.28E-01	1.10E-01	9.09E-01
1.87E+02	2.23E-03	1.68E-01	4.29E-02	3.57E-01
2.40E+02	2.20E-03	6.58E-02	1.69E-02	1.40E-01
3.08E+02	2.08E-03	2.58E-02	6.60E-03	5.49E-02
3.95E+02	1.90E-03	1.01E-02	2.59E-03	2.15E-02
5.06E+02	1.66E-03	3.96E-03	1.02E-03	8.42E-03
6.49E+02	1.38E-03	1.55E-03	3.99E-04	3.30E-03
8.32E+02	1.09E-03	6.10E-04	1.56E-04	1.30E-03
1.07E+03	8.17E-04	2.39E-04	6.12E-05	5.08E-04
1.37E+03	5.80E-04	9.37E-05	2.40E-05	1.99E-04
1.75E+03	3.90E-04	3.67E-05	9.42E-06	7.81E-05
2.25E+03	2.50E-04	1.44E-05	3.70E-06	3.06E-05
2.88E+03	1.53E-04	5.65E-06	1.45E-06	1.20E-05
3.69E+03	8.95E-05	2.21E-06	5.68E-07	4.71E-06
4.74E+03	5.06E-05	8.69E-07	2.22E-07	1.84E-06
6.07E+03	2.77E-05	3.40E-07	8.72E-08	7.24E-07
7.78E+03	1.48E-05	1.33E-07	3.43E-08	2.84E-07
9.98E+03	7.70E-06	5.23E-08	1.35E-08	1.11E-07
1.28E+04	3.94E-06	2.06E-08	5.26E-09	4.37E-08
1.64E+04	1.98E-06	8.05E-09	2.06E-09	1.71E-08
2.10E+04	9.88E-07	3.16E-09	8.09E-10	6.71E-09
2.70E+04	4.87E-07	1.24E-09	3.18E-10	2.63E-09
3.46E+04	2.38E-07	4.85E-10	1.24E-10	1.03E-09
4.43E+04	1.16E-07	1.91E-10	4.88E-11	4.05E-10
5.68E+04	5.59E-08	7.47E-11	1.92E-11	1.59E-10
7.28E+04	2.69E-08	2.92E-11	7.51E-12	6.22E-11
9.33E+04	1.29E-08	1.15E-11	2.95E-12	2.44E-11

Figure 14. CREME96 Galactic Cosmic Ray Energy Spectra for the worst week of a large SEPE (scaled)

Particle Energy [MeV/nuc]	Solar Orbiter – CREME96 GCR Spectra – Worst Week Differential Flux [#/m2/sec/sr/(MeV/nuc)]			
	F (Z=9)	Ne (Z=10)	Na (Z=11)	Mg (Z=12)
1.02E+00	3.31E+01	1.55E+05	1.27E+04	1.50E+05
1.30E+00	2.45E+01	1.14E+05	9.36E+03	1.11E+05
1.67E+00	1.77E+01	8.23E+04	6.74E+03	7.98E+04
2.14E+00	1.24E+01	5.79E+04	4.74E+03	5.60E+04
2.75E+00	8.47E+00	3.96E+04	3.24E+03	3.84E+04
3.52E+00	5.63E+00	2.63E+04	2.16E+03	2.55E+04
4.51E+00	3.63E+00	1.70E+04	1.38E+03	1.64E+04
5.78E+00	2.27E+00	1.06E+04	8.69E+02	1.03E+04
7.42E+00	1.37E+00	6.41E+03	5.25E+02	6.20E+03
9.51E+00	7.99E-01	3.73E+03	3.06E+02	3.61E+03
1.22E+01	4.47E-01	2.10E+03	1.71E+02	2.02E+03
1.56E+01	1.89E-01	8.84E+02	7.24E+01	8.56E+02
2.00E+01	7.42E-02	3.47E+02	2.83E+01	3.35E+02
2.57E+01	2.91E-02	1.36E+02	1.11E+01	1.32E+02
3.29E+01	1.14E-02	5.33E+01	4.37E+00	5.16E+01
4.22E+01	4.47E-03	2.10E+01	1.71E+00	2.02E+01
5.41E+01	1.75E-03	8.19E+00	6.71E-01	7.92E+00
6.94E+01	6.87E-04	3.21E+00	2.63E-01	3.11E+00
8.89E+01	2.69E-04	1.26E+00	1.03E-01	1.22E+00
1.14E+02	1.06E-04	4.94E-01	4.04E-02	4.78E-01
1.46E+02	4.14E-05	1.94E-01	1.59E-02	1.88E-01
1.87E+02	1.63E-05	7.59E-02	6.22E-03	7.35E-02
2.40E+02	6.38E-06	2.98E-02	2.44E-03	2.88E-02
3.08E+02	2.50E-06	1.17E-02	9.56E-04	1.13E-02
3.95E+02	9.80E-07	4.58E-03	3.75E-04	4.43E-03
5.06E+02	3.85E-07	1.79E-03	1.47E-04	1.74E-03
6.49E+02	1.51E-07	7.04E-04	5.77E-05	6.82E-04
8.32E+02	5.91E-08	2.76E-04	2.26E-05	2.67E-04
1.07E+03	2.31E-08	1.08E-04	8.86E-06	1.05E-04
1.37E+03	9.08E-09	4.24E-05	3.48E-06	4.10E-05
1.75E+03	3.56E-09	1.66E-05	1.36E-06	1.61E-05
2.25E+03	1.40E-09	6.53E-06	5.35E-07	6.31E-06
2.88E+03	5.47E-10	2.57E-06	2.10E-07	2.48E-06
3.69E+03	2.15E-10	1.00E-06	8.22E-08	9.72E-07
4.74E+03	8.42E-11	3.94E-07	3.23E-08	3.81E-07
6.07E+03	3.30E-11	1.54E-07	1.26E-08	1.50E-07
7.78E+03	1.30E-11	6.05E-08	4.95E-09	5.85E-08
9.98E+03	5.08E-12	2.37E-08	1.94E-09	2.30E-08
1.28E+04	1.99E-12	9.30E-09	7.62E-10	9.00E-09
1.64E+04	7.81E-13	3.64E-09	2.98E-10	3.53E-09
2.10E+04	3.06E-13	1.44E-09	1.17E-10	1.38E-09
2.70E+04	1.20E-13	5.61E-10	4.58E-11	5.42E-10
3.46E+04	4.71E-14	2.20E-10	1.80E-11	2.13E-10
4.43E+04	1.84E-14	8.62E-11	7.06E-12	8.34E-11
5.68E+04	7.24E-15	3.38E-11	2.77E-12	3.28E-11
7.28E+04	2.83E-15	1.32E-11	1.08E-12	1.28E-11
9.33E+04	1.11E-15	5.19E-12	4.25E-13	5.03E-12

Figure 15. CREME96 Galactic Cosmic Ray Energy Spectra for the worst week of a large SEPE (scaled)

Particle Energy [MeV/nuc]	Solar Orbiter – CREME96 GCR Spectra – Worst Week Differential Flux [#/m2/sec/sr/(MeV/nuc)]			
	Al (Z=13)	Si (Z=14)	Ca (Z=20)	Fe (Z=26)
1.02E+00	1.33E+04	2.62E+05	3.51E+04	1.96E+05
1.30E+00	9.80E+03	1.93E+05	2.59E+04	1.44E+05
1.67E+00	7.06E+03	1.38E+05	1.87E+04	1.04E+05
2.14E+00	4.97E+03	9.75E+04	1.31E+04	7.29E+04
2.75E+00	3.39E+03	6.67E+04	8.97E+03	4.99E+04
3.52E+00	2.26E+03	4.43E+04	5.96E+03	3.31E+04
4.51E+00	1.46E+03	2.86E+04	3.85E+03	2.15E+04
5.78E+00	9.09E+02	1.79E+04	2.40E+03	1.33E+04
7.42E+00	5.50E+02	1.08E+04	1.45E+03	8.08E+03
9.51E+00	3.20E+02	6.29E+03	8.45E+02	4.70E+03
1.22E+01	1.79E+02	3.53E+03	4.74E+02	2.64E+03
1.56E+01	7.58E+01	1.49E+03	2.01E+02	1.42E+03
2.00E+01	2.97E+01	5.84E+02	7.85E+01	6.22E+02
2.57E+01	1.16E+01	2.29E+02	3.07E+01	2.44E+02
3.29E+01	4.57E+00	8.99E+01	1.21E+01	9.60E+01
4.22E+01	1.79E+00	3.52E+01	4.74E+00	3.77E+01
5.41E+01	7.02E-01	1.38E+01	1.85E+00	1.49E+01
6.94E+01	2.76E-01	5.42E+00	7.28E-01	5.82E+00
8.89E+01	1.08E-01	2.12E+00	2.86E-01	2.29E+00
1.14E+02	4.23E-02	8.33E-01	1.12E-01	8.98E-01
1.46E+02	1.66E-02	3.26E-01	4.38E-02	3.98E-01
1.87E+02	6.52E-03	1.28E-01	1.71E-02	1.96E-01
2.40E+02	2.55E-03	5.02E-02	6.74E-03	9.60E-02
3.08E+02	1.00E-03	1.97E-02	2.64E-03	4.71E-02
3.95E+02	3.92E-04	7.72E-03	1.04E-03	2.31E-02
5.06E+02	1.54E-04	3.02E-03	4.06E-04	1.14E-02
6.49E+02	6.03E-05	1.19E-03	1.60E-04	5.59E-03
8.32E+02	2.36E-05	4.66E-04	6.25E-05	2.74E-03
1.07E+03	9.28E-06	1.83E-04	2.45E-05	1.35E-03
1.37E+03	3.64E-06	7.16E-05	9.61E-06	6.63E-04
1.75E+03	1.42E-06	2.81E-05	3.77E-06	3.25E-04
2.25E+03	5.59E-07	1.10E-05	1.47E-06	1.60E-04
2.88E+03	2.20E-07	4.32E-06	5.79E-07	7.86E-05
3.69E+03	8.60E-08	1.69E-06	2.27E-07	3.86E-05
4.74E+03	3.38E-08	6.63E-07	8.92E-08	1.89E-05
6.07E+03	1.32E-08	2.60E-07	3.49E-08	9.32E-06
7.78E+03	5.18E-09	1.02E-07	1.37E-08	4.57E-06
9.98E+03	2.03E-09	4.00E-08	5.37E-09	2.25E-06
1.28E+04	7.98E-10	1.56E-08	2.11E-09	1.10E-06
1.64E+04	3.12E-10	6.15E-09	8.26E-10	5.42E-07
2.10E+04	1.23E-10	2.41E-09	3.24E-10	2.67E-07
2.70E+04	4.80E-11	9.45E-10	1.27E-10	1.31E-07
3.46E+04	1.88E-11	3.71E-10	4.98E-11	6.44E-08
4.43E+04	7.39E-12	1.45E-10	1.96E-11	3.16E-08
5.68E+04	2.90E-12	5.70E-11	7.66E-12	1.55E-08
7.28E+04	1.14E-12	2.24E-11	3.00E-12	7.63E-09
9.33E+04	4.46E-13	8.76E-12	1.18E-12	3.75E-09

Figure 16. CREME96 Galactic Cosmic Ray Energy Spectra for the worst week of a large SEPE (scaled)

Particle Energy [MeV/nuc]	Solar Orbiter – CREME96 GCR Spectra – Worst Day Differential Flux [#/m2/sec/sr/(MeV/nuc)]			
	H (Z=1)	He (Z=2)	Li (Z=3)	Be (Z=4)
1.02E+00	4.05E+09	1.56E+08	1.14E-02	6.08E-04
1.30E+00	3.15E+09	1.15E+08	9.35E-03	5.56E-04
1.67E+00	2.40E+09	8.29E+07	5.93E-03	3.93E-04
2.14E+00	1.80E+09	5.83E+07	3.69E-03	2.71E-04
2.75E+00	1.33E+09	3.99E+07	2.26E-03	1.85E-04
3.52E+00	9.59E+08	2.65E+07	1.39E-03	1.26E-04
4.51E+00	6.76E+08	1.71E+07	8.78E-04	8.84E-05
5.78E+00	4.64E+08	1.07E+07	5.81E-04	6.49E-05
7.42E+00	3.09E+08	6.45E+06	4.15E-04	5.14E-05
9.51E+00	1.99E+08	3.76E+06	3.29E-04	4.53E-05
1.22E+01	1.25E+08	2.11E+06	2.93E-04	4.49E-05
1.56E+01	7.56E+07	1.13E+06	2.94E-04	5.02E-05
2.00E+01	4.39E+07	4.18E+05	3.27E-04	6.21E-05
2.57E+01	2.45E+07	1.50E+05	3.89E-04	8.24E-05
3.29E+01	1.32E+07	5.33E+04	4.77E-04	1.13E-04
4.22E+01	6.74E+06	1.91E+04	5.83E-04	1.54E-04
5.41E+01	3.31E+06	6.82E+03	6.99E-04	2.05E-04
6.94E+01	1.56E+06	2.44E+03	8.13E-04	2.63E-04
8.89E+01	7.04E+05	8.71E+02	9.13E-04	3.27E-04
1.14E+02	3.05E+05	3.11E+02	9.90E-04	3.89E-04
1.46E+02	1.28E+05	1.11E+02	1.03E-03	4.45E-04
1.87E+02	5.19E+04	3.98E+01	1.05E-03	4.88E-04
2.40E+02	2.07E+04	1.42E+01	1.02E-03	5.13E-04
3.08E+02	8.06E+03	5.09E+00	9.63E-04	5.17E-04
3.95E+02	3.10E+03	1.82E+00	8.78E-04	4.99E-04
5.06E+02	1.12E+03	6.50E-01	7.71E-04	4.59E-04
6.49E+02	3.58E+02	2.32E-01	6.49E-04	4.00E-04
8.32E+02	1.28E+02	8.31E-02	5.22E-04	3.30E-04
1.07E+03	4.57E+01	2.97E-02	4.01E-04	2.57E-04
1.37E+03	1.64E+01	1.06E-02	2.93E-04	1.89E-04
1.75E+03	5.84E+00	3.80E-03	2.05E-04	1.31E-04
2.25E+03	2.08E+00	1.36E-03	1.37E-04	8.62E-05
2.88E+03	7.47E-01	4.85E-04	8.79E-05	5.41E-05
3.69E+03	2.67E-01	1.74E-04	5.44E-05	3.25E-05
4.74E+03	9.54E-02	6.20E-05	3.25E-05	1.88E-05
6.07E+03	3.42E-02	2.22E-05	1.89E-05	1.05E-05
7.78E+03	1.22E-02	7.92E-06	1.08E-05	5.75E-06
9.98E+03	4.36E-03	2.83E-06	5.99E-06	3.07E-06
1.28E+04	1.56E-03	1.01E-06	3.28E-06	1.61E-06
1.64E+04	5.58E-04	3.62E-07	1.77E-06	8.29E-07
2.10E+04	1.99E-04	1.30E-07	9.44E-07	4.22E-07
2.70E+04	7.12E-05	4.62E-08	5.00E-07	2.13E-07
3.46E+04	2.54E-05	1.65E-08	2.63E-07	1.07E-07
4.43E+04	9.11E-06	5.92E-09	1.37E-07	5.31E-08
5.68E+04	3.25E-06	2.11E-09	7.13E-08	2.63E-08
7.28E+04	1.16E-06	7.56E-10	3.69E-08	1.30E-08
9.33E+04	4.15E-07	2.71E-10	1.91E-08	6.38E-09

Figure 17. CREME96 Galactic Cosmic Ray Energy Spectra for the worst day of a large SEPE (scaled)

Particle Energy [MeV/nuc]	Solar Orbiter – CREME96 GCR Spectra – Worst Day Differential Flux [#/m2/sec/sr/(MeV/nuc)]			
	B (Z=5)	C (Z=6)	N (Z=7)	O (Z=8)
1.02E+00	1.66E-02	1.50E+06	3.85E+05	3.19E+06
1.30E+00	1.39E-02	1.10E+06	2.83E+05	2.35E+06
1.67E+00	8.92E-03	7.96E+05	2.04E+05	1.69E+06
2.14E+00	5.58E-03	5.59E+05	1.44E+05	1.19E+06
2.75E+00	3.45E-03	3.82E+05	9.80E+04	8.13E+05
3.52E+00	2.13E-03	2.54E+05	6.53E+04	5.41E+05
4.51E+00	1.35E-03	1.64E+05	4.20E+04	3.49E+05
5.78E+00	8.98E-04	1.03E+05	2.63E+04	2.18E+05
7.42E+00	6.46E-04	6.20E+04	1.59E+04	1.32E+05
9.51E+00	5.16E-04	3.61E+04	9.25E+03	7.67E+04
1.22E+01	4.69E-04	2.02E+04	5.18E+03	4.29E+04
1.56E+01	4.80E-04	1.09E+04	2.78E+03	2.31E+04
2.00E+01	5.47E-04	4.01E+03	1.03E+03	8.52E+03
2.57E+01	6.70E-04	1.44E+03	3.67E+02	3.05E+03
3.29E+01	8.48E-04	5.13E+02	1.31E+02	1.09E+03
4.22E+01	1.07E-03	1.83E+02	4.70E+01	3.90E+02
5.41E+01	1.32E-03	6.55E+01	1.68E+01	1.40E+02
6.94E+01	1.59E-03	2.34E+01	5.99E+00	4.98E+01
8.89E+01	1.83E-03	8.37E+00	2.15E+00	1.78E+01
1.14E+02	2.03E-03	3.00E+00	7.67E-01	6.36E+00
1.46E+02	2.17E-03	1.07E+00	2.74E-01	2.27E+00
1.87E+02	2.23E-03	3.82E-01	9.80E-02	8.13E-01
2.40E+02	2.20E-03	1.37E-01	3.51E-02	2.91E-01
3.08E+02	2.08E-03	4.89E-02	1.25E-02	1.04E-01
3.95E+02	1.90E-03	1.75E-02	4.48E-03	3.71E-02
5.06E+02	1.66E-03	6.25E-03	1.60E-03	1.33E-02
6.49E+02	1.38E-03	2.24E-03	5.73E-04	4.75E-03
8.32E+02	1.09E-03	7.98E-04	2.04E-04	1.70E-03
1.07E+03	8.17E-04	2.86E-04	7.32E-05	6.06E-04
1.37E+03	5.80E-04	1.02E-04	2.62E-05	2.17E-04
1.75E+03	3.90E-04	3.64E-05	9.35E-06	7.75E-05
2.25E+03	2.50E-04	1.31E-05	3.34E-06	2.77E-05
2.88E+03	1.53E-04	4.66E-06	1.19E-06	9.91E-06
3.69E+03	8.95E-05	1.66E-06	4.27E-07	3.54E-06
4.74E+03	5.06E-05	5.96E-07	1.52E-07	1.27E-06
6.07E+03	2.77E-05	2.13E-07	5.46E-08	4.52E-07
7.78E+03	1.48E-05	7.61E-08	1.96E-08	1.61E-07
9.98E+03	7.70E-06	2.72E-08	6.97E-09	5.78E-08
1.28E+04	3.94E-06	9.73E-09	2.49E-09	2.07E-08
1.64E+04	1.98E-06	3.48E-09	8.92E-10	7.39E-09
2.10E+04	9.88E-07	1.24E-09	3.19E-10	2.64E-09
2.70E+04	4.87E-07	4.45E-10	1.14E-10	9.45E-10
3.46E+04	2.38E-07	1.59E-10	4.08E-11	3.38E-10
4.43E+04	1.16E-07	5.68E-11	1.46E-11	1.21E-10
5.68E+04	5.59E-08	2.03E-11	5.21E-12	4.32E-11
7.28E+04	2.69E-08	7.25E-12	1.85E-12	1.54E-11
9.33E+04	1.29E-08	2.59E-12	6.65E-13	5.51E-12

Figure 18. CREME96 Galactic Cosmic Ray Energy Spectra for the worst day of a large SEPE (scaled)

Particle Energy [MeV/nuc]	Solar Orbiter – CREME96 GCR Spectra – Worst Day Differential Flux [#/m2/sec/sr/(MeV/nuc)]			
	F (Z=9)	Ne (Z=10)	Na (Z=11)	Mg (Z=12)
1.02E+00	1.45E+02	6.79E+05	5.56E+04	6.57E+05
1.30E+00	1.07E+02	5.00E+05	4.10E+04	4.85E+05
1.67E+00	7.72E+01	3.61E+05	2.96E+04	3.49E+05
2.14E+00	5.42E+01	2.54E+05	2.07E+04	2.45E+05
2.75E+00	3.71E+01	1.73E+05	1.42E+04	1.68E+05
3.52E+00	2.46E+01	1.15E+05	9.44E+03	1.12E+05
4.51E+00	1.59E+01	7.44E+04	6.08E+03	7.20E+04
5.78E+00	9.94E+00	4.65E+04	3.81E+03	4.50E+04
7.42E+00	6.01E+00	2.81E+04	2.30E+03	2.72E+04
9.51E+00	3.49E+00	1.64E+04	1.33E+03	1.59E+04
1.22E+01	1.96E+00	9.16E+03	7.49E+02	8.86E+03
1.56E+01	1.05E+00	4.93E+03	4.03E+02	4.76E+03
2.00E+01	3.89E-01	1.82E+03	1.49E+02	1.75E+03
2.57E+01	1.38E-01	6.49E+02	5.32E+01	6.29E+02
3.29E+01	4.97E-02	2.32E+02	1.91E+01	2.25E+02
4.22E+01	1.78E-02	8.29E+01	6.79E+00	8.03E+01
5.41E+01	6.35E-03	2.97E+01	2.43E+00	2.87E+01
6.94E+01	2.27E-03	1.06E+01	8.69E-01	1.03E+01
8.89E+01	8.12E-04	3.80E+00	3.10E-01	3.67E+00
1.14E+02	2.90E-04	1.36E+00	1.11E-01	1.31E+00
1.46E+02	1.04E-04	4.84E-01	3.96E-02	4.69E-01
1.87E+02	3.71E-05	1.73E-01	1.42E-02	1.68E-01
2.40E+02	1.32E-05	6.20E-02	5.07E-03	5.99E-02
3.08E+02	4.74E-06	2.21E-02	1.82E-03	2.15E-02
3.95E+02	1.69E-06	7.91E-03	6.48E-04	7.66E-03
5.06E+02	6.06E-07	2.83E-03	2.31E-04	2.74E-03
6.49E+02	2.16E-07	1.01E-03	8.28E-05	9.79E-04
8.32E+02	7.73E-08	3.62E-04	2.96E-05	3.49E-04
1.07E+03	2.77E-08	1.30E-04	1.06E-05	1.25E-04
1.37E+03	9.89E-09	4.62E-05	3.78E-06	4.47E-05
1.75E+03	3.53E-09	1.65E-05	1.35E-06	1.60E-05
2.25E+03	1.26E-09	5.91E-06	4.84E-07	5.72E-06
2.88E+03	4.52E-10	2.11E-06	1.73E-07	2.04E-06
3.69E+03	1.61E-10	7.54E-07	6.17E-08	7.30E-07
4.74E+03	5.78E-11	2.69E-07	2.21E-08	2.62E-07
6.07E+03	2.06E-11	9.64E-08	7.90E-09	9.33E-08
7.78E+03	7.38E-12	3.44E-08	2.82E-09	3.34E-08
9.98E+03	2.64E-12	1.23E-08	1.01E-09	1.19E-08
1.28E+04	9.42E-13	4.41E-09	3.61E-10	4.27E-09
1.64E+04	3.37E-13	1.57E-09	1.30E-10	1.52E-09
2.10E+04	1.21E-13	5.63E-10	4.61E-11	5.45E-10
2.70E+04	4.31E-14	2.01E-10	1.65E-11	1.94E-10
3.46E+04	1.54E-14	7.20E-11	5.89E-12	6.96E-11
4.43E+04	5.50E-15	2.58E-11	2.11E-12	2.49E-11
5.68E+04	1.97E-15	9.19E-12	7.53E-13	8.90E-12
7.28E+04	7.04E-16	3.29E-12	2.69E-13	3.18E-12
9.33E+04	2.51E-16	1.17E-12	9.61E-14	1.14E-12

Figure 19. CREME96 Galactic Cosmic Ray Energy Spectra for the worst day of a large SEPE (scaled)

Particle Energy [MeV/nuc]	Solar Orbiter – CREME96 GCR Spectra – Worst Day Differential Flux [#/m2/sec/sr/(MeV/nuc)]			
	Al (Z=13)	Si (Z=14)	Ca (Z=20)	Fe (Z=26)
1.02E+00	5.82E+04	1.15E+06	1.54E+05	1.22E+06
1.30E+00	4.29E+04	8.45E+05	1.13E+05	9.02E+05
1.67E+00	3.09E+04	6.08E+05	8.17E+04	6.49E+05
2.14E+00	2.17E+04	4.27E+05	5.74E+04	4.56E+05
2.75E+00	1.49E+04	2.92E+05	3.92E+04	3.12E+05
3.52E+00	9.88E+03	1.94E+05	2.62E+04	2.07E+05
4.51E+00	6.38E+03	1.25E+05	1.69E+04	1.33E+05
5.78E+00	3.99E+03	7.84E+04	1.05E+04	8.36E+04
7.42E+00	2.40E+03	4.74E+04	6.35E+03	5.05E+04
9.51E+00	1.40E+03	2.76E+04	3.70E+03	2.95E+04
1.22E+01	7.85E+02	1.55E+04	2.07E+03	1.65E+04
1.56E+01	4.22E+02	8.31E+03	1.12E+03	8.86E+03
2.00E+01	1.56E+02	3.06E+03	4.11E+02	4.56E+03
2.57E+01	5.56E+01	1.09E+03	1.47E+02	2.04E+03
3.29E+01	1.99E+01	3.91E+02	5.26E+01	6.63E+02
4.22E+01	7.11E+00	1.40E+02	1.88E+01	2.15E+02
5.41E+01	2.54E+00	5.00E+01	6.72E+00	6.99E+01
6.94E+01	9.09E-01	1.79E+01	2.40E+00	2.26E+01
8.89E+01	3.25E-01	6.39E+00	8.59E-01	7.35E+00
1.14E+02	1.16E-01	2.29E+00	3.07E-01	2.39E+00
1.46E+02	4.15E-02	8.17E-01	1.10E-01	7.75E-01
1.87E+02	1.49E-02	2.92E-01	3.92E-02	2.51E-01
2.40E+02	5.31E-03	1.04E-01	1.40E-02	8.17E-02
3.08E+02	1.89E-03	3.73E-02	5.02E-03	2.65E-02
3.95E+02	6.78E-04	1.33E-02	1.79E-03	8.60E-03
5.06E+02	2.43E-04	4.78E-03	6.40E-04	2.79E-03
6.49E+02	8.67E-05	1.70E-03	2.29E-04	9.06E-04
8.32E+02	3.10E-05	6.10E-04	8.19E-05	2.93E-04
1.07E+03	1.11E-05	2.18E-04	2.92E-05	9.54E-05
1.37E+03	3.96E-06	7.79E-05	1.05E-05	3.10E-05
1.75E+03	1.41E-06	2.78E-05	3.73E-06	1.00E-05
2.25E+03	5.07E-07	9.96E-06	1.33E-06	3.26E-06
2.88E+03	1.80E-07	3.56E-06	4.78E-07	1.06E-06
3.69E+03	6.46E-08	1.27E-06	1.71E-07	3.43E-07
4.74E+03	2.31E-08	4.55E-07	6.11E-08	1.12E-07
6.07E+03	8.27E-09	1.63E-07	2.18E-08	3.62E-08
7.78E+03	2.96E-09	5.82E-08	7.81E-09	1.17E-08
9.98E+03	1.06E-09	2.08E-08	2.79E-09	3.81E-09
1.28E+04	3.77E-10	7.43E-09	9.97E-10	1.24E-09
1.64E+04	1.35E-10	2.65E-09	3.57E-10	4.01E-10
2.10E+04	4.83E-11	9.49E-10	1.27E-10	1.31E-10
2.70E+04	1.73E-11	3.39E-10	4.56E-11	4.23E-11
3.46E+04	6.17E-12	1.21E-10	1.63E-11	1.37E-11
4.43E+04	2.21E-12	4.33E-11	5.83E-12	4.46E-12
5.68E+04	7.89E-13	1.55E-11	2.08E-12	1.45E-12
7.28E+04	2.82E-13	5.54E-12	7.44E-13	4.69E-13
9.33E+04	1.01E-13	1.98E-12	2.67E-13	1.52E-13

Figure 20. CREME96 Galactic Cosmic Ray Energy Spectra for the worst day of a large SEPE (scaled)

Particle Energy [MeV/nuc]	Solar Orbiter – CREME96 GCR Spectra – Peak 5 min Differential Flux [#/m2/sec/sr/(MeV/nuc)]			
	H (Z=1)	He (Z=2)	Li (Z=3)	Be (Z=4)
1.02E+00	1.70E+10	6.54E+08	1.14E-02	6.08E-04
1.30E+00	1.31E+10	4.80E+08	9.35E-03	5.56E-04
1.67E+00	9.97E+09	3.44E+08	5.93E-03	3.93E-04
2.14E+00	7.44E+09	2.40E+08	3.69E-03	2.71E-04
2.75E+00	5.45E+09	1.63E+08	2.26E-03	1.85E-04
3.52E+00	3.90E+09	1.08E+08	1.39E-03	1.26E-04
4.51E+00	2.72E+09	6.90E+07	8.78E-04	8.84E-05
5.78E+00	1.85E+09	4.27E+07	5.81E-04	6.49E-05
7.42E+00	1.22E+09	2.55E+07	4.15E-04	5.14E-05
9.51E+00	7.84E+08	1.47E+07	3.29E-04	4.53E-05
1.22E+01	4.85E+08	8.17E+06	2.93E-04	4.49E-05
1.56E+01	2.90E+08	4.34E+06	2.94E-04	5.02E-05
2.00E+01	1.66E+08	1.59E+06	3.27E-04	6.21E-05
2.57E+01	9.19E+07	5.60E+05	3.89E-04	8.24E-05
3.29E+01	4.88E+07	1.98E+05	4.77E-04	1.13E-04
4.22E+01	2.48E+07	7.00E+04	5.83E-04	1.54E-04
5.41E+01	1.21E+07	2.48E+04	6.99E-04	2.05E-04
6.94E+01	5.63E+06	8.80E+03	8.13E-04	2.63E-04
8.89E+01	2.53E+06	3.14E+03	9.13E-04	3.27E-04
1.14E+02	1.10E+06	1.12E+03	9.90E-04	3.89E-04
1.46E+02	4.61E+05	4.01E+02	1.03E-03	4.45E-04
1.87E+02	1.89E+05	1.45E+02	1.05E-03	4.88E-04
2.40E+02	7.70E+04	5.31E+01	1.02E-03	5.13E-04
3.08E+02	3.11E+04	1.97E+01	9.63E-04	5.17E-04
3.95E+02	1.26E+04	7.39E+00	8.78E-04	4.99E-04
5.06E+02	4.83E+03	2.65E+00	7.71E-04	4.59E-04
6.49E+02	1.59E+03	9.47E-01	6.49E-04	4.00E-04
8.32E+02	5.69E+02	3.39E-01	5.22E-04	3.30E-04
1.07E+03	2.03E+02	1.21E-01	4.01E-04	2.57E-04
1.37E+03	7.28E+01	4.33E-02	2.93E-04	1.89E-04
1.75E+03	2.60E+01	1.55E-02	2.05E-04	1.31E-04
2.25E+03	9.30E+00	5.54E-03	1.37E-04	8.62E-05
2.88E+03	3.33E+00	1.98E-03	8.79E-05	5.41E-05
3.69E+03	1.19E+00	7.07E-04	5.44E-05	3.25E-05
4.74E+03	4.24E-01	2.53E-04	3.25E-05	1.88E-05
6.07E+03	1.52E-01	9.03E-05	1.89E-05	1.05E-05
7.78E+03	5.42E-02	3.23E-05	1.08E-05	5.75E-06
9.98E+03	1.94E-02	1.15E-05	5.99E-06	3.07E-06
1.28E+04	6.93E-03	4.13E-06	3.28E-06	1.61E-06
1.64E+04	2.48E-03	1.47E-06	1.77E-06	8.29E-07
2.10E+04	8.86E-04	5.27E-07	9.44E-07	4.22E-07
2.70E+04	3.18E-04	1.88E-07	5.00E-07	2.13E-07
3.46E+04	1.13E-04	6.74E-08	2.63E-07	1.07E-07
4.43E+04	4.05E-05	2.41E-08	1.37E-07	5.31E-08
5.68E+04	1.45E-05	8.61E-09	7.13E-08	2.63E-08
7.28E+04	5.17E-06	3.09E-09	3.69E-08	1.30E-08
9.33E+04	1.85E-06	1.10E-09	1.91E-08	6.38E-09

Figure 21. CREME96 Galactic Cosmic Ray Energy Spectra for the peak 5 min of a large SEPE (scaled)

Particle Energy [MeV/nuc]	Solar Orbiter – CREME96 GCR Spectra – Peak 5 min Differential Flux [#/m2/sec/sr/(MeV/nuc)]			
	B (Z=5)	C (Z=6)	N (Z=7)	O (Z=8)
1.02E+00	1.66E-02	6.29E+06	1.61E+06	1.33E+07
1.30E+00	1.39E-02	4.61E+06	1.18E+06	9.80E+06
1.67E+00	8.92E-03	3.30E+06	8.47E+05	7.02E+06
2.14E+00	5.58E-03	2.31E+06	5.91E+05	4.90E+06
2.75E+00	3.45E-03	1.56E+06	4.01E+05	3.33E+06
3.52E+00	2.13E-03	1.03E+06	2.65E+05	2.20E+06
4.51E+00	1.35E-03	6.62E+05	1.70E+05	1.41E+06
5.78E+00	8.98E-04	4.10E+05	1.05E+05	8.71E+05
7.42E+00	6.46E-04	2.45E+05	6.29E+04	5.22E+05
9.51E+00	5.16E-04	1.41E+05	3.62E+04	3.01E+05
1.22E+01	4.69E-04	7.84E+04	2.01E+04	1.66E+05
1.56E+01	4.80E-04	4.17E+04	1.07E+04	8.86E+04
2.00E+01	5.47E-04	1.52E+04	3.90E+03	3.23E+04
2.57E+01	6.70E-04	5.37E+03	1.37E+03	1.14E+04
3.29E+01	8.48E-04	1.91E+03	4.86E+02	4.04E+03
4.22E+01	1.07E-03	6.72E+02	1.73E+02	1.42E+03
5.41E+01	1.32E-03	2.37E+02	6.10E+01	5.05E+02
6.94E+01	1.59E-03	8.45E+01	2.16E+01	1.79E+02
8.89E+01	1.83E-03	3.01E+01	7.71E+00	6.39E+01
1.14E+02	2.03E-03	1.07E+01	2.76E+00	2.29E+01
1.46E+02	2.17E-03	3.86E+00	9.89E-01	8.20E+00
1.87E+02	2.23E-03	1.40E+00	3.58E-01	2.97E+00
2.40E+02	2.20E-03	5.09E-01	1.31E-01	1.08E+00
3.08E+02	2.08E-03	1.89E-01	4.84E-02	4.01E-01
3.95E+02	1.90E-03	7.10E-02	1.82E-02	1.51E-01
5.06E+02	1.66E-03	2.54E-02	6.53E-03	5.41E-02
6.49E+02	1.38E-03	9.09E-03	2.34E-03	1.93E-02
8.32E+02	1.09E-03	3.25E-03	8.33E-04	6.91E-03
1.07E+03	8.17E-04	1.16E-03	2.98E-04	2.48E-03
1.37E+03	5.80E-04	4.15E-04	1.07E-04	8.84E-04
1.75E+03	3.90E-04	1.49E-04	3.81E-05	3.16E-04
2.25E+03	2.50E-04	5.31E-05	1.36E-05	1.13E-04
2.88E+03	1.53E-04	1.91E-05	4.86E-06	4.04E-05
3.69E+03	8.95E-05	6.79E-06	1.74E-06	1.45E-05
4.74E+03	5.06E-05	2.43E-06	6.22E-07	5.16E-06
6.07E+03	2.77E-05	8.67E-07	2.22E-07	1.84E-06
7.78E+03	1.48E-05	3.10E-07	7.95E-08	6.59E-07
9.98E+03	7.70E-06	1.11E-07	2.84E-08	2.36E-07
1.28E+04	3.94E-06	3.96E-08	1.02E-08	8.42E-08
1.64E+04	1.98E-06	1.42E-08	3.63E-09	3.01E-08
2.10E+04	9.88E-07	5.07E-09	1.30E-09	1.08E-08
2.70E+04	4.87E-07	1.82E-09	4.65E-10	3.85E-09
3.46E+04	2.38E-07	6.48E-10	1.66E-10	1.37E-09
4.43E+04	1.16E-07	2.31E-10	5.93E-11	4.91E-10
5.68E+04	5.59E-08	8.27E-11	2.12E-11	1.75E-10
7.28E+04	2.69E-08	2.96E-11	7.58E-12	6.29E-11
9.33E+04	1.29E-08	1.06E-11	2.71E-12	2.25E-11

Figure 22. CREME96 Galactic Cosmic Ray Energy Spectra for the peak 5 min of a large SEPE (scaled)

Particle Energy [MeV/nuc]	Solar Orbiter – CREME96 GCR Spectra – Peak 5 min Differential Flux [#/m2/sec/sr/(MeV/nuc)]			
	F (Z=9)	Ne (Z=10)	Na (Z=11)	Mg (Z=12)
1.02E+00	6.10E+02	2.84E+06	2.34E+05	2.76E+06
1.30E+00	4.47E+02	2.08E+06	1.71E+05	2.02E+06
1.67E+00	3.20E+02	1.50E+06	1.23E+05	1.45E+06
2.14E+00	2.24E+02	1.05E+06	8.55E+04	1.01E+06
2.75E+00	1.52E+02	7.10E+05	5.82E+04	6.87E+05
3.52E+00	1.00E+02	4.69E+05	3.84E+04	4.53E+05
4.51E+00	6.41E+01	3.00E+05	2.45E+04	2.90E+05
5.78E+00	3.98E+01	1.85E+05	1.52E+04	1.80E+05
7.42E+00	2.37E+01	1.11E+05	9.09E+03	1.08E+05
9.51E+00	1.37E+01	6.40E+04	5.25E+03	6.20E+04
1.22E+01	7.59E+00	3.56E+04	2.91E+03	3.44E+04
1.56E+01	4.04E+00	1.89E+04	1.55E+03	1.83E+04
2.00E+01	1.47E+00	6.88E+03	5.64E+02	6.67E+03
2.57E+01	5.21E-01	2.44E+03	1.99E+02	2.35E+03
3.29E+01	1.84E-01	8.60E+02	7.05E+01	8.33E+02
4.22E+01	6.52E-02	3.05E+02	2.49E+01	2.95E+02
5.41E+01	2.31E-02	1.08E+02	8.83E+00	1.04E+02
6.94E+01	8.19E-03	3.82E+01	3.14E+00	3.71E+01
8.89E+01	2.92E-03	1.36E+01	1.12E+00	1.32E+01
1.14E+02	1.04E-03	4.86E+00	3.99E-01	4.71E+00
1.46E+02	3.75E-04	1.75E+00	1.44E-01	1.69E+00
1.87E+02	1.36E-04	6.32E-01	5.18E-02	6.12E-01
2.40E+02	4.94E-05	2.31E-01	1.89E-02	2.24E-01
3.08E+02	1.83E-05	8.55E-02	7.00E-03	8.27E-02
3.95E+02	6.88E-06	3.21E-02	2.63E-03	3.11E-02
5.06E+02	2.46E-06	1.15E-02	9.44E-04	1.12E-02
6.49E+02	8.83E-07	4.13E-03	3.38E-04	3.99E-03
8.32E+02	3.15E-07	1.47E-03	1.21E-04	1.42E-03
1.07E+03	1.13E-07	5.27E-04	4.32E-05	5.09E-04
1.37E+03	4.03E-08	1.88E-04	1.54E-05	1.82E-04
1.75E+03	1.44E-08	6.73E-05	5.51E-06	6.52E-05
2.25E+03	5.16E-09	2.40E-05	1.97E-06	2.32E-05
2.88E+03	1.84E-09	8.60E-06	7.05E-07	8.33E-06
3.69E+03	6.58E-10	3.07E-06	2.51E-07	2.97E-06
4.74E+03	2.35E-10	1.10E-06	9.00E-08	1.06E-06
6.07E+03	8.41E-11	3.92E-07	3.21E-08	3.80E-07
7.78E+03	3.01E-11	1.41E-07	1.15E-08	1.36E-07
9.98E+03	1.07E-11	5.03E-08	4.11E-09	4.86E-08
1.28E+04	3.85E-12	1.79E-08	1.47E-09	1.74E-08
1.64E+04	1.37E-12	6.41E-09	5.26E-10	6.21E-09
2.10E+04	4.91E-13	2.30E-09	1.88E-10	2.22E-09
2.70E+04	1.75E-13	8.20E-10	6.72E-11	7.94E-10
3.46E+04	6.27E-14	2.93E-10	2.40E-11	2.83E-10
4.43E+04	2.25E-14	1.05E-10	8.59E-12	1.01E-10
5.68E+04	8.03E-15	3.75E-11	3.07E-12	3.63E-11
7.28E+04	2.87E-15	1.35E-11	1.10E-12	1.30E-11
9.33E+04	1.02E-15	4.79E-12	3.92E-13	4.64E-12

Figure 23. CREME96 Galactic Cosmic Ray Energy Spectra for the peak 5 min of a large SEPE (scaled)

Particle Energy [MeV/nuc]	Solar Orbiter – CREME96 GCR Spectra – Peak 5 min Differential Flux [#/m2/sec/sr/(MeV/nuc)]			
	Al (Z=13)	Si (Z=14)	Ca (Z=20)	Fe (Z=26)
1.02E+00	2.44E+05	4.80E+06	6.45E+05	5.12E+06
1.30E+00	1.79E+05	3.52E+06	4.72E+05	3.76E+06
1.67E+00	1.28E+05	2.53E+06	3.39E+05	2.69E+06
2.14E+00	8.95E+04	1.77E+06	2.36E+05	1.88E+06
2.75E+00	6.08E+04	1.20E+06	1.61E+05	1.28E+06
3.52E+00	4.01E+04	7.90E+05	1.06E+05	8.43E+05
4.51E+00	2.57E+04	5.05E+05	6.79E+04	5.40E+05
5.78E+00	1.59E+04	3.14E+05	4.20E+04	3.34E+05
7.42E+00	9.53E+03	1.88E+05	2.51E+04	1.99E+05
9.51E+00	5.49E+03	1.08E+05	1.45E+04	1.15E+05
1.22E+01	3.05E+03	5.99E+04	8.04E+03	6.39E+04
1.56E+01	1.61E+03	3.19E+04	4.28E+03	3.40E+04
2.00E+01	5.91E+02	1.16E+04	1.56E+03	1.73E+04
2.57E+01	2.08E+02	4.10E+03	5.51E+02	7.66E+03
3.29E+01	7.38E+01	1.45E+03	1.94E+02	2.45E+03
4.22E+01	2.60E+01	5.13E+02	6.90E+01	7.89E+02
5.41E+01	9.25E+00	1.82E+02	2.44E+01	2.54E+02
6.94E+01	3.28E+00	6.45E+01	8.66E+00	8.18E+01
8.89E+01	1.17E+00	2.30E+01	3.09E+00	2.64E+01
1.14E+02	4.17E-01	8.20E+00	1.10E+00	8.57E+00
1.46E+02	1.50E-01	2.95E+00	3.96E-01	2.79E+00
1.87E+02	5.42E-02	1.07E+00	1.44E-01	9.18E-01
2.40E+02	1.98E-02	3.90E-01	5.23E-02	3.05E-01
3.08E+02	7.33E-03	1.44E-01	1.93E-02	1.02E-01
3.95E+02	2.76E-03	5.42E-02	7.28E-03	3.49E-02
5.06E+02	9.88E-04	1.94E-02	2.62E-03	1.14E-02
6.49E+02	3.53E-04	6.95E-03	9.33E-04	3.70E-03
8.32E+02	1.26E-04	2.49E-03	3.34E-04	1.20E-03
1.07E+03	4.52E-05	8.88E-04	1.19E-04	3.89E-04
1.37E+03	1.61E-05	3.18E-04	4.27E-05	1.26E-04
1.75E+03	5.77E-06	1.14E-04	1.52E-05	4.09E-05
2.25E+03	2.06E-06	4.06E-05	5.45E-06	1.33E-05
2.88E+03	7.38E-07	1.45E-05	1.94E-06	4.32E-06
3.69E+03	2.64E-07	5.18E-06	6.96E-07	1.40E-06
4.74E+03	9.42E-08	1.85E-06	2.49E-07	4.55E-07
6.07E+03	3.37E-08	6.63E-07	8.90E-08	1.47E-07
7.78E+03	1.20E-08	2.37E-07	3.19E-08	4.79E-08
9.98E+03	4.31E-09	8.47E-08	1.14E-08	1.55E-08
1.28E+04	1.54E-09	3.02E-08	4.06E-09	5.04E-09
1.64E+04	5.50E-10	1.08E-08	1.45E-09	1.64E-09
2.10E+04	1.97E-10	3.87E-09	5.19E-10	5.31E-10
2.70E+04	7.04E-11	1.38E-09	1.85E-10	1.73E-10
3.46E+04	2.51E-11	4.94E-10	6.64E-11	5.59E-11
4.43E+04	8.99E-12	1.77E-10	2.37E-11	1.82E-11
5.68E+04	3.21E-12	6.32E-11	8.48E-12	5.89E-12
7.28E+04	1.15E-12	2.26E-11	3.04E-12	1.92E-12
9.33E+04	4.10E-13	8.08E-12	1.08E-12	6.21E-13

Figure 24. CREME96 Galactic Cosmic Ray Energy Spectra for the peak 5 min of a large SEPE (scaled)

LET [MeV cm2/g]	Solar Orbiter – CREME96 GCR Spectra – Solmin Integral Flux [#/m2/sec/sr]			
	Z=1-92	H (Z=1)	He (Z=2)	Li (Z=3)
1.07E+00	3.90E+03	3.54E+03	3.27E+02	1.34E+00
1.32E+00	3.90E+03	3.54E+03	3.27E+02	1.34E+00
1.75E+00	2.45E+03	2.10E+03	3.27E+02	1.34E+00
2.31E+00	1.14E+03	7.85E+02	3.27E+02	1.34E+00
3.04E+00	7.47E+02	3.90E+02	3.27E+02	1.34E+00
4.02E+00	5.55E+02	1.98E+02	3.27E+02	1.34E+00
5.31E+00	4.58E+02	1.01E+02	3.27E+02	1.34E+00
7.02E+00	3.03E+02	5.13E+01	2.21E+02	1.34E+00
9.27E+00	1.68E+02	2.59E+01	1.12E+02	1.34E+00
1.22E+01	1.10E+02	1.31E+01	6.68E+01	1.34E+00
1.62E+01	7.73E+01	6.79E+00	4.06E+01	7.92E-01
2.14E+01	5.78E+01	3.56E+00	2.47E+01	3.82E-01
2.82E+01	4.61E+01	1.89E+00	1.51E+01	2.14E-01
3.73E+01	3.92E+01	1.00E+00	9.45E+00	1.21E-01
4.92E+01	3.37E+01	5.33E-01	5.94E+00	6.72E-02
6.50E+01	2.70E+01	2.81E-01	3.55E+00	3.67E-02
8.59E+01	2.18E+01	1.47E-01	2.09E+00	1.97E-02
1.14E+02	1.59E+01	7.60E-02	1.16E+00	1.05E-02
1.50E+02	1.15E+01	3.84E-02	6.38E-01	5.61E-03
1.98E+02	8.78E+00	1.86E-02	3.49E-01	3.00E-03
2.62E+02	6.52E+00	8.38E-03	1.89E-01	1.62E-03
3.45E+02	4.60E+00	3.42E-03	1.01E-01	8.69E-04
4.56E+02	3.30E+00	9.13E-04	5.36E-02	4.66E-04
6.03E+02	2.55E+00	0.00E+00	2.78E-02	2.49E-04
7.96E+02	1.96E+00	0.00E+00	1.38E-02	1.32E-04
1.05E+03	1.51E+00	0.00E+00	6.15E-03	6.76E-05
1.39E+03	6.71E-01	0.00E+00	1.95E-03	3.14E-05
1.84E+03	3.52E-01	0.00E+00	0.00E+00	9.73E-06
2.42E+03	1.92E-01	0.00E+00	0.00E+00	0.00E+00
3.20E+03	1.05E-01	0.00E+00	0.00E+00	0.00E+00
4.23E+03	5.66E-02	0.00E+00	0.00E+00	0.00E+00
5.59E+03	2.98E-02	0.00E+00	0.00E+00	0.00E+00
7.38E+03	1.54E-02	0.00E+00	0.00E+00	0.00E+00
9.75E+03	8.07E-03	0.00E+00	0.00E+00	0.00E+00
1.29E+04	3.96E-03	0.00E+00	0.00E+00	0.00E+00
1.70E+04	1.81E-03	0.00E+00	0.00E+00	0.00E+00
2.25E+04	6.59E-04	0.00E+00	0.00E+00	0.00E+00
2.97E+04	6.96E-06	0.00E+00	0.00E+00	0.00E+00
3.92E+04	3.54E-07	0.00E+00	0.00E+00	0.00E+00
5.18E+04	1.36E-07	0.00E+00	0.00E+00	0.00E+00
6.84E+04	3.89E-08	0.00E+00	0.00E+00	0.00E+00
9.03E+04	1.57E-09	0.00E+00	0.00E+00	0.00E+00

Figure 25. CREME96 Galactic Cosmic Ray LET Spectra for solar minimum conditions and nominal (quiet) activity.

LET [MeV cm2/g]	Solar Orbiter – CREME96 GCR Spectra – Solmin Integral Flux [#/m2/sec/sr]			
	Be (Z=4)	B (Z=5)	C (Z=6)	N (Z=7)
1.07E+00	7.58E-01	2.53E+00	8.50E+00	2.31E+00
1.32E+00	7.58E-01	2.53E+00	8.50E+00	2.31E+00
1.75E+00	7.58E-01	2.53E+00	8.50E+00	2.31E+00
2.31E+00	7.58E-01	2.53E+00	8.50E+00	2.31E+00
3.04E+00	7.58E-01	2.53E+00	8.50E+00	2.31E+00
4.02E+00	7.58E-01	2.53E+00	8.50E+00	2.31E+00
5.31E+00	7.58E-01	2.53E+00	8.50E+00	2.31E+00
7.02E+00	7.58E-01	2.53E+00	8.50E+00	2.31E+00
9.27E+00	7.58E-01	2.53E+00	8.50E+00	2.31E+00
1.22E+01	7.58E-01	2.53E+00	8.50E+00	2.31E+00
1.62E+01	7.58E-01	2.53E+00	8.50E+00	2.31E+00
2.14E+01	7.58E-01	2.53E+00	8.50E+00	2.31E+00
2.82E+01	4.62E-01	2.53E+00	8.50E+00	2.31E+00
3.73E+01	1.91E-01	2.53E+00	8.50E+00	2.31E+00
4.92E+01	9.49E-02	1.21E+00	8.50E+00	2.31E+00
6.50E+01	4.78E-02	6.41E-01	5.12E+00	2.31E+00
8.59E+01	2.40E-02	3.54E-01	2.58E+00	1.57E+00
1.14E+02	1.20E-02	1.94E-01	1.48E+00	7.33E-01
1.50E+02	6.04E-03	1.05E-01	8.50E-01	4.05E-01
1.98E+02	3.07E-03	5.59E-02	4.79E-01	2.25E-01
2.62E+02	1.59E-03	2.97E-02	2.65E-01	1.24E-01
3.45E+02	8.35E-04	1.58E-02	1.45E-01	6.74E-02
4.56E+02	4.45E-04	8.45E-03	7.83E-02	3.66E-02
6.03E+02	2.38E-04	4.55E-03	4.24E-02	1.99E-02
7.96E+02	1.28E-04	2.46E-03	2.31E-02	1.08E-02
1.05E+03	6.84E-05	1.33E-03	1.26E-02	5.89E-03
1.39E+03	3.58E-05	7.15E-04	6.83E-03	3.22E-03
1.84E+03	1.76E-05	3.75E-04	3.66E-03	1.75E-03
2.42E+03	7.28E-06	1.86E-04	1.92E-03	9.36E-04
3.20E+03	0.00E+00	8.07E-05	9.40E-04	4.82E-04
4.23E+03	0.00E+00	0.00E+00	3.96E-04	2.30E-04
5.59E+03	0.00E+00	0.00E+00	0.00E+00	8.18E-05
7.38E+03	0.00E+00	0.00E+00	0.00E+00	0.00E+00
9.75E+03	0.00E+00	0.00E+00	0.00E+00	0.00E+00
1.29E+04	0.00E+00	0.00E+00	0.00E+00	0.00E+00
1.70E+04	0.00E+00	0.00E+00	0.00E+00	0.00E+00
2.25E+04	0.00E+00	0.00E+00	0.00E+00	0.00E+00
2.97E+04	0.00E+00	0.00E+00	0.00E+00	0.00E+00
3.92E+04	0.00E+00	0.00E+00	0.00E+00	0.00E+00
5.18E+04	0.00E+00	0.00E+00	0.00E+00	0.00E+00
6.84E+04	0.00E+00	0.00E+00	0.00E+00	0.00E+00
9.03E+04	0.00E+00	0.00E+00	0.00E+00	0.00E+00

Figure 26. CREME96 Galactic Cosmic Ray LET Spectra for solar minimum conditions and nominal (quiet) activity.

LET [MeV cm2/g]	Solar Orbiter – CREME96 GCR Spectra – Solmin Integral Flux [#/m2/sec/sr]			
	O (Z=8)	F (Z=9)	Ne (Z=10)	Na (Z=11)
1.07E+00	8.00E+00	1.90E-01	1.29E+00	2.78E-01
1.32E+00	8.00E+00	1.90E-01	1.29E+00	2.78E-01
1.75E+00	8.00E+00	1.90E-01	1.29E+00	2.78E-01
2.31E+00	8.00E+00	1.90E-01	1.29E+00	2.78E-01
3.04E+00	8.00E+00	1.90E-01	1.29E+00	2.78E-01
4.02E+00	8.00E+00	1.90E-01	1.29E+00	2.78E-01
5.31E+00	8.00E+00	1.90E-01	1.29E+00	2.78E-01
7.02E+00	8.00E+00	1.90E-01	1.29E+00	2.78E-01
9.27E+00	8.00E+00	1.90E-01	1.29E+00	2.78E-01
1.22E+01	8.00E+00	1.90E-01	1.29E+00	2.78E-01
1.62E+01	8.00E+00	1.90E-01	1.29E+00	2.78E-01
2.14E+01	8.00E+00	1.90E-01	1.29E+00	2.78E-01
2.82E+01	8.00E+00	1.90E-01	1.29E+00	2.78E-01
3.73E+01	8.00E+00	1.90E-01	1.29E+00	2.78E-01
4.92E+01	8.00E+00	1.90E-01	1.29E+00	2.78E-01
6.50E+01	8.00E+00	1.90E-01	1.29E+00	2.78E-01
8.59E+01	8.00E+00	1.90E-01	1.29E+00	2.78E-01
1.14E+02	5.15E+00	1.90E-01	1.29E+00	2.78E-01
1.50E+02	2.48E+00	1.10E-01	1.29E+00	2.78E-01
1.98E+02	1.42E+00	5.61E-02	5.99E-01	2.78E-01
2.62E+02	8.18E-01	3.10E-02	3.24E-01	1.09E-01
3.45E+02	4.64E-01	1.71E-02	1.85E-01	6.12E-02
4.56E+02	2.59E-01	9.36E-03	1.05E-01	3.48E-02
6.03E+02	1.44E-01	5.05E-03	5.88E-02	1.95E-02
7.96E+02	7.88E-02	2.72E-03	3.24E-02	1.08E-02
1.05E+03	4.32E-02	1.46E-03	1.77E-02	5.88E-03
1.39E+03	2.37E-02	7.93E-04	9.66E-03	3.20E-03
1.84E+03	1.30E-02	4.33E-04	5.29E-03	1.74E-03
2.42E+03	7.06E-03	2.36E-04	2.91E-03	9.55E-04
3.20E+03	3.73E-03	1.26E-04	1.58E-03	5.21E-04
4.23E+03	1.88E-03	6.52E-05	8.32E-04	2.79E-04
5.59E+03	8.51E-04	3.16E-05	4.18E-04	1.43E-04
7.38E+03	0.00E+00	1.21E-05	1.87E-04	6.84E-05
9.75E+03	0.00E+00	0.00E+00	0.00E+00	2.30E-05
1.29E+04	0.00E+00	0.00E+00	0.00E+00	0.00E+00
1.70E+04	0.00E+00	0.00E+00	0.00E+00	0.00E+00
2.25E+04	0.00E+00	0.00E+00	0.00E+00	0.00E+00
2.97E+04	0.00E+00	0.00E+00	0.00E+00	0.00E+00
3.92E+04	0.00E+00	0.00E+00	0.00E+00	0.00E+00
5.18E+04	0.00E+00	0.00E+00	0.00E+00	0.00E+00
6.84E+04	0.00E+00	0.00E+00	0.00E+00	0.00E+00
9.03E+04	0.00E+00	0.00E+00	0.00E+00	0.00E+00

Figure 27. CREME96 Galactic Cosmic Ray LET Spectra for solar minimum conditions and nominal (quiet) activity.

LET [MeV cm2/g]	Solar Orbiter – CREME96 GCR Spectra – Solmin Integral Flux [#/m2/sec/sr]			
	Mg (Z=12)	Al (Z=13)	Si (Z=14)	Z=15-19
1.07E+00	1.67E+00	3.01E-01	1.19E+00	5.35E-01
1.32E+00	1.67E+00	3.01E-01	1.19E+00	5.35E-01
1.75E+00	1.67E+00	3.01E-01	1.19E+00	5.35E-01
2.31E+00	1.67E+00	3.01E-01	1.19E+00	5.35E-01
3.04E+00	1.67E+00	3.01E-01	1.19E+00	5.35E-01
4.02E+00	1.67E+00	3.01E-01	1.19E+00	5.35E-01
5.31E+00	1.67E+00	3.01E-01	1.19E+00	5.35E-01
7.02E+00	1.67E+00	3.01E-01	1.19E+00	5.35E-01
9.27E+00	1.67E+00	3.01E-01	1.19E+00	5.35E-01
1.22E+01	1.67E+00	3.01E-01	1.19E+00	5.35E-01
1.62E+01	1.67E+00	3.01E-01	1.19E+00	5.35E-01
2.14E+01	1.67E+00	3.01E-01	1.19E+00	5.35E-01
2.82E+01	1.67E+00	3.01E-01	1.19E+00	5.35E-01
3.73E+01	1.67E+00	3.01E-01	1.19E+00	5.35E-01
4.92E+01	1.67E+00	3.01E-01	1.19E+00	5.35E-01
6.50E+01	1.67E+00	3.01E-01	1.19E+00	5.35E-01
8.59E+01	1.67E+00	3.01E-01	1.19E+00	5.35E-01
1.14E+02	1.67E+00	3.01E-01	1.19E+00	5.35E-01
1.50E+02	1.67E+00	3.01E-01	1.19E+00	5.35E-01
1.98E+02	1.67E+00	3.01E-01	1.19E+00	5.35E-01
2.62E+02	9.92E-01	3.01E-01	1.19E+00	5.35E-01
3.45E+02	4.91E-01	1.31E-01	7.84E-01	5.35E-01
4.56E+02	2.79E-01	7.20E-02	3.53E-01	4.15E-01
6.03E+02	1.59E-01	4.09E-02	1.97E-01	2.36E-01
7.96E+02	8.87E-02	2.30E-02	1.10E-01	1.02E-01
1.05E+03	4.90E-02	1.28E-02	6.13E-02	5.32E-02
1.39E+03	2.68E-02	6.98E-03	3.37E-02	2.80E-02
1.84E+03	1.46E-02	3.81E-03	1.84E-02	1.48E-02
2.42E+03	7.99E-03	2.07E-03	9.97E-03	7.84E-03
3.20E+03	4.38E-03	1.14E-03	5.46E-03	4.18E-03
4.23E+03	2.37E-03	6.20E-04	2.99E-03	2.26E-03
5.59E+03	1.24E-03	3.29E-04	1.60E-03	1.22E-03
7.38E+03	6.12E-04	1.66E-04	8.22E-04	6.50E-04
9.75E+03	2.54E-04	7.53E-05	3.91E-04	3.30E-04
1.29E+04	0.00E+00	1.12E-05	1.28E-04	1.50E-04
1.70E+04	0.00E+00	0.00E+00	0.00E+00	3.07E-05
2.25E+04	0.00E+00	0.00E+00	0.00E+00	0.00E+00
2.97E+04	0.00E+00	0.00E+00	0.00E+00	0.00E+00
3.92E+04	0.00E+00	0.00E+00	0.00E+00	0.00E+00
5.18E+04	0.00E+00	0.00E+00	0.00E+00	0.00E+00
6.84E+04	0.00E+00	0.00E+00	0.00E+00	0.00E+00
9.03E+04	0.00E+00	0.00E+00	0.00E+00	0.00E+00

Figure 28. CREME96 Galactic Cosmic Ray LET Spectra for solar minimum conditions and nominal (quiet) activity.

LET [MeV cm2/g]	Solar Orbiter – CREME96 GCR Spectra – Solmin Integral Flux [#/m2/sec/sr]			
	Ca (Z=20)	Z=21-25	Fe (Z=26)	Z=27-92
1.07E+00	2.15E-01	4.74E-01	8.59E-01	4.93E-02
1.32E+00	2.15E-01	4.74E-01	8.59E-01	4.93E-02
1.75E+00	2.15E-01	4.74E-01	8.59E-01	4.93E-02
2.31E+00	2.15E-01	4.74E-01	8.59E-01	4.93E-02
3.04E+00	2.15E-01	4.74E-01	8.59E-01	4.93E-02
4.02E+00	2.15E-01	4.74E-01	8.59E-01	4.93E-02
5.31E+00	2.15E-01	4.74E-01	8.59E-01	4.93E-02
7.02E+00	2.15E-01	4.74E-01	8.59E-01	4.93E-02
9.27E+00	2.15E-01	4.74E-01	8.59E-01	4.93E-02
1.22E+01	2.15E-01	4.74E-01	8.59E-01	4.93E-02
1.62E+01	2.15E-01	4.74E-01	8.59E-01	4.93E-02
2.14E+01	2.15E-01	4.74E-01	8.59E-01	4.93E-02
2.82E+01	2.15E-01	4.74E-01	8.59E-01	4.93E-02
3.73E+01	2.15E-01	4.74E-01	8.59E-01	4.93E-02
4.92E+01	2.15E-01	4.74E-01	8.59E-01	4.93E-02
6.50E+01	2.15E-01	4.74E-01	8.59E-01	4.93E-02
8.59E+01	2.15E-01	4.74E-01	8.59E-01	4.93E-02
1.14E+02	2.15E-01	4.74E-01	8.59E-01	4.93E-02
1.50E+02	2.15E-01	4.74E-01	8.59E-01	4.93E-02
1.98E+02	2.15E-01	4.74E-01	8.59E-01	4.93E-02
2.62E+02	2.15E-01	4.74E-01	8.59E-01	4.93E-02
3.45E+02	2.15E-01	4.74E-01	8.59E-01	4.93E-02
4.56E+02	2.15E-01	4.74E-01	8.59E-01	4.93E-02
6.03E+02	2.15E-01	4.74E-01	8.59E-01	4.93E-02
7.96E+02	9.69E-02	4.59E-01	8.59E-01	4.93E-02
1.05E+03	5.04E-02	2.78E-01	8.59E-01	4.93E-02
1.39E+03	2.78E-02	1.30E-01	3.35E-01	3.26E-02
1.84E+03	1.53E-02	7.24E-02	1.73E-01	1.34E-02
2.42E+03	8.37E-03	4.05E-02	9.45E-02	7.08E-03
3.20E+03	4.53E-03	2.23E-02	5.16E-02	3.83E-03
4.23E+03	2.44E-03	1.22E-02	2.80E-02	2.07E-03
5.59E+03	1.33E-03	6.55E-03	1.49E-02	1.11E-03
7.38E+03	7.23E-04	3.56E-03	7.98E-03	5.89E-04
9.75E+03	3.80E-04	1.93E-03	4.36E-03	3.21E-04
1.29E+04	1.88E-04	1.00E-03	2.31E-03	1.72E-04
1.70E+04	7.77E-05	4.72E-04	1.14E-03	8.68E-05
2.25E+04	0.00E+00	1.50E-04	4.71E-04	3.90E-05
2.97E+04	0.00E+00	0.00E+00	0.00E+00	6.96E-06
3.92E+04	0.00E+00	0.00E+00	0.00E+00	3.54E-07
5.18E+04	0.00E+00	0.00E+00	0.00E+00	1.36E-07
6.84E+04	0.00E+00	0.00E+00	0.00E+00	3.89E-08
9.03E+04	0.00E+00	0.00E+00	0.00E+00	1.57E-09

Figure 29. CREME96 Galactic Cosmic Ray LET Spectra for solar minimum conditions and nominal (quiet) activity.

LET [MeV cm2/g]	Solar Orbiter – CREME96 GCR Spectra – Worst Week Integral Flux [#/m2/sec/sr]			
	Z=1-92	H (Z=1)	He (Z=2)	Li (Z=3)
1.07E+00	7.54E+07	7.52E+07	2.01E+05	2.67E+00
1.32E+00	7.54E+07	7.52E+07	2.01E+05	2.67E+00
1.75E+00	7.54E+07	7.52E+07	2.01E+05	2.67E+00
2.31E+00	7.53E+07	7.51E+07	2.01E+05	2.67E+00
3.04E+00	7.48E+07	7.45E+07	2.01E+05	2.67E+00
4.02E+00	7.35E+07	7.34E+07	2.01E+05	2.67E+00
5.31E+00	7.09E+07	7.06E+07	2.01E+05	2.67E+00
7.02E+00	6.58E+07	6.57E+07	2.01E+05	2.67E+00
9.27E+00	5.77E+07	5.75E+07	2.01E+05	2.67E+00
1.22E+01	4.67E+07	4.66E+07	2.01E+05	2.67E+00
1.62E+01	3.45E+07	3.44E+07	1.99E+05	2.67E+00
2.14E+01	2.34E+07	2.31E+07	1.98E+05	2.65E+00
2.82E+01	1.46E+07	1.44E+07	1.92E+05	2.60E+00
3.73E+01	8.60E+06	8.41E+06	1.80E+05	2.51E+00
4.92E+01	4.88E+06	4.71E+06	1.60E+05	2.36E+00
6.50E+01	2.69E+06	2.57E+06	1.28E+05	2.11E+00
8.59E+01	1.46E+06	1.37E+06	9.30E+04	1.75E+00
1.14E+02	7.73E+05	7.11E+05	6.01E+04	1.32E+00
1.50E+02	3.99E+05	3.61E+05	3.63E+04	9.11E-01
1.98E+02	1.97E+05	1.75E+05	2.10E+04	5.78E-01
2.62E+02	9.21E+04	7.90E+04	1.17E+04	3.45E-01
3.45E+02	3.99E+04	3.23E+04	6.40E+03	1.97E-01
4.56E+02	1.31E+04	8.60E+03	3.42E+03	1.10E-01
6.03E+02	2.60E+03	0.00E+00	1.78E+03	6.02E-02
7.96E+02	1.52E+03	0.00E+00	8.84E+02	3.25E-02
1.05E+03	8.61E+02	0.00E+00	3.96E+02	1.68E-02
1.39E+03	4.55E+02	0.00E+00	1.25E+02	7.90E-03
1.84E+03	2.27E+02	0.00E+00	0.00E+00	2.49E-03
2.42E+03	1.51E+02	0.00E+00	0.00E+00	0.00E+00
3.20E+03	9.78E+01	0.00E+00	0.00E+00	0.00E+00
4.23E+03	6.02E+01	0.00E+00	0.00E+00	0.00E+00
5.59E+03	3.44E+01	0.00E+00	0.00E+00	0.00E+00
7.38E+03	1.75E+01	0.00E+00	0.00E+00	0.00E+00
9.75E+03	9.40E+00	0.00E+00	0.00E+00	0.00E+00
1.29E+04	4.56E+00	0.00E+00	0.00E+00	0.00E+00
1.70E+04	1.97E+00	0.00E+00	0.00E+00	0.00E+00
2.25E+04	7.89E-01	0.00E+00	0.00E+00	0.00E+00
2.97E+04	5.61E-03	0.00E+00	0.00E+00	0.00E+00
3.92E+04	1.17E-04	0.00E+00	0.00E+00	0.00E+00
5.18E+04	3.92E-05	0.00E+00	0.00E+00	0.00E+00
6.84E+04	9.53E-06	0.00E+00	0.00E+00	0.00E+00
9.03E+04	6.78E-07	0.00E+00	0.00E+00	0.00E+00

Figure 30. CREME96 Galactic Cosmic Ray LET Spectra for the worst week of a large SEPE (scaled).

LET [MeV cm2/g]	Solar Orbiter – CREME96 GCR Spectra – Worst Week Integral Flux [#/m2/sec/sr]			
	Be (Z=4)	B (Z=5)	C (Z=6)	N (Z=7)
1.07E+00	1.09E+00	2.10E+00	4.18E+02	8.64E+01
1.32E+00	1.09E+00	2.10E+00	4.18E+02	8.64E+01
1.75E+00	1.09E+00	2.10E+00	4.18E+02	8.64E+01
2.31E+00	1.09E+00	2.10E+00	4.18E+02	8.64E+01
3.04E+00	1.09E+00	2.10E+00	4.18E+02	8.64E+01
4.02E+00	1.09E+00	2.10E+00	4.18E+02	8.64E+01
5.31E+00	1.09E+00	2.10E+00	4.18E+02	8.64E+01
7.02E+00	1.09E+00	2.10E+00	4.18E+02	8.64E+01
9.27E+00	1.09E+00	2.10E+00	4.18E+02	8.64E+01
1.22E+01	1.09E+00	2.10E+00	4.18E+02	8.64E+01
1.62E+01	1.09E+00	2.10E+00	4.18E+02	8.64E+01
2.14E+01	1.09E+00	2.10E+00	4.18E+02	8.64E+01
2.82E+01	1.09E+00	2.10E+00	4.18E+02	8.64E+01
3.73E+01	1.09E+00	2.10E+00	4.18E+02	8.64E+01
4.92E+01	1.07E+00	2.10E+00	4.18E+02	8.64E+01
6.50E+01	1.03E+00	2.08E+00	4.18E+02	8.64E+01
8.59E+01	9.61E-01	2.06E+00	4.18E+02	8.64E+01
1.14E+02	8.52E-01	1.98E+00	4.14E+02	8.61E+01
1.50E+02	7.00E-01	1.84E+00	4.04E+02	8.53E+01
1.98E+02	5.21E-01	1.59E+00	3.82E+02	8.32E+01
2.62E+02	3.53E-01	1.26E+00	3.42E+02	7.82E+01
3.45E+02	2.21E-01	8.99E-01	2.79E+02	6.91E+01
4.56E+02	1.31E-01	5.87E-01	2.06E+02	5.58E+01
6.03E+02	7.48E-02	3.57E-01	1.37E+02	4.05E+01
7.96E+02	4.17E-02	2.08E-01	8.53E+01	2.67E+01
1.05E+03	2.29E-02	1.17E-01	5.03E+01	1.64E+01
1.39E+03	1.21E-02	6.46E-02	2.86E+01	9.64E+00
1.84E+03	6.03E-03	3.44E-02	1.57E+01	5.46E+00
2.42E+03	2.53E-03	1.73E-02	8.33E+00	2.98E+00
3.20E+03	0.00E+00	7.59E-03	4.13E+00	1.56E+00
4.23E+03	0.00E+00	0.00E+00	1.74E+00	7.49E-01
5.59E+03	0.00E+00	0.00E+00	0.00E+00	2.68E-01
7.38E+03	0.00E+00	0.00E+00	0.00E+00	0.00E+00
9.75E+03	0.00E+00	0.00E+00	0.00E+00	0.00E+00
1.29E+04	0.00E+00	0.00E+00	0.00E+00	0.00E+00
1.70E+04	0.00E+00	0.00E+00	0.00E+00	0.00E+00
2.25E+04	0.00E+00	0.00E+00	0.00E+00	0.00E+00
2.97E+04	0.00E+00	0.00E+00	0.00E+00	0.00E+00
3.92E+04	0.00E+00	0.00E+00	0.00E+00	0.00E+00
5.18E+04	0.00E+00	0.00E+00	0.00E+00	0.00E+00
6.84E+04	0.00E+00	0.00E+00	0.00E+00	0.00E+00
9.03E+04	0.00E+00	0.00E+00	0.00E+00	0.00E+00

Figure 31. CREME96 Galactic Cosmic Ray LET Spectra for the worst week of a large SEPE (scaled).

LET [MeV cm2/g]	Solar Orbiter – CREME96 GCR Spectra – Worst Week Integral Flux [#/m2/sec/sr]			
	O (Z=8)	F (Z=9)	Ne (Z=10)	Na (Z=11)
1.07E+00	5.65E+02	4.32E-01	8.66E+01	6.95E+00
1.32E+00	5.65E+02	4.32E-01	8.66E+01	6.95E+00
1.75E+00	5.65E+02	4.32E-01	8.66E+01	6.95E+00
2.31E+00	5.65E+02	4.32E-01	8.66E+01	6.95E+00
3.04E+00	5.65E+02	4.32E-01	8.66E+01	6.95E+00
4.02E+00	5.65E+02	4.32E-01	8.66E+01	6.95E+00
5.31E+00	5.65E+02	4.32E-01	8.66E+01	6.95E+00
7.02E+00	5.65E+02	4.32E-01	8.66E+01	6.95E+00
9.27E+00	5.65E+02	4.32E-01	8.66E+01	6.95E+00
1.22E+01	5.65E+02	4.32E-01	8.66E+01	6.95E+00
1.62E+01	5.65E+02	4.32E-01	8.66E+01	6.95E+00
2.14E+01	5.65E+02	4.32E-01	8.66E+01	6.95E+00
2.82E+01	5.65E+02	4.32E-01	8.66E+01	6.95E+00
3.73E+01	5.65E+02	4.32E-01	8.66E+01	6.95E+00
4.92E+01	5.65E+02	4.32E-01	8.66E+01	6.95E+00
6.50E+01	5.65E+02	4.32E-01	8.66E+01	6.95E+00
8.59E+01	5.65E+02	4.32E-01	8.66E+01	6.95E+00
1.14E+02	5.64E+02	4.32E-01	8.66E+01	6.95E+00
1.50E+02	5.63E+02	4.31E-01	8.66E+01	6.95E+00
1.98E+02	5.56E+02	4.27E-01	8.65E+01	6.95E+00
2.62E+02	5.38E+02	4.17E-01	8.57E+01	6.93E+00
3.45E+02	5.00E+02	3.92E-01	8.38E+01	6.85E+00
4.56E+02	4.33E+02	3.52E-01	7.90E+01	6.60E+00
6.03E+02	3.40E+02	2.90E-01	7.00E+01	6.10E+00
7.96E+02	2.41E+02	2.16E-01	5.65E+01	5.21E+00
1.05E+03	1.56E+02	1.45E-01	4.11E+01	4.03E+00
1.39E+03	9.49E+01	9.03E-02	2.72E+01	2.81E+00
1.84E+03	5.52E+01	5.36E-02	1.68E+01	1.80E+00
2.42E+03	3.10E+01	3.07E-02	9.87E+00	1.09E+00
3.20E+03	1.66E+01	1.70E-02	5.58E+00	6.27E-01
4.23E+03	8.48E+00	8.93E-03	3.01E+00	3.47E-01
5.59E+03	3.87E+00	4.38E-03	1.54E+00	1.82E-01
7.38E+03	0.00E+00	1.69E-03	6.91E-01	8.79E-02
9.75E+03	0.00E+00	0.00E+00	0.00E+00	2.97E-02
1.29E+04	0.00E+00	0.00E+00	0.00E+00	0.00E+00
1.70E+04	0.00E+00	0.00E+00	0.00E+00	0.00E+00
2.25E+04	0.00E+00	0.00E+00	0.00E+00	0.00E+00
2.97E+04	0.00E+00	0.00E+00	0.00E+00	0.00E+00
3.92E+04	0.00E+00	0.00E+00	0.00E+00	0.00E+00
5.18E+04	0.00E+00	0.00E+00	0.00E+00	0.00E+00
6.84E+04	0.00E+00	0.00E+00	0.00E+00	0.00E+00
9.03E+04	0.00E+00	0.00E+00	0.00E+00	0.00E+00

Figure 32. CREME96 Galactic Cosmic Ray LET Spectra for the worst week of a large SEPE (scaled).

LET [MeV cm2/g]	Solar Orbiter – CREME96 GCR Spectra – Worst Week Integral Flux [#/m2/sec/sr]			
	Mg (Z=12)	Al (Z=13)	Si (Z=14)	Z=15-19
1.07E+00	6.38E+01	5.58E+00	8.57E+01	1.98E+01
1.32E+00	6.38E+01	5.58E+00	8.57E+01	1.98E+01
1.75E+00	6.38E+01	5.58E+00	8.57E+01	1.98E+01
2.31E+00	6.38E+01	5.58E+00	8.57E+01	1.98E+01
3.04E+00	6.38E+01	5.58E+00	8.57E+01	1.98E+01
4.02E+00	6.38E+01	5.58E+00	8.57E+01	1.98E+01
5.31E+00	6.38E+01	5.58E+00	8.57E+01	1.98E+01
7.02E+00	6.38E+01	5.58E+00	8.57E+01	1.98E+01
9.27E+00	6.38E+01	5.58E+00	8.57E+01	1.98E+01
1.22E+01	6.38E+01	5.58E+00	8.57E+01	1.98E+01
1.62E+01	6.38E+01	5.58E+00	8.57E+01	1.98E+01
2.14E+01	6.38E+01	5.58E+00	8.57E+01	1.98E+01
2.82E+01	6.38E+01	5.58E+00	8.57E+01	1.98E+01
3.73E+01	6.38E+01	5.58E+00	8.57E+01	1.98E+01
4.92E+01	6.38E+01	5.58E+00	8.57E+01	1.98E+01
6.50E+01	6.38E+01	5.58E+00	8.57E+01	1.98E+01
8.59E+01	6.38E+01	5.58E+00	8.57E+01	1.98E+01
1.14E+02	6.38E+01	5.58E+00	8.57E+01	1.98E+01
1.50E+02	6.38E+01	5.58E+00	8.57E+01	1.98E+01
1.98E+02	6.38E+01	5.58E+00	8.57E+01	1.98E+01
2.62E+02	6.36E+01	5.58E+00	8.57E+01	1.98E+01
3.45E+02	6.32E+01	5.56E+00	8.57E+01	1.98E+01
4.56E+02	6.18E+01	5.50E+00	8.51E+01	1.98E+01
6.03E+02	5.85E+01	5.30E+00	8.31E+01	1.97E+01
7.96E+02	5.21E+01	4.86E+00	7.81E+01	1.91E+01
1.05E+03	4.22E+01	4.14E+00	6.87E+01	1.77E+01
1.39E+03	3.07E+01	3.18E+00	5.49E+01	1.52E+01
1.84E+03	2.04E+01	2.20E+00	3.95E+01	1.19E+01
2.42E+03	1.26E+01	1.40E+00	2.58E+01	8.33E+00
3.20E+03	7.42E+00	8.42E-01	1.57E+01	5.33E+00
4.23E+03	4.18E+00	4.84E-01	9.22E+00	3.23E+00
5.59E+03	2.25E+00	2.65E-01	5.13E+00	1.87E+00
7.38E+03	1.12E+00	1.36E-01	2.69E+00	1.02E+00
9.75E+03	4.70E-01	6.24E-02	1.30E+00	5.21E-01
1.29E+04	0.00E+00	9.32E-03	4.29E-01	2.29E-01
1.70E+04	0.00E+00	0.00E+00	0.00E+00	4.22E-03
2.25E+04	0.00E+00	0.00E+00	0.00E+00	0.00E+00
2.97E+04	0.00E+00	0.00E+00	0.00E+00	0.00E+00
3.92E+04	0.00E+00	0.00E+00	0.00E+00	0.00E+00
5.18E+04	0.00E+00	0.00E+00	0.00E+00	0.00E+00
6.84E+04	0.00E+00	0.00E+00	0.00E+00	0.00E+00
9.03E+04	0.00E+00	0.00E+00	0.00E+00	0.00E+00

Figure 33. CREME96 Galactic Cosmic Ray LET Spectra for the worst week of a large SEPE (scaled).

LET [MeV cm2/g]	Solar Orbiter – CREME96 GCR Spectra – Worst Week Integral Flux [#/m2/sec/sr]			
	Ca (Z=20)	Z=21-25	Fe (Z=26)	Z=27-92
1.07E+00	6.73E+00	2.93E+00	5.31E+01	2.27E+00
1.32E+00	6.73E+00	2.93E+00	5.31E+01	2.27E+00
1.75E+00	6.73E+00	2.93E+00	5.31E+01	2.27E+00
2.31E+00	6.73E+00	2.93E+00	5.31E+01	2.27E+00
3.04E+00	6.73E+00	2.93E+00	5.31E+01	2.27E+00
4.02E+00	6.73E+00	2.93E+00	5.31E+01	2.27E+00
5.31E+00	6.73E+00	2.93E+00	5.31E+01	2.27E+00
7.02E+00	6.73E+00	2.93E+00	5.31E+01	2.27E+00
9.27E+00	6.73E+00	2.93E+00	5.31E+01	2.27E+00
1.22E+01	6.73E+00	2.93E+00	5.31E+01	2.27E+00
1.62E+01	6.73E+00	2.93E+00	5.31E+01	2.27E+00
2.14E+01	6.73E+00	2.93E+00	5.31E+01	2.27E+00
2.82E+01	6.73E+00	2.93E+00	5.31E+01	2.27E+00
3.73E+01	6.73E+00	2.93E+00	5.31E+01	2.27E+00
4.92E+01	6.73E+00	2.93E+00	5.31E+01	2.27E+00
6.50E+01	6.73E+00	2.93E+00	5.31E+01	2.27E+00
8.59E+01	6.73E+00	2.93E+00	5.31E+01	2.27E+00
1.14E+02	6.73E+00	2.93E+00	5.31E+01	2.27E+00
1.50E+02	6.73E+00	2.93E+00	5.31E+01	2.27E+00
1.98E+02	6.73E+00	2.93E+00	5.31E+01	2.27E+00
2.62E+02	6.73E+00	2.93E+00	5.31E+01	2.27E+00
3.45E+02	6.73E+00	2.93E+00	5.31E+01	2.27E+00
4.56E+02	6.73E+00	2.93E+00	5.31E+01	2.27E+00
6.03E+02	6.73E+00	2.93E+00	5.31E+01	2.27E+00
7.96E+02	6.69E+00	2.93E+00	5.31E+01	2.27E+00
1.05E+03	6.57E+00	2.90E+00	5.31E+01	2.27E+00
1.39E+03	6.18E+00	2.76E+00	5.14E+01	2.25E+00
1.84E+03	5.46E+00	2.50E+00	4.78E+01	2.12E+00
2.42E+03	4.37E+00	2.13E+00	4.17E+01	1.89E+00
3.20E+03	3.14E+00	1.66E+00	3.34E+01	1.57E+00
4.23E+03	2.03E+00	1.19E+00	2.44E+01	1.18E+00
5.59E+03	1.24E+00	7.80E-01	1.63E+01	8.03E-01
7.38E+03	7.19E-01	4.80E-01	1.01E+01	5.04E-01
9.75E+03	3.94E-01	2.82E-01	6.03E+00	3.05E-01
1.29E+04	1.99E-01	1.54E-01	3.37E+00	1.75E-01
1.70E+04	8.32E-02	7.52E-02	1.71E+00	9.18E-02
2.25E+04	0.00E+00	2.65E-02	7.20E-01	4.15E-02
2.97E+04	0.00E+00	0.00E+00	0.00E+00	5.61E-03
3.92E+04	0.00E+00	0.00E+00	0.00E+00	1.17E-04
5.18E+04	0.00E+00	0.00E+00	0.00E+00	3.92E-05
6.84E+04	0.00E+00	0.00E+00	0.00E+00	9.53E-06
9.03E+04	0.00E+00	0.00E+00	0.00E+00	6.78E-07

Figure 34. CREME96 Galactic Cosmic Ray LET Spectra for the worst week of a large SEPE (scaled).

LET [MeV cm2/g]	Solar Orbiter – CREME96 GCR Spectra – Worst Day Integral Flux [#/m2/sec/sr]			
	Z=1-92	H (Z=1)	He (Z=2)	Li (Z=3)
1.07E+00	3.19E+08	3.19E+08	1.01E+06	8.85E+00
1.32E+00	3.19E+08	3.19E+08	1.01E+06	8.85E+00
1.75E+00	3.19E+08	3.19E+08	1.01E+06	8.85E+00
2.31E+00	3.19E+08	3.19E+08	1.01E+06	8.85E+00
3.04E+00	3.19E+08	3.18E+08	1.01E+06	8.85E+00
4.02E+00	3.15E+08	3.14E+08	1.01E+06	8.85E+00
5.31E+00	3.07E+08	3.06E+08	1.01E+06	8.85E+00
7.02E+00	2.91E+08	2.90E+08	1.01E+06	8.85E+00
9.27E+00	2.60E+08	2.59E+08	1.01E+06	8.85E+00
1.22E+01	2.16E+08	2.15E+08	1.01E+06	8.85E+00
1.62E+01	1.63E+08	1.61E+08	1.00E+06	8.85E+00
2.14E+01	1.12E+08	1.11E+08	9.97E+05	8.84E+00
2.82E+01	7.05E+07	6.95E+07	9.77E+05	8.78E+00
3.73E+01	4.19E+07	4.09E+07	9.31E+05	8.60E+00
4.92E+01	2.39E+07	2.31E+07	8.39E+05	8.22E+00
6.50E+01	1.32E+07	1.26E+07	6.86E+05	7.52E+00
8.59E+01	7.21E+06	6.69E+06	5.09E+05	6.40E+00
1.14E+02	3.84E+06	3.49E+06	3.34E+05	4.97E+00
1.50E+02	1.98E+06	1.78E+06	2.03E+05	3.48E+00
1.98E+02	9.82E+05	8.60E+05	1.18E+05	2.25E+00
2.62E+02	4.58E+05	3.89E+05	6.64E+04	1.36E+00
3.45E+02	1.98E+05	1.59E+05	3.63E+04	7.79E-01
4.56E+02	6.48E+04	4.23E+04	1.94E+04	4.36E-01
6.03E+02	1.27E+04	0.00E+00	1.01E+04	2.39E-01
7.96E+02	6.99E+03	0.00E+00	5.02E+03	1.28E-01
1.05E+03	3.67E+03	0.00E+00	2.25E+03	6.65E-02
1.39E+03	1.70E+03	0.00E+00	7.12E+02	3.12E-02
1.84E+03	6.64E+02	0.00E+00	0.00E+00	9.86E-03
2.42E+03	4.36E+02	0.00E+00	0.00E+00	0.00E+00
3.20E+03	2.79E+02	0.00E+00	0.00E+00	0.00E+00
4.23E+03	1.74E+02	0.00E+00	0.00E+00	0.00E+00
5.59E+03	9.93E+01	0.00E+00	0.00E+00	0.00E+00
7.38E+03	4.95E+01	0.00E+00	0.00E+00	0.00E+00
9.75E+03	2.64E+01	0.00E+00	0.00E+00	0.00E+00
1.29E+04	1.27E+01	0.00E+00	0.00E+00	0.00E+00
1.70E+04	5.41E+00	0.00E+00	0.00E+00	0.00E+00
2.25E+04	2.16E+00	0.00E+00	0.00E+00	0.00E+00
2.97E+04	1.46E-02	0.00E+00	0.00E+00	0.00E+00
3.92E+04	2.12E-04	0.00E+00	0.00E+00	0.00E+00
5.18E+04	6.29E-05	0.00E+00	0.00E+00	0.00E+00
6.84E+04	1.31E-05	0.00E+00	0.00E+00	0.00E+00
9.03E+04	9.25E-07	0.00E+00	0.00E+00	0.00E+00

Figure 35. CREME96 Galactic Cosmic Ray LET Spectra for the worst day of a large SEPE (scaled).

LET [MeV cm2/g]	Solar Orbiter – CREME96 GCR Spectra – Worst Day Integral Flux [#/m2/sec/sr]			
	Be (Z=4)	B (Z=5)	C (Z=6)	N (Z=7)
1.07E+00	3.53E+00	6.82E+00	1.37E+03	2.73E+02
1.32E+00	3.53E+00	6.82E+00	1.37E+03	2.73E+02
1.75E+00	3.53E+00	6.82E+00	1.37E+03	2.73E+02
2.31E+00	3.53E+00	6.82E+00	1.37E+03	2.73E+02
3.04E+00	3.53E+00	6.82E+00	1.37E+03	2.73E+02
4.02E+00	3.53E+00	6.82E+00	1.37E+03	2.73E+02
5.31E+00	3.53E+00	6.82E+00	1.37E+03	2.73E+02
7.02E+00	3.53E+00	6.82E+00	1.37E+03	2.73E+02
9.27E+00	3.53E+00	6.82E+00	1.37E+03	2.73E+02
1.22E+01	3.53E+00	6.82E+00	1.37E+03	2.73E+02
1.62E+01	3.53E+00	6.82E+00	1.37E+03	2.73E+02
2.14E+01	3.53E+00	6.82E+00	1.37E+03	2.73E+02
2.82E+01	3.53E+00	6.82E+00	1.37E+03	2.73E+02
3.73E+01	3.53E+00	6.82E+00	1.37E+03	2.73E+02
4.92E+01	3.51E+00	6.82E+00	1.37E+03	2.73E+02
6.50E+01	3.43E+00	6.81E+00	1.37E+03	2.73E+02
8.59E+01	3.26E+00	6.74E+00	1.37E+03	2.73E+02
1.14E+02	2.96E+00	6.59E+00	1.36E+03	2.73E+02
1.50E+02	2.49E+00	6.21E+00	1.33E+03	2.72E+02
1.98E+02	1.91E+00	5.51E+00	1.28E+03	2.67E+02
2.62E+02	1.31E+00	4.46E+00	1.17E+03	2.54E+02
3.45E+02	8.33E-01	3.24E+00	9.75E+02	2.30E+02
4.56E+02	4.98E-01	2.15E+00	7.33E+02	1.89E+02
6.03E+02	2.86E-01	1.32E+00	4.98E+02	1.40E+02
7.96E+02	1.60E-01	7.72E-01	3.12E+02	9.37E+01
1.05E+03	8.75E-02	4.37E-01	1.85E+02	5.82E+01
1.39E+03	4.65E-02	2.41E-01	1.05E+02	3.43E+01
1.84E+03	2.31E-02	1.28E-01	5.82E+01	1.96E+01
2.42E+03	9.70E-03	6.48E-02	3.09E+01	1.07E+01
3.20E+03	0.00E+00	2.84E-02	1.52E+01	5.59E+00
4.23E+03	0.00E+00	0.00E+00	6.46E+00	2.69E+00
5.59E+03	0.00E+00	0.00E+00	0.00E+00	9.60E-01
7.38E+03	0.00E+00	0.00E+00	0.00E+00	0.00E+00
9.75E+03	0.00E+00	0.00E+00	0.00E+00	0.00E+00
1.29E+04	0.00E+00	0.00E+00	0.00E+00	0.00E+00
1.70E+04	0.00E+00	0.00E+00	0.00E+00	0.00E+00
2.25E+04	0.00E+00	0.00E+00	0.00E+00	0.00E+00
2.97E+04	0.00E+00	0.00E+00	0.00E+00	0.00E+00
3.92E+04	0.00E+00	0.00E+00	0.00E+00	0.00E+00
5.18E+04	0.00E+00	0.00E+00	0.00E+00	0.00E+00
6.84E+04	0.00E+00	0.00E+00	0.00E+00	0.00E+00
9.03E+04	0.00E+00	0.00E+00	0.00E+00	0.00E+00

Figure 36. CREME96 Galactic Cosmic Ray LET Spectra for the worst day of a large SEPE (scaled).

LET [MeV cm2/g]	Solar Orbiter – CREME96 GCR Spectra – Worst Day Integral Flux [#/m2/sec/sr]			
	O (Z=8)	F (Z=9)	Ne (Z=10)	Na (Z=11)
1.07E+00	1.74E+03	1.24E+00	2.55E+02	2.02E+01
1.32E+00	1.74E+03	1.24E+00	2.55E+02	2.02E+01
1.75E+00	1.74E+03	1.24E+00	2.55E+02	2.02E+01
2.31E+00	1.74E+03	1.24E+00	2.55E+02	2.02E+01
3.04E+00	1.74E+03	1.24E+00	2.55E+02	2.02E+01
4.02E+00	1.74E+03	1.24E+00	2.55E+02	2.02E+01
5.31E+00	1.74E+03	1.24E+00	2.55E+02	2.02E+01
7.02E+00	1.74E+03	1.24E+00	2.55E+02	2.02E+01
9.27E+00	1.74E+03	1.24E+00	2.55E+02	2.02E+01
1.22E+01	1.74E+03	1.24E+00	2.55E+02	2.02E+01
1.62E+01	1.74E+03	1.24E+00	2.55E+02	2.02E+01
2.14E+01	1.74E+03	1.24E+00	2.55E+02	2.02E+01
2.82E+01	1.74E+03	1.24E+00	2.55E+02	2.02E+01
3.73E+01	1.74E+03	1.24E+00	2.55E+02	2.02E+01
4.92E+01	1.74E+03	1.24E+00	2.55E+02	2.02E+01
6.50E+01	1.74E+03	1.24E+00	2.55E+02	2.02E+01
8.59E+01	1.74E+03	1.24E+00	2.55E+02	2.02E+01
1.14E+02	1.74E+03	1.24E+00	2.55E+02	2.02E+01
1.50E+02	1.74E+03	1.24E+00	2.55E+02	2.02E+01
1.98E+02	1.73E+03	1.24E+00	2.55E+02	2.02E+01
2.62E+02	1.69E+03	1.22E+00	2.54E+02	2.02E+01
3.45E+02	1.59E+03	1.18E+00	2.50E+02	2.01E+01
4.56E+02	1.41E+03	1.08E+00	2.39E+02	1.96E+01
6.03E+02	1.13E+03	9.09E-01	2.16E+02	1.83E+01
7.96E+02	8.15E+02	6.92E-01	1.79E+02	1.60E+01
1.05E+03	5.35E+02	4.74E-01	1.32E+02	1.26E+01
1.39E+03	3.28E+02	2.98E-01	8.88E+01	8.98E+00
1.84E+03	1.92E+02	1.79E-01	5.52E+01	5.82E+00
2.42E+03	1.08E+02	1.03E-01	3.28E+01	3.54E+00
3.20E+03	5.80E+01	5.69E-02	1.85E+01	2.06E+00
4.23E+03	2.96E+01	3.00E-02	1.00E+01	1.14E+00
5.59E+03	1.35E+01	1.47E-02	5.12E+00	5.98E-01
7.38E+03	0.00E+00	5.68E-03	2.31E+00	2.90E-01
9.75E+03	0.00E+00	0.00E+00	0.00E+00	9.80E-02
1.29E+04	0.00E+00	0.00E+00	0.00E+00	0.00E+00
1.70E+04	0.00E+00	0.00E+00	0.00E+00	0.00E+00
2.25E+04	0.00E+00	0.00E+00	0.00E+00	0.00E+00
2.97E+04	0.00E+00	0.00E+00	0.00E+00	0.00E+00
3.92E+04	0.00E+00	0.00E+00	0.00E+00	0.00E+00
5.18E+04	0.00E+00	0.00E+00	0.00E+00	0.00E+00
6.84E+04	0.00E+00	0.00E+00	0.00E+00	0.00E+00
9.03E+04	0.00E+00	0.00E+00	0.00E+00	0.00E+00

Figure 37. CREME96 Galactic Cosmic Ray LET Spectra for the worst day of a large SEPE (scaled).

LET [MeV cm2/g]	Solar Orbiter – CREME96 GCR Spectra – Worst Day Integral Flux [#/m2/sec/sr]			
	Mg (Z=12)	Al (Z=13)	Si (Z=14)	Z=15-19
1.07E+00	1.82E+02	1.56E+01	2.35E+02	5.27E+01
1.32E+00	1.82E+02	1.56E+01	2.35E+02	5.27E+01
1.75E+00	1.82E+02	1.56E+01	2.35E+02	5.27E+01
2.31E+00	1.82E+02	1.56E+01	2.35E+02	5.27E+01
3.04E+00	1.82E+02	1.56E+01	2.35E+02	5.27E+01
4.02E+00	1.82E+02	1.56E+01	2.35E+02	5.27E+01
5.31E+00	1.82E+02	1.56E+01	2.35E+02	5.27E+01
7.02E+00	1.82E+02	1.56E+01	2.35E+02	5.27E+01
9.27E+00	1.82E+02	1.56E+01	2.35E+02	5.27E+01
1.22E+01	1.82E+02	1.56E+01	2.35E+02	5.27E+01
1.62E+01	1.82E+02	1.56E+01	2.35E+02	5.27E+01
2.14E+01	1.82E+02	1.56E+01	2.35E+02	5.27E+01
2.82E+01	1.82E+02	1.56E+01	2.35E+02	5.27E+01
3.73E+01	1.82E+02	1.56E+01	2.35E+02	5.27E+01
4.92E+01	1.82E+02	1.56E+01	2.35E+02	5.27E+01
6.50E+01	1.82E+02	1.56E+01	2.35E+02	5.27E+01
8.59E+01	1.82E+02	1.56E+01	2.35E+02	5.27E+01
1.14E+02	1.82E+02	1.56E+01	2.35E+02	5.27E+01
1.50E+02	1.82E+02	1.56E+01	2.35E+02	5.27E+01
1.98E+02	1.82E+02	1.56E+01	2.35E+02	5.27E+01
2.62E+02	1.80E+02	1.56E+01	2.35E+02	5.27E+01
3.45E+02	1.80E+02	1.56E+01	2.35E+02	5.27E+01
4.56E+02	1.78E+02	1.55E+01	2.35E+02	5.27E+01
6.03E+02	1.70E+02	1.51E+01	2.31E+02	5.25E+01
7.96E+02	1.55E+02	1.41E+01	2.21E+02	5.14E+01
1.05E+03	1.28E+02	1.23E+01	1.98E+02	4.86E+01
1.39E+03	9.54E+01	9.63E+00	1.61E+02	4.28E+01
1.84E+03	6.41E+01	6.79E+00	1.18E+02	3.42E+01
2.42E+03	4.00E+01	4.37E+00	7.84E+01	2.44E+01
3.20E+03	2.37E+01	2.65E+00	4.85E+01	1.59E+01
4.23E+03	1.35E+01	1.54E+00	2.86E+01	9.68E+00
5.59E+03	7.21E+00	8.41E-01	1.59E+01	5.61E+00
7.38E+03	3.61E+00	4.33E-01	8.38E+00	3.07E+00
9.75E+03	1.51E+00	1.98E-01	4.04E+00	1.57E+00
1.29E+04	0.00E+00	2.97E-02	1.33E+00	6.92E-01
1.70E+04	0.00E+00	0.00E+00	0.00E+00	1.26E-02
2.25E+04	0.00E+00	0.00E+00	0.00E+00	0.00E+00
2.97E+04	0.00E+00	0.00E+00	0.00E+00	0.00E+00
3.92E+04	0.00E+00	0.00E+00	0.00E+00	0.00E+00
5.18E+04	0.00E+00	0.00E+00	0.00E+00	0.00E+00
6.84E+04	0.00E+00	0.00E+00	0.00E+00	0.00E+00
9.03E+04	0.00E+00	0.00E+00	0.00E+00	0.00E+00

Figure 38. CREME96 Galactic Cosmic Ray LET Spectra for the worst day of a large SEPE (scaled).

LET [MeV cm2/g]	Solar Orbiter – CREME96 GCR Spectra – Worst Day Integral Flux [#/m2/sec/sr]			
	Ca (Z=20)	Z=21-25	Fe (Z=26)	Z=27-92
1.07E+00	1.71E+01	5.26E+00	8.75E+01	3.53E+00
1.32E+00	1.71E+01	5.26E+00	8.75E+01	3.53E+00
1.75E+00	1.71E+01	5.26E+00	8.75E+01	3.53E+00
2.31E+00	1.71E+01	5.26E+00	8.75E+01	3.53E+00
3.04E+00	1.71E+01	5.26E+00	8.75E+01	3.53E+00
4.02E+00	1.71E+01	5.26E+00	8.75E+01	3.53E+00
5.31E+00	1.71E+01	5.26E+00	8.75E+01	3.53E+00
7.02E+00	1.71E+01	5.26E+00	8.75E+01	3.53E+00
9.27E+00	1.71E+01	5.26E+00	8.75E+01	3.53E+00
1.22E+01	1.71E+01	5.26E+00	8.75E+01	3.53E+00
1.62E+01	1.71E+01	5.26E+00	8.75E+01	3.53E+00
2.14E+01	1.71E+01	5.26E+00	8.75E+01	3.53E+00
2.82E+01	1.71E+01	5.26E+00	8.75E+01	3.53E+00
3.73E+01	1.71E+01	5.26E+00	8.75E+01	3.53E+00
4.92E+01	1.71E+01	5.26E+00	8.75E+01	3.53E+00
6.50E+01	1.71E+01	5.26E+00	8.75E+01	3.53E+00
8.59E+01	1.71E+01	5.26E+00	8.75E+01	3.53E+00
1.14E+02	1.71E+01	5.26E+00	8.75E+01	3.53E+00
1.50E+02	1.71E+01	5.26E+00	8.75E+01	3.53E+00
1.98E+02	1.71E+01	5.26E+00	8.75E+01	3.53E+00
2.62E+02	1.71E+01	5.26E+00	8.75E+01	3.53E+00
3.45E+02	1.71E+01	5.26E+00	8.75E+01	3.53E+00
4.56E+02	1.71E+01	5.26E+00	8.75E+01	3.53E+00
6.03E+02	1.71E+01	5.26E+00	8.75E+01	3.53E+00
7.96E+02	1.70E+01	5.26E+00	8.75E+01	3.53E+00
1.05E+03	1.69E+01	5.26E+00	8.75E+01	3.53E+00
1.39E+03	1.61E+01	5.22E+00	8.74E+01	3.53E+00
1.84E+03	1.46E+01	5.09E+00	8.64E+01	3.52E+00
2.42E+03	1.19E+01	4.74E+00	8.26E+01	3.42E+00
3.20E+03	8.74E+00	4.05E+00	7.37E+01	3.14E+00
4.23E+03	5.75E+00	3.09E+00	5.91E+01	2.63E+00
5.59E+03	3.54E+00	2.10E+00	4.19E+01	1.94E+00
7.38E+03	2.07E+00	1.32E+00	2.68E+01	1.28E+00
9.75E+03	1.14E+00	7.84E-01	1.63E+01	7.91E-01
1.29E+04	5.75E-01	4.31E-01	9.18E+00	4.60E-01
1.70E+04	2.41E-01	2.12E-01	4.70E+00	2.43E-01
2.25E+04	0.00E+00	7.48E-02	1.98E+00	1.10E-01
2.97E+04	0.00E+00	0.00E+00	0.00E+00	1.46E-02
3.92E+04	0.00E+00	0.00E+00	0.00E+00	2.12E-04
5.18E+04	0.00E+00	0.00E+00	0.00E+00	6.29E-05
6.84E+04	0.00E+00	0.00E+00	0.00E+00	1.31E-05
9.03E+04	0.00E+00	0.00E+00	0.00E+00	9.25E-07

Figure 39. CREME96 Galactic Cosmic Ray LET Spectra for the worst day of a large SEPE (scaled).

LET [MeV cm2/g]	Solar Orbiter – CREME96 GCR Spectra – Peak 5 min Integral Flux [#/m2/sec/sr]			
	Z=1-92	H (Z=1)	He (Z=2)	Li (Z=3)
1.07E+00	1.17E+09	1.17E+09	3.72E+06	3.21E+01
1.32E+00	1.17E+09	1.17E+09	3.72E+06	3.21E+01
1.75E+00	1.17E+09	1.17E+09	3.72E+06	3.21E+01
2.31E+00	1.17E+09	1.17E+09	3.72E+06	3.21E+01
3.04E+00	1.17E+09	1.16E+09	3.72E+06	3.21E+01
4.02E+00	1.16E+09	1.15E+09	3.72E+06	3.21E+01
5.31E+00	1.13E+09	1.13E+09	3.72E+06	3.21E+01
7.02E+00	1.07E+09	1.07E+09	3.72E+06	3.21E+01
9.27E+00	9.60E+08	9.56E+08	3.72E+06	3.21E+01
1.22E+01	7.99E+08	7.95E+08	3.71E+06	3.21E+01
1.62E+01	6.05E+08	6.01E+08	3.71E+06	3.21E+01
2.14E+01	4.15E+08	4.11E+08	3.68E+06	3.21E+01
2.82E+01	2.63E+08	2.59E+08	3.61E+06	3.19E+01
3.73E+01	1.56E+08	1.52E+08	3.44E+06	3.12E+01
4.92E+01	8.93E+07	8.61E+07	3.11E+06	2.98E+01
6.50E+01	4.95E+07	4.70E+07	2.55E+06	2.73E+01
8.59E+01	2.69E+07	2.50E+07	1.89E+06	2.32E+01
1.14E+02	1.44E+07	1.31E+07	1.24E+06	1.82E+01
1.50E+02	7.40E+06	6.63E+06	7.61E+05	1.27E+01
1.98E+02	3.67E+06	3.21E+06	4.42E+05	8.20E+00
2.62E+02	1.71E+06	1.45E+06	2.48E+05	4.95E+00
3.45E+02	7.40E+05	5.92E+05	1.36E+05	2.86E+00
4.56E+02	2.41E+05	1.57E+05	7.25E+04	1.60E+00
6.03E+02	4.71E+04	0.00E+00	3.77E+04	8.75E-01
7.96E+02	2.59E+04	0.00E+00	1.88E+04	4.72E-01
1.05E+03	1.36E+04	0.00E+00	8.41E+03	2.44E-01
1.39E+03	6.24E+03	0.00E+00	2.67E+03	1.15E-01
1.84E+03	2.40E+03	0.00E+00	0.00E+00	3.61E-02
2.42E+03	1.57E+03	0.00E+00	0.00E+00	0.00E+00
3.20E+03	1.01E+03	0.00E+00	0.00E+00	0.00E+00
4.23E+03	6.26E+02	0.00E+00	0.00E+00	0.00E+00
5.59E+03	3.57E+02	0.00E+00	0.00E+00	0.00E+00
7.38E+03	1.78E+02	0.00E+00	0.00E+00	0.00E+00
9.75E+03	9.49E+01	0.00E+00	0.00E+00	0.00E+00
1.29E+04	4.56E+01	0.00E+00	0.00E+00	0.00E+00
1.70E+04	1.94E+01	0.00E+00	0.00E+00	0.00E+00
2.25E+04	7.76E+00	0.00E+00	0.00E+00	0.00E+00
2.97E+04	5.23E-02	0.00E+00	0.00E+00	0.00E+00
3.92E+04	7.67E-04	0.00E+00	0.00E+00	0.00E+00
5.18E+04	2.27E-04	0.00E+00	0.00E+00	0.00E+00
6.84E+04	4.79E-05	0.00E+00	0.00E+00	0.00E+00
9.03E+04	3.37E-06	0.00E+00	0.00E+00	0.00E+00

Figure 40. CREME96 Galactic Cosmic Ray LET Spectra for the peak 5 min of a large SEPE (scaled).

LET [MeV cm2/g]	Solar Orbiter – CREME96 GCR Spectra – Peak 5 min Integral Flux [#/m2/sec/sr]			
	Be (Z=4)	B (Z=5)	C (Z=6)	N (Z=7)
1.07E+00	1.28E+01	2.48E+01	4.95E+03	9.88E+02
1.32E+00	1.28E+01	2.48E+01	4.95E+03	9.88E+02
1.75E+00	1.28E+01	2.48E+01	4.95E+03	9.88E+02
2.31E+00	1.28E+01	2.48E+01	4.95E+03	9.88E+02
3.04E+00	1.28E+01	2.48E+01	4.95E+03	9.88E+02
4.02E+00	1.28E+01	2.48E+01	4.95E+03	9.88E+02
5.31E+00	1.28E+01	2.48E+01	4.95E+03	9.88E+02
7.02E+00	1.28E+01	2.48E+01	4.95E+03	9.88E+02
9.27E+00	1.28E+01	2.48E+01	4.95E+03	9.88E+02
1.22E+01	1.28E+01	2.48E+01	4.95E+03	9.88E+02
1.62E+01	1.28E+01	2.48E+01	4.95E+03	9.88E+02
2.14E+01	1.28E+01	2.48E+01	4.95E+03	9.88E+02
2.82E+01	1.28E+01	2.48E+01	4.95E+03	9.88E+02
3.73E+01	1.28E+01	2.48E+01	4.95E+03	9.88E+02
4.92E+01	1.27E+01	2.46E+01	4.95E+03	9.88E+02
6.50E+01	1.24E+01	2.46E+01	4.95E+03	9.88E+02
8.59E+01	1.18E+01	2.44E+01	4.94E+03	9.88E+02
1.14E+02	1.07E+01	2.39E+01	4.93E+03	9.87E+02
1.50E+02	9.06E+00	2.25E+01	4.84E+03	9.80E+02
1.98E+02	6.92E+00	1.99E+01	4.65E+03	9.64E+02
2.62E+02	4.79E+00	1.61E+01	4.23E+03	9.19E+02
3.45E+02	3.04E+00	1.18E+01	3.53E+03	8.28E+02
4.56E+02	1.82E+00	7.81E+00	2.67E+03	6.83E+02
6.03E+02	1.04E+00	4.80E+00	1.80E+03	5.07E+02
7.96E+02	5.83E-01	2.81E+00	1.14E+03	3.39E+02
1.05E+03	3.20E-01	1.59E+00	6.73E+02	2.11E+02
1.39E+03	1.70E-01	8.80E-01	3.84E+02	1.25E+02
1.84E+03	8.45E-02	4.70E-01	2.12E+02	7.09E+01
2.42E+03	3.54E-02	2.36E-01	1.12E+02	3.89E+01
3.20E+03	0.00E+00	1.04E-01	5.56E+01	2.03E+01
4.23E+03	0.00E+00	0.00E+00	2.35E+01	9.77E+00
5.59E+03	0.00E+00	0.00E+00	0.00E+00	3.49E+00
7.38E+03	0.00E+00	0.00E+00	0.00E+00	0.00E+00
9.75E+03	0.00E+00	0.00E+00	0.00E+00	0.00E+00
1.29E+04	0.00E+00	0.00E+00	0.00E+00	0.00E+00
1.70E+04	0.00E+00	0.00E+00	0.00E+00	0.00E+00
2.25E+04	0.00E+00	0.00E+00	0.00E+00	0.00E+00
2.97E+04	0.00E+00	0.00E+00	0.00E+00	0.00E+00
3.92E+04	0.00E+00	0.00E+00	0.00E+00	0.00E+00
5.18E+04	0.00E+00	0.00E+00	0.00E+00	0.00E+00
6.84E+04	0.00E+00	0.00E+00	0.00E+00	0.00E+00
9.03E+04	0.00E+00	0.00E+00	0.00E+00	0.00E+00

Figure 41. CREME96 Galactic Cosmic Ray LET Spectra for the peak 5 min of a large SEPE (scaled).

LET [MeV cm2/g]	Solar Orbiter – CREME96 GCR Spectra – Peak 5 min Integral Flux [#/m2/sec/sr]			
	O (Z=8)	F (Z=9)	Ne (Z=10)	Na (Z=11)
1.07E+00	6.29E+03	4.50E+00	9.19E+02	7.28E+01
1.32E+00	6.29E+03	4.50E+00	9.19E+02	7.28E+01
1.75E+00	6.29E+03	4.50E+00	9.19E+02	7.28E+01
2.31E+00	6.29E+03	4.50E+00	9.19E+02	7.28E+01
3.04E+00	6.29E+03	4.50E+00	9.19E+02	7.28E+01
4.02E+00	6.29E+03	4.50E+00	9.19E+02	7.28E+01
5.31E+00	6.29E+03	4.50E+00	9.19E+02	7.28E+01
7.02E+00	6.29E+03	4.50E+00	9.19E+02	7.28E+01
9.27E+00	6.29E+03	4.50E+00	9.19E+02	7.28E+01
1.22E+01	6.29E+03	4.50E+00	9.19E+02	7.28E+01
1.62E+01	6.29E+03	4.50E+00	9.19E+02	7.28E+01
2.14E+01	6.29E+03	4.50E+00	9.19E+02	7.28E+01
2.82E+01	6.29E+03	4.50E+00	9.19E+02	7.28E+01
3.73E+01	6.29E+03	4.50E+00	9.19E+02	7.28E+01
4.92E+01	6.29E+03	4.50E+00	9.19E+02	7.28E+01
6.50E+01	6.29E+03	4.50E+00	9.19E+02	7.28E+01
8.59E+01	6.29E+03	4.50E+00	9.19E+02	7.28E+01
1.14E+02	6.27E+03	4.50E+00	9.19E+02	7.28E+01
1.50E+02	6.27E+03	4.48E+00	9.19E+02	7.28E+01
1.98E+02	6.22E+03	4.47E+00	9.19E+02	7.28E+01
2.62E+02	6.08E+03	4.41E+00	9.16E+02	7.26E+01
3.45E+02	5.74E+03	4.24E+00	9.00E+02	7.21E+01
4.56E+02	5.08E+03	3.89E+00	8.61E+02	7.02E+01
6.03E+02	4.08E+03	3.28E+00	7.77E+02	6.59E+01
7.96E+02	2.95E+03	2.49E+00	6.43E+02	5.75E+01
1.05E+03	1.93E+03	1.70E+00	4.76E+02	4.55E+01
1.39E+03	1.19E+03	1.08E+00	3.20E+02	3.24E+01
1.84E+03	6.93E+02	6.45E-01	1.99E+02	2.10E+01
2.42E+03	3.91E+02	3.71E-01	1.18E+02	1.28E+01
3.20E+03	2.11E+02	2.06E-01	6.71E+01	7.42E+00
4.23E+03	1.07E+02	1.08E-01	3.62E+01	4.11E+00
5.59E+03	4.90E+01	5.32E-02	1.84E+01	2.16E+00
7.38E+03	0.00E+00	2.04E-02	8.34E+00	1.04E+00
9.75E+03	0.00E+00	0.00E+00	0.00E+00	3.54E-01
1.29E+04	0.00E+00	0.00E+00	0.00E+00	0.00E+00
1.70E+04	0.00E+00	0.00E+00	0.00E+00	0.00E+00
2.25E+04	0.00E+00	0.00E+00	0.00E+00	0.00E+00
2.97E+04	0.00E+00	0.00E+00	0.00E+00	0.00E+00
3.92E+04	0.00E+00	0.00E+00	0.00E+00	0.00E+00
5.18E+04	0.00E+00	0.00E+00	0.00E+00	0.00E+00
6.84E+04	0.00E+00	0.00E+00	0.00E+00	0.00E+00
9.03E+04	0.00E+00	0.00E+00	0.00E+00	0.00E+00

Figure 42. CREME96 Galactic Cosmic Ray LET Spectra for the peak 5 min of a large SEPE (scaled).

LET [MeV cm2/g]	Solar Orbiter – CREME96 GCR Spectra – Peak 5 min Integral Flux [#/m2/sec/sr]			
	Mg (Z=12)	Al (Z=13)	Si (Z=14)	Z=15-19
1.07E+00	6.53E+02	5.64E+01	8.50E+02	1.91E+02
1.32E+00	6.53E+02	5.64E+01	8.50E+02	1.91E+02
1.75E+00	6.53E+02	5.64E+01	8.50E+02	1.91E+02
2.31E+00	6.53E+02	5.64E+01	8.50E+02	1.91E+02
3.04E+00	6.53E+02	5.64E+01	8.50E+02	1.91E+02
4.02E+00	6.53E+02	5.64E+01	8.50E+02	1.91E+02
5.31E+00	6.53E+02	5.64E+01	8.50E+02	1.91E+02
7.02E+00	6.53E+02	5.64E+01	8.50E+02	1.91E+02
9.27E+00	6.53E+02	5.64E+01	8.50E+02	1.91E+02
1.22E+01	6.53E+02	5.64E+01	8.50E+02	1.91E+02
1.62E+01	6.53E+02	5.64E+01	8.50E+02	1.91E+02
2.14E+01	6.53E+02	5.64E+01	8.50E+02	1.91E+02
2.82E+01	6.53E+02	5.64E+01	8.50E+02	1.91E+02
3.73E+01	6.53E+02	5.64E+01	8.50E+02	1.91E+02
4.92E+01	6.53E+02	5.64E+01	8.50E+02	1.91E+02
6.50E+01	6.53E+02	5.64E+01	8.50E+02	1.91E+02
8.59E+01	6.53E+02	5.64E+01	8.50E+02	1.91E+02
1.14E+02	6.53E+02	5.64E+01	8.50E+02	1.91E+02
1.50E+02	6.53E+02	5.64E+01	8.50E+02	1.91E+02
1.98E+02	6.53E+02	5.64E+01	8.50E+02	1.91E+02
2.62E+02	6.53E+02	5.64E+01	8.50E+02	1.91E+02
3.45E+02	6.50E+02	5.63E+01	8.50E+02	1.91E+02
4.56E+02	6.40E+02	5.59E+01	8.46E+02	1.91E+02
6.03E+02	6.13E+02	5.44E+01	8.32E+02	1.89E+02
7.96E+02	5.55E+02	5.08E+01	7.92E+02	1.85E+02
1.05E+03	4.61E+02	4.42E+01	7.11E+02	1.75E+02
1.39E+03	3.43E+02	3.47E+01	5.80E+02	1.54E+02
1.84E+03	2.31E+02	2.44E+01	4.25E+02	1.23E+02
2.42E+03	1.44E+02	1.57E+01	2.82E+02	8.76E+01
3.20E+03	8.55E+01	9.54E+00	1.74E+02	5.69E+01
4.23E+03	4.84E+01	5.51E+00	1.03E+02	3.48E+01
5.59E+03	2.59E+01	3.02E+00	5.73E+01	2.02E+01
7.38E+03	1.30E+01	1.56E+00	3.01E+01	1.10E+01
9.75E+03	5.45E+00	7.14E-01	1.45E+01	5.65E+00
1.29E+04	0.00E+00	1.07E-01	4.81E+00	2.49E+00
1.70E+04	0.00E+00	0.00E+00	0.00E+00	4.53E-02
2.25E+04	0.00E+00	0.00E+00	0.00E+00	0.00E+00
2.97E+04	0.00E+00	0.00E+00	0.00E+00	0.00E+00
3.92E+04	0.00E+00	0.00E+00	0.00E+00	0.00E+00
5.18E+04	0.00E+00	0.00E+00	0.00E+00	0.00E+00
6.84E+04	0.00E+00	0.00E+00	0.00E+00	0.00E+00
9.03E+04	0.00E+00	0.00E+00	0.00E+00	0.00E+00

Figure 43. CREME96 Galactic Cosmic Ray LET Spectra for the peak 5 min of a large SEPE (scaled).

LET [MeV cm2/g]	Solar Orbiter – CREME96 GCR Spectra – Peak 5 min Integral Flux [#/m2/sec/sr]			
	Ca (Z=20)	Z=21-25	Fe (Z=26)	Z=27-92
1.07E+00	6.18E+01	1.91E+01	3.18E+02	1.28E+01
1.32E+00	6.18E+01	1.91E+01	3.18E+02	1.28E+01
1.75E+00	6.18E+01	1.91E+01	3.18E+02	1.28E+01
2.31E+00	6.18E+01	1.91E+01	3.18E+02	1.28E+01
3.04E+00	6.18E+01	1.91E+01	3.18E+02	1.28E+01
4.02E+00	6.18E+01	1.91E+01	3.18E+02	1.28E+01
5.31E+00	6.18E+01	1.91E+01	3.18E+02	1.28E+01
7.02E+00	6.18E+01	1.91E+01	3.18E+02	1.28E+01
9.27E+00	6.18E+01	1.91E+01	3.18E+02	1.28E+01
1.22E+01	6.18E+01	1.91E+01	3.18E+02	1.28E+01
1.62E+01	6.18E+01	1.91E+01	3.18E+02	1.28E+01
2.14E+01	6.18E+01	1.91E+01	3.18E+02	1.28E+01
2.82E+01	6.18E+01	1.91E+01	3.18E+02	1.28E+01
3.73E+01	6.18E+01	1.91E+01	3.18E+02	1.28E+01
4.92E+01	6.18E+01	1.91E+01	3.18E+02	1.28E+01
6.50E+01	6.18E+01	1.91E+01	3.18E+02	1.28E+01
8.59E+01	6.18E+01	1.91E+01	3.18E+02	1.28E+01
1.14E+02	6.18E+01	1.91E+01	3.18E+02	1.28E+01
1.50E+02	6.18E+01	1.91E+01	3.18E+02	1.28E+01
1.98E+02	6.18E+01	1.91E+01	3.18E+02	1.28E+01
2.62E+02	6.18E+01	1.91E+01	3.18E+02	1.28E+01
3.45E+02	6.18E+01	1.91E+01	3.18E+02	1.28E+01
4.56E+02	6.18E+01	1.91E+01	3.18E+02	1.28E+01
6.03E+02	6.18E+01	1.91E+01	3.18E+02	1.28E+01
7.96E+02	6.17E+01	1.91E+01	3.18E+02	1.28E+01
1.05E+03	6.10E+01	1.91E+01	3.18E+02	1.28E+01
1.39E+03	5.83E+01	1.89E+01	3.16E+02	1.28E+01
1.84E+03	5.25E+01	1.84E+01	3.12E+02	1.27E+01
2.42E+03	4.29E+01	1.70E+01	2.98E+02	1.24E+01
3.20E+03	3.14E+01	1.46E+01	2.65E+02	1.13E+01
4.23E+03	2.07E+01	1.11E+01	2.12E+02	9.46E+00
5.59E+03	1.27E+01	7.54E+00	1.51E+02	6.99E+00
7.38E+03	7.43E+00	4.75E+00	9.63E+01	4.60E+00
9.75E+03	4.08E+00	2.82E+00	5.84E+01	2.84E+00
1.29E+04	2.07E+00	1.55E+00	3.29E+01	1.65E+00
1.70E+04	8.65E-01	7.61E-01	1.69E+01	8.71E-01
2.25E+04	0.00E+00	2.68E-01	7.10E+00	3.95E-01
2.97E+04	0.00E+00	0.00E+00	0.00E+00	5.23E-02
3.92E+04	0.00E+00	0.00E+00	0.00E+00	7.67E-04
5.18E+04	0.00E+00	0.00E+00	0.00E+00	2.27E-04
6.84E+04	0.00E+00	0.00E+00	0.00E+00	4.79E-05
9.03E+04	0.00E+00	0.00E+00	0.00E+00	3.37E-06

Figure 44. CREME96 Galactic Cosmic Ray LET Spectra for the peak 5 min of a large SEPE (scaled).
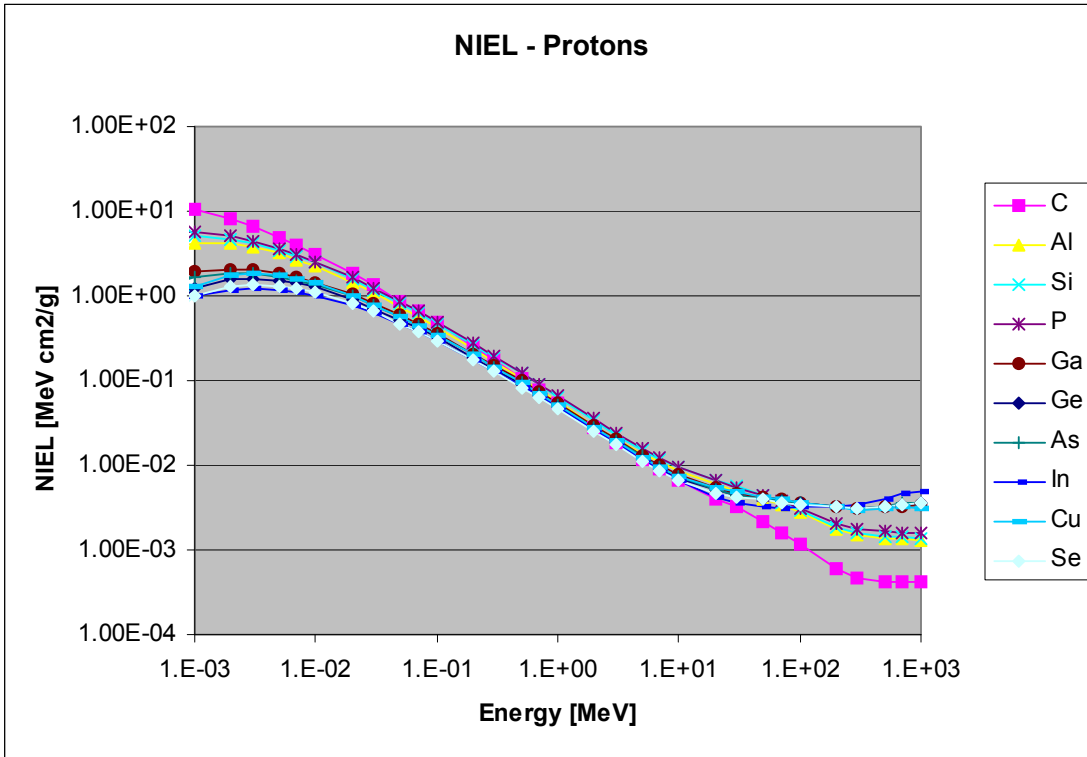
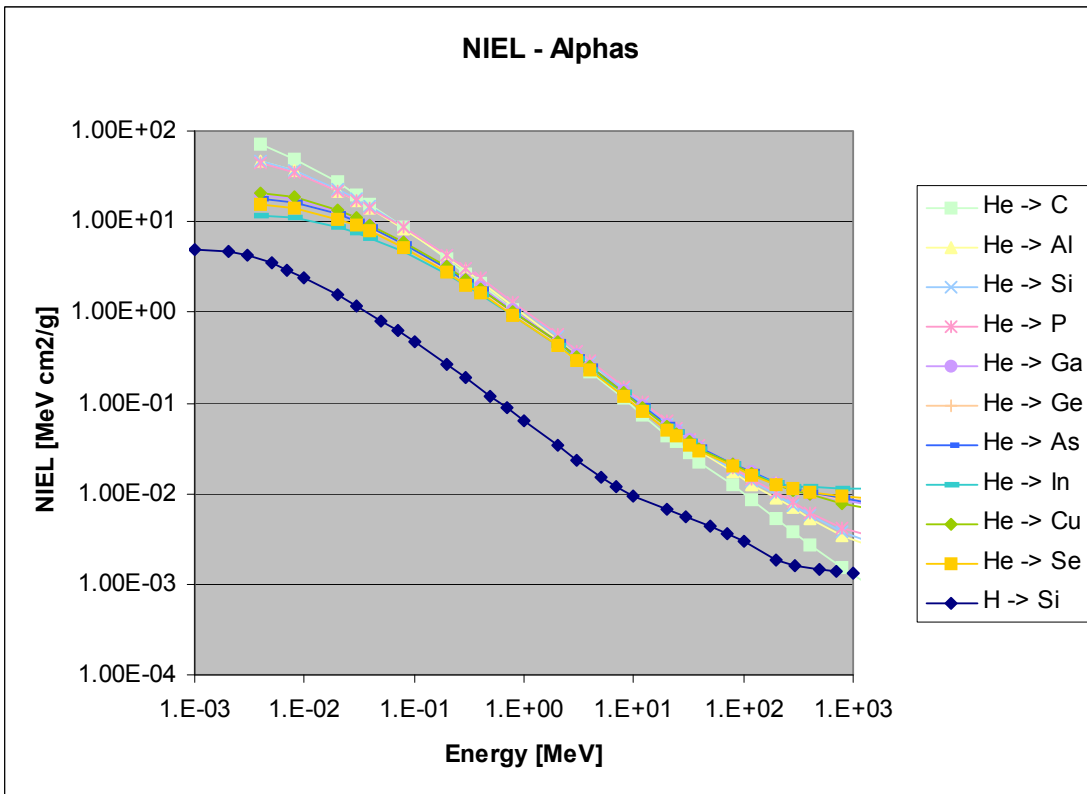**Figure 45. Proton NIEL for various target materials**

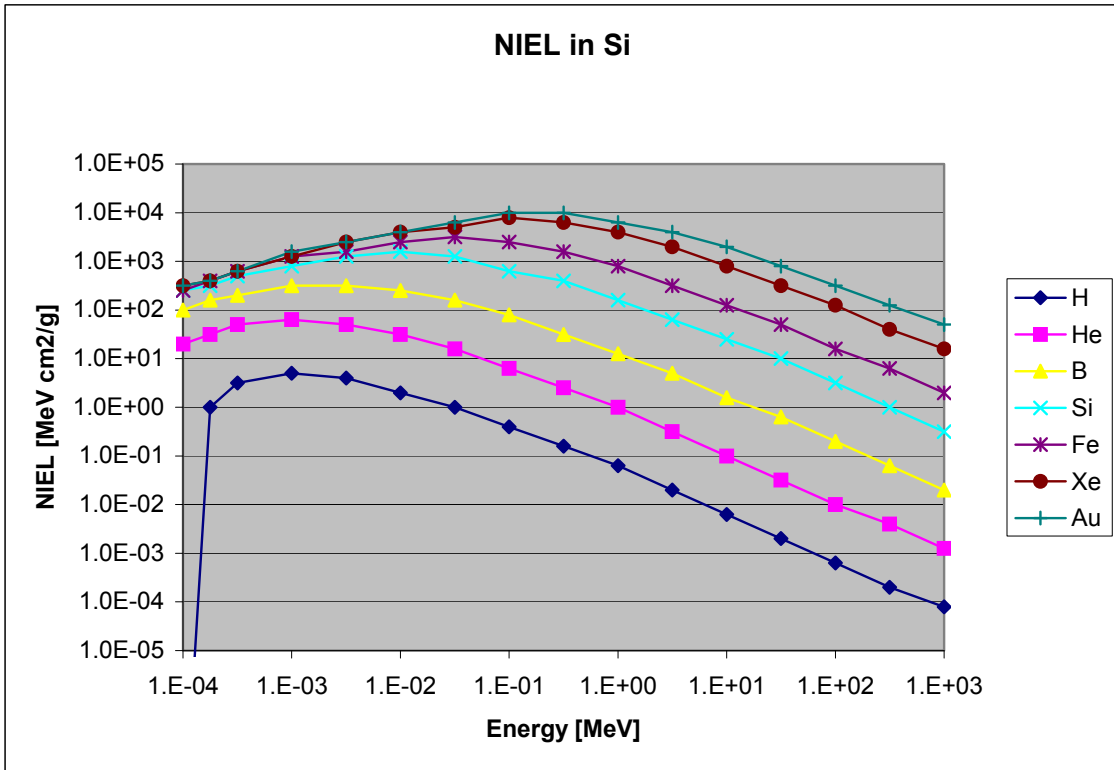**Figure 46. Alpha NIEL for various target materials**

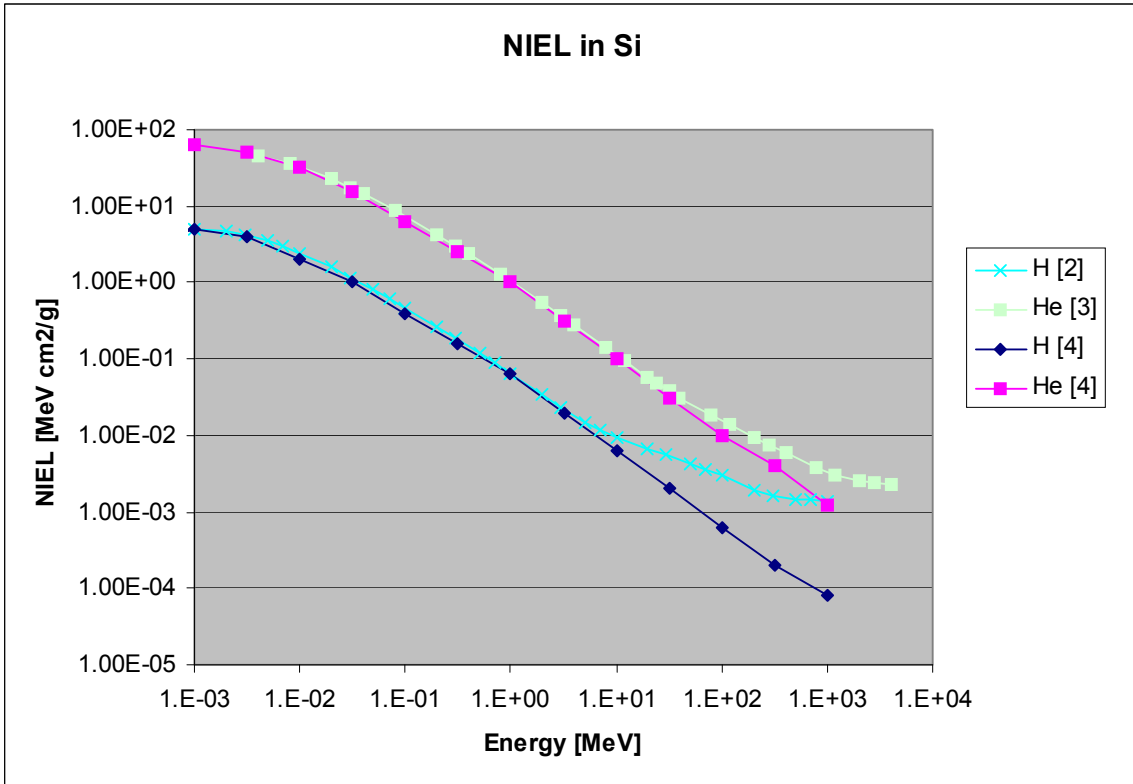**Figure 47. NIEL in Silicium for selected heavier ions**

Figure 48. NIEL in Silicium for H and He from different data sources

Energy [MeV]	Proton NIEL for Target Material [MeV cm2/g]				
	C	Al	Si	P	Ga
1.00E-03	1.03E+01	4.26E+00	5.03E+00	5.61E+00	1.90E+00
2.00E-03	8.09E+00	4.23E+00	4.72E+00	5.09E+00	2.06E+00
3.00E-03	6.62E+00	3.88E+00	4.22E+00	4.46E+00	2.05E+00
5.00E-03	4.97E+00	3.20E+00	3.49E+00	3.67E+00	1.86E+00
7.00E-03	3.99E+00	2.69E+00	2.96E+00	3.11E+00	1.68E+00
1.00E-02	3.11E+00	2.24E+00	2.46E+00	2.53E+00	1.46E+00
2.00E-02	1.86E+00	1.44E+00	1.57E+00	1.65E+00	1.04E+00
3.00E-02	1.34E+00	1.08E+00	1.18E+00	1.24E+00	8.17E-01
5.00E-02	8.74E-01	7.28E-01	8.16E-01	8.51E-01	5.91E-01
7.00E-02	6.49E-01	5.64E-01	6.23E-01	6.53E-01	4.64E-01
1.00E-01	4.80E-01	4.26E-01	4.72E-01	4.89E-01	3.59E-01
2.00E-01	2.53E-01	2.35E-01	2.62E-01	2.73E-01	2.08E-01
3.00E-01	1.76E-01	1.67E-01	1.87E-01	1.95E-01	1.51E-01
5.00E-01	1.07E-01	1.07E-01	1.20E-01	1.24E-01	9.89E-02
7.00E-01	7.71E-02	7.88E-02	8.84E-02	9.15E-02	7.41E-02
1.00E+00	5.45E-02	5.67E-02	6.38E-02	6.63E-02	5.43E-02
2.00E+00	2.76E-02	2.97E-02	3.36E-02	3.51E-02	2.94E-02
3.00E+00	1.85E-02	2.06E-02	2.29E-02	2.42E-02	2.04E-02
5.00E+00	1.18E-02	1.36E-02	1.48E-02	1.58E-02	1.28E-02
7.00E+00	8.84E-03	1.08E-02	1.17E-02	1.22E-02	9.78E-03
1.00E+01	6.76E-03	8.69E-03	9.43E-03	9.72E-03	7.58E-03
2.00E+01	3.93E-03	5.97E-03	6.65E-03	6.70E-03	5.40E-03
3.00E+01	3.23E-03	4.94E-03	5.58E-03	5.47E-03	4.74E-03
5.00E+01	2.16E-03	3.99E-03	4.30E-03	4.35E-03	4.19E-03
7.00E+01	1.60E-03	3.35E-03	3.65E-03	3.71E-03	3.90E-03
1.00E+02	1.16E-03	2.72E-03	2.97E-03	3.08E-03	3.62E-03
2.00E+02	6.09E-04	1.73E-03	1.88E-03	2.03E-03	3.20E-03
3.00E+02	4.66E-04	1.48E-03	1.62E-03	1.79E-03	3.03E-03
5.00E+02	4.21E-04	1.34E-03	1.43E-03	1.65E-03	3.17E-03
7.00E+02	4.24E-04	1.33E-03	1.41E-03	1.59E-03	3.32E-03
1.00E+03	4.17E-04	1.29E-03	1.34E-03	1.58E-03	3.34E-03

Figure 49. Proton NIEL for various target materials

Energy [MeV]	Proton NIEL for Target Material [MeV cm2/g]				
	Ge	As	In	Cu	Se
1.00E-03	1.21E+00	1.63E+00	9.88E-01	1.30E+00	9.76E-01
2.00E-03	1.55E+00	1.85E+00	1.18E+00	1.79E+00	1.29E+00
3.00E-03	1.61E+00	1.82E+00	1.20E+00	1.85E+00	1.36E+00
5.00E-03	1.51E+00	1.68E+00	1.16E+00	1.72E+00	1.31E+00
7.00E-03	1.41E+00	1.53E+00	1.10E+00	1.58E+00	1.23E+00
1.00E-02	1.26E+00	1.36E+00	1.00E+00	1.40E+00	1.11E+00
2.00E-02	9.05E-01	9.79E-01	7.65E-01	9.91E-01	8.12E-01
3.00E-02	7.15E-01	7.76E-01	6.25E-01	7.91E-01	6.58E-01
5.00E-02	5.19E-01	5.58E-01	4.69E-01	5.59E-01	4.73E-01
7.00E-02	4.14E-01	4.46E-01	3.77E-01	4.44E-01	3.79E-01
1.00E-01	3.21E-01	3.42E-01	2.98E-01	3.43E-01	2.96E-01
2.00E-01	1.89E-01	2.02E-01	1.78E-01	2.00E-01	1.75E-01
3.00E-01	1.35E-01	1.45E-01	1.31E-01	1.42E-01	1.27E-01
5.00E-01	8.83E-02	9.51E-02	8.73E-02	9.27E-02	8.36E-02
7.00E-01	6.61E-02	7.13E-02	6.60E-02	7.05E-02	6.27E-02
1.00E+00	4.92E-02	5.23E-02	4.88E-02	5.15E-02	4.60E-02
2.00E+00	2.66E-02	2.84E-02	2.68E-02	2.78E-02	2.49E-02
3.00E+00	1.84E-02	1.97E-02	1.87E-02	1.92E-02	1.73E-02
5.00E+00	1.17E-02	1.26E-02	1.18E-02	1.24E-02	1.11E-02
7.00E+00	8.87E-03	9.57E-03	8.80E-03	9.52E-03	8.43E-03
1.00E+01	6.89E-03	7.27E-03	6.59E-03	7.48E-03	6.52E-03
2.00E+01	5.04E-03	5.15E-03	4.23E-03	5.49E-03	4.74E-03
3.00E+01	4.51E-03	4.49E-03	3.54E-03	4.87E-03	4.18E-03
5.00E+01	4.08E-03	4.04E-03	3.23E-03	4.29E-03	3.89E-03
7.00E+01	3.79E-03	3.73E-03	3.13E-03	3.92E-03	3.65E-03
1.00E+02	3.56E-03	3.58E-03	3.18E-03	3.64E-03	3.48E-03
2.00E+02	3.22E-03	3.29E-03	3.25E-03	3.17E-03	3.22E-03
3.00E+02	3.12E-03	3.13E-03	3.38E-03	2.99E-03	3.15E-03
5.00E+02	3.27E-03	3.28E-03	4.02E-03	3.06E-03	3.24E-03
7.00E+02	3.48E-03	3.54E-03	4.54E-03	3.20E-03	3.39E-03
1.00E+03	3.51E-03	3.58E-03	4.96E-03	3.14E-03	3.65E-03

Figure 50. Proton NIEL for various target materials

Energy [MeV]	Alpha NIEL for Target Material [MeV cm2/g]				
	C	Al	Si	P	Ga
4.00E-03	7.21E+01	4.67E+01	4.65E+01	4.43E+01	2.01E+01
8.00E-03	4.98E+01	3.61E+01	3.64E+01	3.47E+01	1.79E+01
2.00E-02	2.69E+01	2.21E+01	2.26E+01	2.18E+01	1.30E+01
3.00E-02	1.99E+01	1.70E+01	1.77E+01	1.71E+01	1.07E+01
4.00E-02	1.58E+01	1.40E+01	1.46E+01	1.42E+01	9.14E+00
8.00E-02	8.83E+00	8.46E+00	8.80E+00	8.70E+00	6.01E+00
2.00E-01	3.91E+00	4.02E+00	4.26E+00	4.25E+00	3.16E+00
3.00E-01	2.68E+00	2.88E+00	3.02E+00	3.04E+00	2.32E+00
4.00E-01	2.05E+00	2.22E+00	2.36E+00	2.39E+00	1.85E+00
8.00E-01	1.06E+00	1.19E+00	1.26E+00	1.29E+00	1.05E+00
2.00E+00	4.34E-01	5.07E-01	5.46E-01	5.60E-01	4.79E-01
3.00E+00	2.92E-01	3.45E-01	3.66E-01	3.79E-01	3.31E-01
4.00E+00	2.17E-01	2.63E-01	2.79E-01	2.90E-01	2.56E-01
8.00E+00	1.11E-01	1.33E-01	1.42E-01	1.48E-01	1.35E-01
1.20E+01	7.29E-02	9.02E-02	9.56E-02	1.01E-01	9.23E-02
2.00E+01	4.41E-02	5.53E-02	5.86E-02	6.21E-02	5.76E-02
2.40E+01	3.76E-02	4.63E-02	4.92E-02	5.24E-02	4.89E-02
3.20E+01	2.81E-02	3.53E-02	3.82E-02	4.02E-02	3.87E-02
4.00E+01	2.26E-02	2.97E-02	3.15E-02	3.35E-02	3.27E-02
8.00E+01	1.23E-02	1.73E-02	1.84E-02	1.95E-02	2.15E-02
1.20E+02	8.47E-03	1.26E-02	1.39E-02	1.46E-02	1.73E-02
2.00E+02	5.28E-03	8.91E-03	9.61E-03	1.03E-02	1.32E-02
2.80E+02	3.82E-03	6.89E-03	7.47E-03	8.05E-03	1.14E-02
4.00E+02	2.76E-03	5.28E-03	5.82E-03	6.17E-03	1.00E-02
8.00E+02	1.54E-03	3.37E-03	3.79E-03	4.18E-03	8.43E-03
1.20E+03	1.11E-03	2.83E-03	3.10E-03	3.58E-03	7.78E-03
2.00E+03	7.90E-04	2.31E-03	2.57E-03	2.89E-03	7.33E-03
2.80E+03	6.93E-04	2.00E-03	2.41E-03	2.51E-03	6.95E-03
4.00E+03	5.42E-04	1.95E-03	2.22E-03	2.41E-03	6.48E-03

Figure 51. Alpha NIEL for various target materials

Energy [MeV]	Alpha NIEL for Target Material [MeV cm2/g]				
	Ge	As	In	Cu	Se
4.00E-03	1.80E+01	1.80E+01	1.15E+01	2.08E+01	1.58E+01
8.00E-03	1.63E+01	1.63E+01	1.10E+01	1.86E+01	1.44E+01
2.00E-02	1.20E+01	1.20E+01	8.83E+00	1.34E+01	1.08E+01
3.00E-02	9.94E+00	1.00E+01	7.56E+00	1.10E+01	9.04E+00
4.00E-02	8.52E+00	8.60E+00	6.69E+00	9.35E+00	7.78E+00
8.00E-02	5.62E+00	5.68E+00	4.64E+00	6.08E+00	5.17E+00
2.00E-01	2.95E+00	3.02E+00	2.59E+00	3.15E+00	2.74E+00
3.00E-01	2.16E+00	2.22E+00	1.94E+00	2.29E+00	2.03E+00
4.00E-01	1.72E+00	1.78E+00	1.57E+00	1.82E+00	1.63E+00
8.00E-01	9.76E-01	1.02E+00	9.17E-01	1.02E+00	9.25E-01
2.00E+00	4.46E-01	4.63E-01	4.30E-01	4.64E-01	4.20E-01
3.00E+00	3.11E-01	3.24E-01	3.04E-01	3.22E-01	2.93E-01
4.00E+00	2.37E-01	2.51E-01	2.35E-01	2.49E-01	2.27E-01
8.00E+00	1.26E-01	1.33E-01	1.28E-01	1.29E-01	1.19E-01
1.20E+01	8.62E-02	9.11E-02	8.76E-02	8.84E-02	8.18E-02
2.00E+01	5.38E-02	5.71E-02	5.50E-02	5.49E-02	5.10E-02
2.40E+01	4.57E-02	4.82E-02	4.74E-02	4.64E-02	4.39E-02
3.20E+01	3.64E-02	3.78E-02	3.71E-02	3.72E-02	3.46E-02
4.00E+01	3.08E-02	3.25E-02	3.16E-02	3.13E-02	2.99E-02
8.00E+01	2.04E-02	2.14E-02	2.08E-02	2.08E-02	2.00E-02
1.20E+02	1.65E-02	1.72E-02	1.69E-02	1.65E-02	1.59E-02
2.00E+02	1.31E-02	1.32E-02	1.31E-02	1.27E-02	1.27E-02
2.80E+02	1.12E-02	1.13E-02	1.17E-02	1.09E-02	1.11E-02
4.00E+02	1.01E-02	1.01E-02	1.17E-02	9.61E-03	1.03E-02
8.00E+02	8.67E-03	8.89E-03	1.13E-02	7.90E-03	9.20E-03
1.20E+03	8.34E-03	8.32E-03	1.13E-02	7.19E-03	8.78E-03
2.00E+03	7.82E-03	7.80E-03	1.13E-02	6.88E-03	8.13E-03
2.80E+03	7.17E-03	7.38E-03	1.11E-02	6.50E-03	7.80E-03
4.00E+03	6.89E-03	6.90E-03	1.09E-02	6.33E-03	7.13E-03

Figure 52. Alpha NIEL for various target materials

Energy [MeV]	NIEL in Si for selected Ions [MeV cm2/g]			
	H	He	B	Si
1.00E-04	1.0E-09	2.0E+01	1.0E+02	2.5E+02
1.78E-04	1.0E+00	3.2E+01	1.6E+02	3.2E+02
3.16E-04	3.2E+00	5.0E+01	2.0E+02	5.0E+02
1.00E-03	5.0E+00	6.3E+01	3.2E+02	7.9E+02
3.16E-03	4.0E+00	5.0E+01	3.2E+02	1.3E+03
1.00E-02	2.0E+00	3.2E+01	2.5E+02	1.6E+03
3.16E-02	1.0E+00	1.6E+01	1.6E+02	1.3E+03
1.00E-01	4.0E-01	6.3E+00	7.9E+01	6.3E+02
3.16E-01	1.6E-01	2.5E+00	3.2E+01	4.0E+02
1.00E+00	6.3E-02	1.0E+00	1.3E+01	1.6E+02
3.16E+00	2.0E-02	3.2E-01	5.0E+00	6.3E+01
1.00E+01	6.3E-03	1.0E-01	1.6E+00	2.5E+01
3.16E+01	2.0E-03	3.2E-02	6.3E-01	1.0E+01
1.00E+02	6.3E-04	1.0E-02	2.0E-01	3.2E+00
3.16E+02	2.0E-04	4.0E-03	6.3E-02	1.0E+00
1.00E+03	7.9E-05	1.3E-03	2.0E-02	3.2E-01

Figure 53. NIEL in Si for selected Ions

Energy [MeV]	NIEL in Si for selected Ions [MeV cm2/g]		
	Fe	Xe	Au
1.00E-04	2.5E+02	3.2E+02	3.2E+02
1.78E-04	4.0E+02	4.0E+02	4.0E+02
3.16E-04	6.3E+02	6.3E+02	6.3E+02
1.00E-03	1.3E+03	1.3E+03	1.6E+03
3.16E-03	1.6E+03	2.5E+03	2.5E+03
1.00E-02	2.5E+03	4.0E+03	4.0E+03
3.16E-02	3.2E+03	5.0E+03	6.3E+03
1.00E-01	2.5E+03	7.9E+03	1.0E+04
3.16E-01	1.6E+03	6.3E+03	1.0E+04
1.00E+00	7.9E+02	4.0E+03	6.3E+03
3.16E+00	3.2E+02	2.0E+03	4.0E+03
1.00E+01	1.3E+02	7.9E+02	2.0E+03
3.16E+01	5.0E+01	3.2E+02	7.9E+02
1.00E+02	1.6E+01	1.3E+02	3.2E+02
3.16E+02	6.3E+00	4.0E+01	1.3E+02
1.00E+03	2.0E+00	1.6E+01	5.0E+01

Figure 54. NIEL in Si for selected Ions